



**US Army Corps
of Engineers**
Waterways Experiment
Station

Geophysical Investigation of Cluster 11, Edgewood Area, Aberdeen Proving Ground, Maryland

by Michael K. Sharp, Janet E. Simms, Landris T. Lee, Jr., Jerry L. Burgess

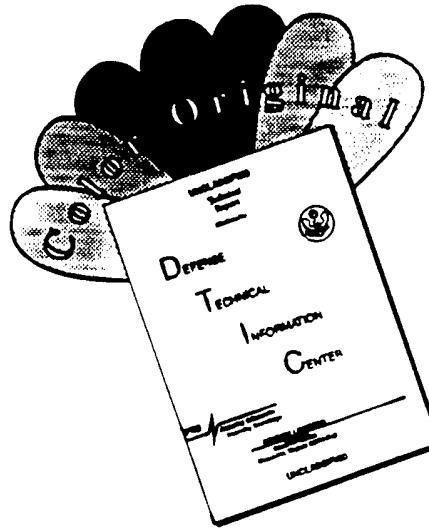
Approved for Public Release; Distribution Is Unlimited

Approved for Public Release; Distribution Is Unlimited

Approved For Public Release; Distribution Is Unlimited

19960409 167

DISCLAIMER NOTICE



THIS DOCUMENT IS BEST
QUALITY AVAILABLE. THE COPY
FURNISHED TO DTIC CONTAINED
A SIGNIFICANT NUMBER OF
COLOR PAGES WHICH DO NOT
REPRODUCE LEGIBLY ON BLACK
AND WHITE MICROFICHE.

Geophysical Investigation of Cluster 11, Edgewood Area, Aberdeen Proving Ground, Maryland

by Michael K. Sharp, Janet E. Simms, Landris T. Lee, Jr.

U.S. Army Corps of Engineers
Waterways Experiment Station
3909 Halls Ferry Road
Vicksburg, MS 39180-6199

Jerry L. Burgess

Environmental, Conservation and Restoration Division
Directorate of Safety, Health, and Environment
STEAP-SH-ER
Aberdeen Proving Ground
Edgewood, MD 21005

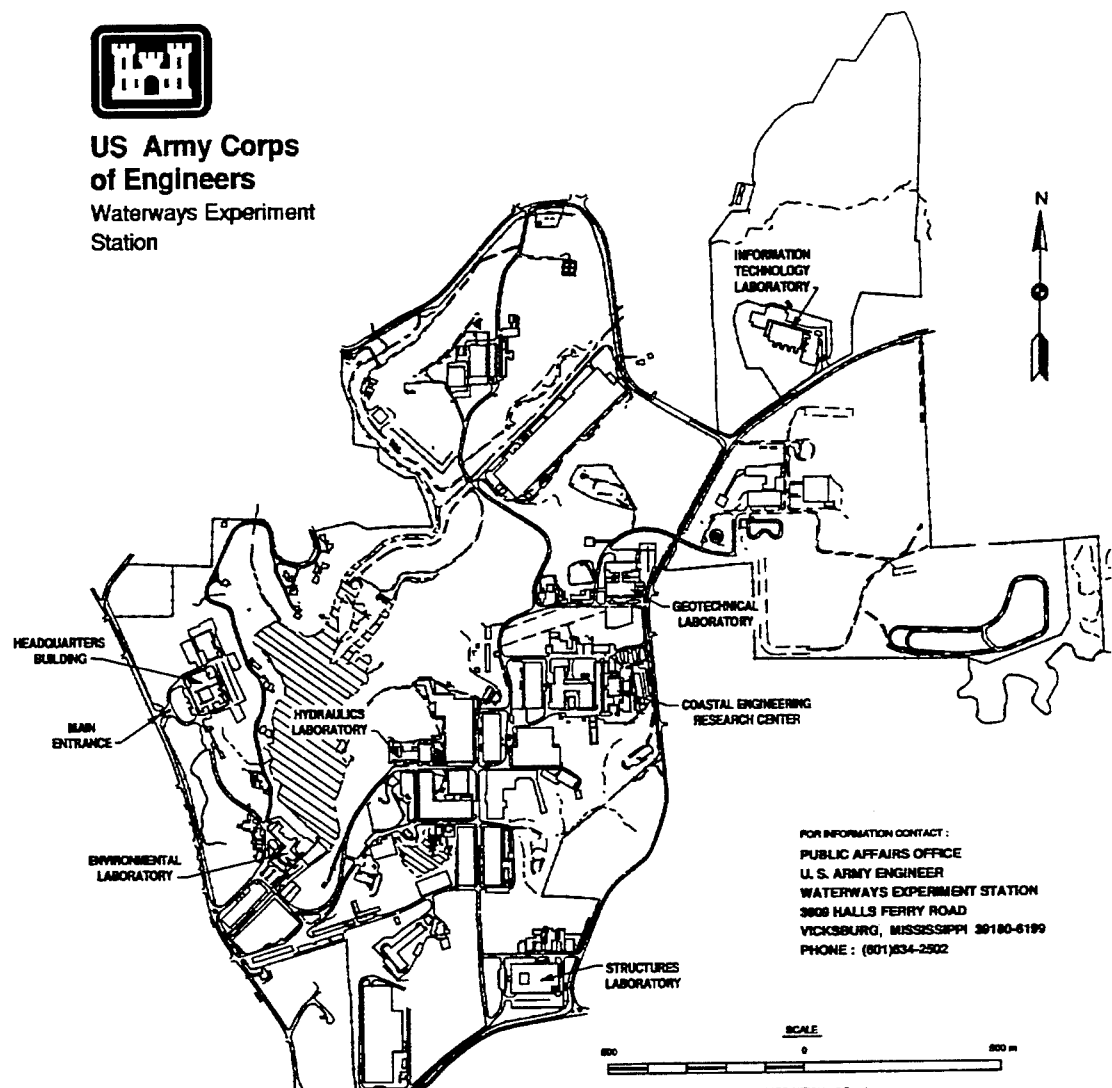
Final report

Approved for public release; distribution is unlimited

Prepared for Installation Restoration Program, Directorate of Safety, Health,
and Environment
Aberdeen Proving Ground, MD 21005



**US Army Corps
of Engineers**
Waterways Experiment
Station



Waterways Experiment Station Cataloging-in-Publication Data

Geophysical investigation of Cluster 11, Edgewood Area, Aberdeen Proving Ground, Maryland / by Michael K. Sharp .. [et al.] ; prepared for Installation Restoration Program, Directorate of Safety, Health, and Environment.

183 p. : ill. ; 28 cm. — (Miscellaneous paper ; GL-96-4)

Includes bibliographic references.

1. Geophysics — Maryland — Aberdeen Proving Ground. 2. Ground penetration radar. 3. Hazardous waste sites — Maryland — Aberdeen Proving Ground. 4. Aberdeen Proving Ground (Md.) I. Sharp, Michael K. II. United States. Army. Corps of Engineers. III. U.S. Army Engineer Waterways Experiment Station. IV. Geotechnical Laboratory (U.S. Army Engineer Waterways Experiment Station) V. Installation Restoration Program. VI. Aberdeen Proving Ground (Md.). Directorate of Safety, Health, and Environment. VII. Series: Miscellaneous paper (U.S. Army Engineer Waterways Experiment Station) ; GL-96-4.

TA7 W34m no.GL-96-4

Contents

Preface	viii
Conversion Factors, Non-SI to SI Units of Measurement	ix
1—Introduction	1
Background	1
22nd Street landfill	1
Ton container steamout site	1
Adamsite storage pit	3
Radioactive material disposal facility	3
Approach and Scope of Work	3
2—Site Geology	7
3—Geophysical Test Principles and Field Procedures	13
Geophysical Test Principles	13
Electromagnetic surveys	13
Magnetic surveys	14
Ground penetrating radar surveys	15
Electrical resistivity surveys	16
Surface seismic surveys	17
Field Procedures	18
Land surveys	18
Offshore surveys	22
4—Test Results and Interpretation	25
Site 1 Results	25
Site 2 Results	26
Site 3 Results	59
Site 4 Results	93
Site 5 Results	103
Site 6 Results	113
Offshore Results	123
5—Summary	145
Onshore Sites 1-6	145
Offshore Sites 1 and 2	146
Geological	147

References	149
Appendix A	A1
SF 298	

List of Figures

Figure 1. Site map showing locations of SWMU's on a portion of Bush River peninsula (APG/EA) as identified by Nemeth 1989	2
Figure 2. Site map showing locations of onshore and offshore grids at Bush River peninsula	5
Figure 3. Location of regional borings and monitoring wells relative to the Cluster 11 area. Metric scale: 1 cm = 60 m	9
Figure 4. Stratigraphic cross section from regional borings BR-1 through BR-5, Bush River area (from Thurmond 1993). Metric horizontal scale: 1 cm = 96 m	11
Figure 5. Grid map for Site 1 geophysical investigation. Stations are gridded at 10 ft (3 m) intervals	19
Figure 6. Grid map for Site 2 geophysical investigation. Stations are gridded at 10 ft (3 m) intervals	20
Figure 7. Grid map for Site 3 geophysical investigation. Stations are gridded at 10 ft (3 m) intervals	21
Figure 8. Grid map for Site 4 geophysical investigation. Stations are gridded at 10 ft (3 m) intervals	22
Figure 9. Grid map for Site 5 geophysical investigation. Stations are gridded at 10 ft (3 m) intervals	23
Figure 10. Grid map for Site 6 geophysical investigation. Stations are gridded at 10 ft (3 m) intervals	24
Figure 11. EM-31 conductivity survey for Site 1. Contours are 2 mS/m Station intervals are 10 ft (3 m)	27
Figure 12. EM-31 inphase survey for Site 1. Contours are 1 ppt. Station intervals are 10 ft (3 m)	29
Figure 13. Magnetic total field survey for Site 1. Contours intervals are 50 gammas, and station intervals are 10 ft (3 m)	31
Figure 14. Magnetic gradient survey for Site 1. Contours are 25 gammas/m. Station intervals are 10 ft (3 m)	33
Figure 15. EM-31 conductivity survey for Site 2. Contours are 5 mS/m, and station intervals are 10 ft (3 m)	35

Figure 16.	EM-31 inphase survey for Site 2. Contours are 1 ppt, and station intervals are 10 ft (3 m)	37
Figure 17.	Magnetic total field survey for Site 2. Contours are 250 gammas, and station intervals are 10 ft (3 m)	41
Figure 18.	Magnetic gradient survey for Site 2. Contours are 125 gammas/m, and station intervals are 10 ft (3 m)	43
Figure 19.	EM-61 bottom coil survey for Site 2. Contours are 100 mV, and station intervals are 10 ft (3 m)	45
Figure 20.	EM-61 top coil survey for Site 2. Contours are 100 mV, and station intervals are 10 ft (3 m)	47
Figure 21.	EM-61 difference between top and bottom coil survey for Site 2. Contours are 100 mV, and station intervals are 10 ft (3 m)	49
Figure 22.	Seismic reflection and resistivity sounding lines at Site 2. Station intervals are 10 ft (3 m)	52
Figure 23.	Seismic reflection line 100 survey results showing depth section (top) and layer interpreted depth section (bottom). Horizontal axis is station intervals of 10 ft (3 m). Vertical axis is depth intervals of 10 ft (3 m).	53
Figure 24.	Resistivity sounding line 1 at Site 2, showing inversion curve (left) and interpreted layers (right)	55
Figure 25.	Inversion curve (left) and equivalence models (right) for resistivity sounding line 1 at Site 2	56
Figure 26.	Resistivity sounding line 2 at Site 2, showing inversion curve (left) and interpreted layers (right)	57
Figure 27.	Inversion curve (left) and equivalence models (right) for resistivity sounding line 2 at Site 2	58
Figure 28.	EM-31 conductivity survey for Site 3. Contours are 2.5 mS/m, and station intervals are 10 ft (3 m)	61
Figure 29.	EM-31 inphase survey for Site 3. Contours are 1 ppt, and station intervals are 10 ft (3 m)	63
Figure 30.	Magnetic total field survey for Site 3. Contours are 100 gammas, and station intervals are 10 ft (3 m)	65
Figure 31.	Magnetic gradient survey for Site 3. Contours are 100 gammas/m, and station intervals are 10 ft (3 m)	67
Figure 32.	EM-61 bottom coil survey for Site 3. Contours are 100 mV, and station intervals are 10 ft (3 m)	69
Figure 33.	EM-61 top coil survey for Site 3. Contours are 100 mV, and station intervals are 10 ft (3 m)	71

Figure 34.	EM-61 difference between top and bottom coils survey for Site 3. Contours are 20 mV, and station intervals are 10 ft (3 m)	73
Figure 35.	Seismic reflection lines 200 and GPR survey lines at Site 3. Metric scale: 1 3m = 25 m	77
Figure 36.	Seismic reflection line 200 showing depth section (top) and layer interpreted depth section (bottom). Horizontal and vertical intervals are 10 ft (3 m).	79
Figure 37.	Geologic cross section A-A' from Bush River monitoring wells (Bailey 1995). Metric scale: 1 cm = 50 m.	83
Figure 38.	Geologic cross section B-B' from Bush River monitoring wells (Bailey 1995). Metric scale: 1 cm = 50 m.	85
Figure 39.	GPR line 1 at Site 3, stations 0 to 150, 280 nanosecond (ns) window. Station intervals are 2 ft (0.6 m)	87
Figure 40.	GPR line 2 at Site 3, stations 0 to 170, 200 nanosecond (ns) window. Station intervals are 2 ft (0.6 m)	89
Figure 41.	GPR line 2 at Site 3, stations 0 to 170, 460 nanosecond (ns) window. Station intervals are 2 ft (0.6 m)	91
Figure 42.	EM-31 conductivity survey for Site 4. Contours are 10 mS/m, and station intervals are 10 ft (3 m)	95
Figure 43.	EM-31 inphase survey for Site 4. Contours are 2.5 ppt, and station intervals are 10 ft (3 m)	97
Figure 44.	Magnetic total field survey for Site 4. Contours are 250 gammas, and station intervals are 10 ft (3 m)	99
Figure 45.	Magnetic gradient survey for Site 4. Contours are 200 gammas/m, and station intervals are 10 ft (3 m)	101
Figure 46.	EM-31 conductivity survey for Site 5. Contours are 10 mS/m, and station intervals are 10 ft (3 m)	105
Figure 47.	EM-31 inphase survey for Site 5. Contours are 2.5 ppt, and station intervals are 10 ft (3 m)	107
Figure 48.	Magnetic total field survey for Site 5. Contours are 250 gammas, and station intervals are 10 ft (3 m)	109
Figure 49.	Magnetic gradient survey for Site 5. Contours are 250 gammas/m, and station intervals are 10 ft (3 m)	111
Figure 50.	EM-31 conductivity survey for Site 6. Contours are 5 mS/m, and station intervals are 10 ft (3 m)	115
Figure 51.	EM-31 inphase survey for Site 6. Contours are 1 ppt, and station intervals are 10 ft (3 m)	117
Figure 52.	Magnetic total field survey for Site 6. Contours are 250 gammas, and station intervals are 10 ft (3 m)	119

Figure 53.	Magnetic gradient survey for Site 6. Contours are 200 gammas/m, and station intervals are 10 ft (3 m)	121
Figure 54.	EM-61 bottom coil survey for Site 6. Contours are 50 mV, and station intervals are 10 ft (3 m)	125
Figure 55.	EM-61 top coil survey for Site 6. Contours are 50 mV, and station intervals are 10 ft (3 m)	127
Figure 56.	EM-61 difference between top and bottom coil survey for Site 6. Contours are 10 mV, and station intervals are 10 ft (3 m)	129
Figure 57.	EM-31 conductivity survey for Offshore Site 1. Contours are 5 mS/m, and station intervals are 10 ft (3 m)	133
Figure 58.	EM-31 inphase survey for Offshore Site 1. Contours are 0.5 ppt, and station intervals are 10 ft (3 m)	135
Figure 59.	Magnetic total field survey for Offshore Site 1. Contours are 20 gammas, and station intervals are 10 ft (3 m)	137
Figure 60.	EM-31 conductivity survey for Offshore Site 2. Contours are 5 gammas/m, and station intervals are 10 ft (3 m)	139
Figure 61.	EM-31 inphase survey for Offshore Site 2. Contours are 0.5 ppt, and station intervals are 10 ft (3 m)	141
Figure 62.	Magnetic total field survey for Offshore Site 2. Contours are 50 gammas, and station intervals are 10 ft (3 m)	143

List of Tables

Table 1.	Anomalies Detected at Site 1	39
Table 2.	Anomalies Detected at Site 3	75
Table 3.	Anomalies Detected at Site 4	103
Table 4.	Anomalies Detected at Site 5	113
Table 5.	Anomalies Detected at Site 6	131
Table 6.	Anomalies Detected at Offshore Site 1	132
Table 7.	Anomalies Detected at Offshore Site 2	132

Preface

A geophysical investigation was conducted at the Bush River Study Area, Cluster 11 Site, Edgewood Area, Aberdeen Proving Ground (APG), Maryland, by personnel of the Geotechnical Laboratory (GL), U.S. Army Engineer Waterways Experiment Station (WES), during the period 3 - 7 June 1994. The investigation was conducted for the Installation Restoration Program, Directorate of Safety, Health, and Environment, APG. The Technical Monitor was Mr. Jerry Burgess. Mr. Don Green was the APG Area Manager.

This report was prepared by Mr. Michael K. Sharp, Earthquake Engineering and Geosciences Division (EEGD), and Mr. Jerry Burgess, Aberdeen Proving Ground (APG). The work was performed under the direct supervision of Mr. Joseph R. Curro, Jr., Chief, Engineering Geophysics Branch. The work was performed under the general supervision of Drs. A. G. Franklin, Chief, EEGD, and W. F. Marcuson, III, Director, GL. Field work and data analysis were performed by Messrs. Sharp and Landris T. Lee, Jr., and Dr. Janet E. Simms.

At the time of publication of this report, Director of WES was Dr. Robert W. Whalin. Commander was COL Bruce K. Howard, EN.

The contents of this report are not to be used for advertising, publication, or promotional purposes. Citation of trade names does not constitute an official endorsement or approval of the use of such commercial products.

Conversion Factors, SI to Non-SI Units of Measurement

SI units of measurement used in this report can be converted to Non-SI units as follows:

Multiply	By	To Obtain
meters	3.28	feet
nanotesla	1.0	gamma
centimeters	0.393	inches
millisiemens per meter	0.3048	millimhos per foot
square meters	10.758	square feet

1 Introduction

Background

A geophysical investigation was conducted on a portion of the Bush River Study Area (BRSA) at Edgewood Area (EA) Aberdeen Proving Ground (APG), designated as Cluster 11 or the Eastern Chemical Depot Area. This area of investigation consists of four solid waste management units (SWMU) termed 22nd street landfill, ton container steamout site, adamsite storage pit and radioactive material disposal facility. These SWMU's are shown in Figure 1 and were identified in the RCRA Facility Assessment Report for the EA, APG, by Nemeth 1989. Following is a brief discussion of each SWMU as presented in the RCRA Facility Assessment Report.

22nd Street landfill

The 22nd street landfill is a SWMU located east of 22nd street (Figure 1). The landfill was reportedly in use during the late 1960's and early 1970's. Approximately 40,470 square metres are involved in the landfill which was operated as a sanitary fill using normal fill methods. The area is grass covered and routinely mowed except for a marshy portion to the east (adjacent to the Bush River) and a wooded area to the northwest. The area is bounded to the north by a small creek draining into the Bush River. There is also a small creek that runs through the approximate center of the area.

Reportedly the landfill received sanitary waste consisting of asphalt roofing material, concrete, and steel which can be seen at various locations scattered around the site. It is not known if the landfill received debris from chemical plant buildings being demolished during that time period. Prior to land filling in the area, the marsh which existed in the eastern portion of the site received wastes from the ton container steamout site. These wastes were primarily sulfur sludges heavily contaminated with mustard. It is also possible that the marsh area was used as a dump site for chemical agent filled munitions.

Ton container steamout site

The ton container steamout site is located adjacent to the southeast portion of the 22nd street landfill (Figure 1). This SWMU was a facility used to

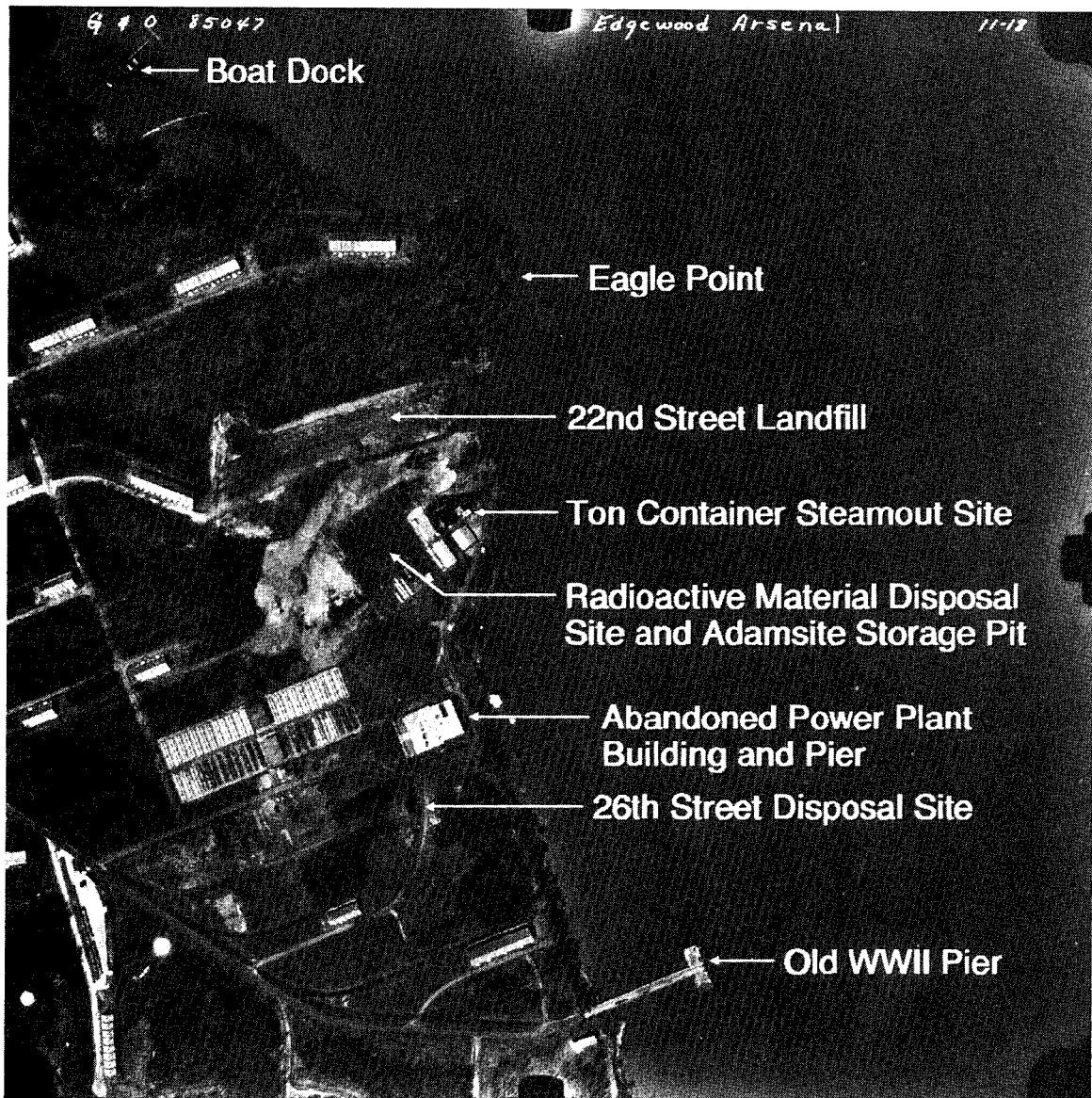


Figure 1. Site map showing locations of SWMU's on a portion of Bush River peninsula (APG/EA) as identified by Nemeth 1989

decontaminate ton containers in which mustard, chloropicrin, lewisite, and other chemical agents had been stored. The facility was operated until the late 1950's or early 1960's. The refuge from the cleaning process was initially placed in an earth pit at the edge of the marsh. The sludge later went into a wooden box set into a pit at the edge of the marsh. Sludge was periodically removed from the box and placed in one of the disposal fields (O-field or J-field). The amount of sludge which went into the marsh area is not known. There is no surface evidence of the sludge box, possibly due to the land filling action discussed previously.

Adamsite storage pit

This SWMU is located in Building 934 (E2370) in the ton container steamout site (Figure 1). The building is a roofed concrete pit divided into two sections originally constructed during 1931. The floor of the building is located 1.8 m below ground level. During the 1960's, drums of Adamsite (DM) were buried in the southwest half of the building. The drums were placed in the building and surrounded with sand. A concrete cap was poured over the top of the drums and sand. The drums were subsequently removed from the building in 1983.

Radioactive material disposal facility

The radioactive material disposal facility is located as shown in Figure 1. The facility had been previously used for chemical agent storage from the time of its construction in 1931 until it became a dedicated facility for radioactive waste material handling in the late 1950's or early 1960's. While used for chemical storage, the facility was referred to as the toxic gas yard. The facility is now commonly referred to as the 'rad yard'. This SWMU is a facility at which radioactive waste material is processed, packaged, and temporarily stored prior to disposal. There has never been any actual disposal of radioactive waste at this site. The facility is fenced and approximately 29.73 m square.

Approach and Scope of Work

A geophysical investigation was conducted at Cluster 11 by WES personnel during June 1994. The objective of the investigation was to delineate anomalies indicative of a landfill or other burial activities (such as tanks, barrels, etc.) and to collect information to aid in the geological site characterization. Five geophysical methods were used in this investigation: electric, magnetic, electromagnetic (EM), ground penetrating radar (GPR) and surface seismic surveys.

The success of using geophysical surveying methods for delineating targets of interest is based on there being a sufficient contrast in material properties, i.e., electrical, magnetic, chemical, etc. between the target and its surrounding environment. Other factors affecting the ability to detect a target using geophysical methods are the size, depth and orientation of the target.

To accomplish the objectives of the investigation, a plan was devised to fully survey the areas of interest. The areas surveyed for this investigation are shown in Figure 2. This figure is an aerial photograph of the site with the location of the surveyed areas indicated by the red grids and labeled Site 1 through Site 6. All four SWMU's discussed previously were fully investigated, except for a portion of the 22nd street landfill which was heavily covered with tall grasses (phragmites). In addition to the land areas surveyed, a

portion of the offshore was also surveyed. The offshore grids are shown in Figure 2 and labeled offshore Sites 1 and 2. The grids extend from the old WWII pier north to Eagle Point. This area was surveyed to determine if any of the proposed fill material extended into Bush River.

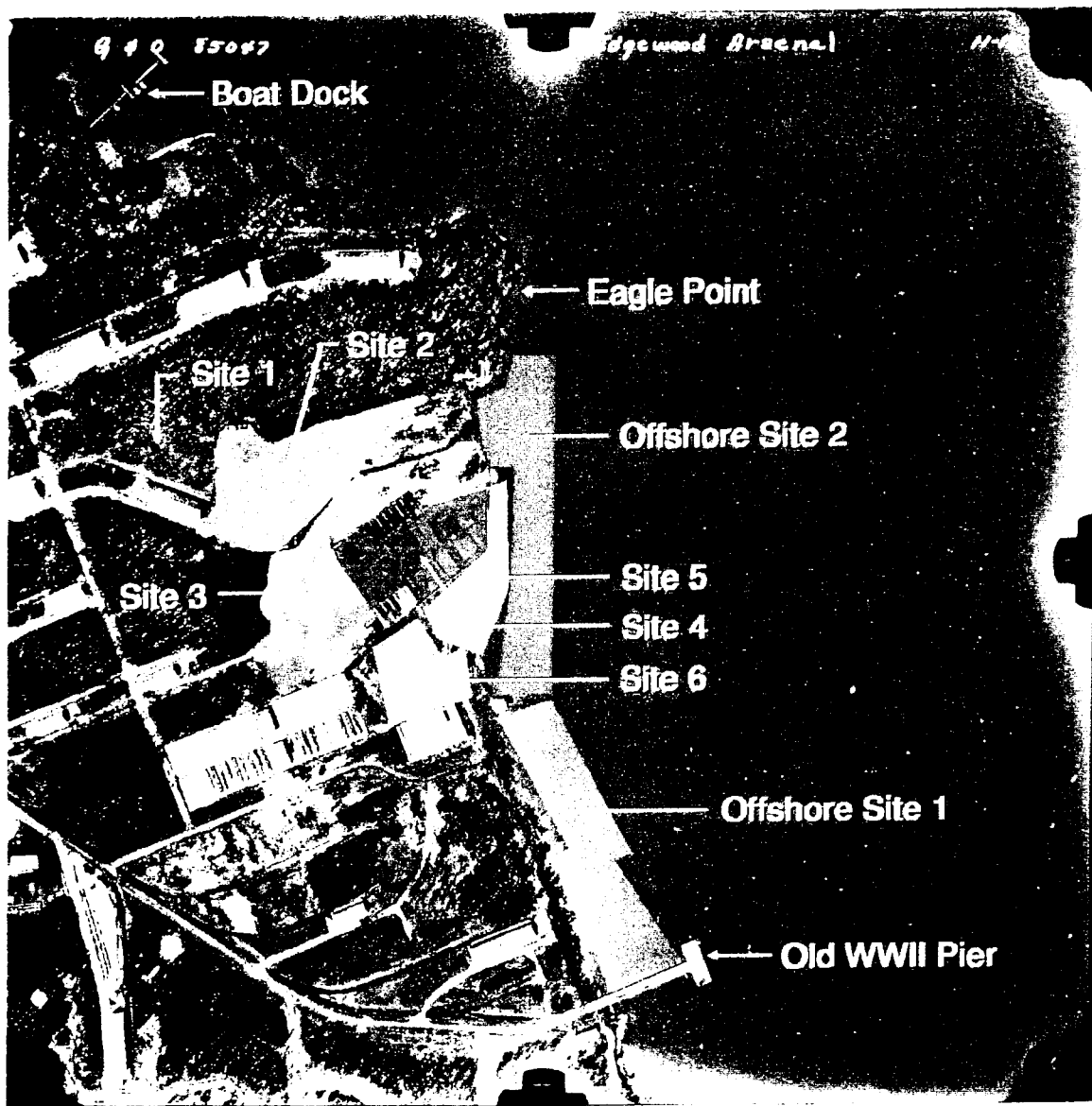


Figure 2. Site map showing locations of onshore and offshore grids at Bush River peninsula

2 Site Geology

Cluster 11 lies southeast of the Fall Line in the Atlantic Coastal Plain physiographic province of Maryland. The Coastal Plain here is underlain by gently southeast dipping crystalline basement. Depth to basement in this area is likely to be around 152 m below MSL. The underlying Coastal Plain sediments consist of the Cretaceous Patapsco Formation of the Potomac Group and the Pleistocene Talbot Formation (Owens 1969; Thurmond 1993).

Geotechnical borings in the BRSA aid in understanding the deeper stratigraphy of Cluster 11 while the shallow monitoring wells define the near surface sediments (locations of geotechnical borings and monitoring wells shown in Figure 3). The stratigraphic cross section from the geotechnical borings is shown in Figure 4. Lithologic logs from regional borings BR-1 through BR-5 combined with palynologic analysis indicate that the top of the Cretaceous deposits vary from surface outcropping in the northwestern portion of the BRSA to approximate depths of 6 m below ground surface in the Cluster 11 area. In Cluster 11 this buried Cretaceous-Tertiary surface slopes to the south and east as a result of erosion during lowering sea levels consummate with the Pleistocene. Thus, this boundary is an erosional unconformity. The Cretaceous deposits in the study area comprise fine-medium grained quartz sands and massive red or dark grey clays. The upper Cretaceous unit in this area is composed of approximately 21 m of stiff clay which serves as an aquitard to the underlying confined aquifer system. Aside from the continuous upper Cretaceous clay the sandy lithotypes are variable in thickness and laterally discontinuous which is typical of alluvial facies sediments. Thus, these Potomac Group sediments were likely to have been deposited in a complex river system as suggested by Minard and others (1980).

Deposition during the Pleistocene consists of gravel, sand and clay deposits found associated with paleochannels eroded during low stands of sea level as a result of Pleistocene glaciation. These fluvial, estuarine and marginal-marine sediments were deposited in the channel environment during interglacial periods resulting in rising sea levels. These deposits generally consist of fluvial sediments overlain by fine grained sands and clays. Pleistocene deposits in the study area are part of the Talbot Formation. The Talbot Formation can be divided into three lithologic units. These are Unit A, composed of sand and gravel of fluvial origin containing clasts of piedmont metamorphics. Unit B is a sandy and silty clay of estuarine origin as indicated by the presence of organics and bivalve shells (see Thurmond 1993). Unit C consists of a

mixture of medium to fine grained sand and interbedded clay. The lithotypes are generally laterally discontinuous, and the sands are colored red to gray. Unit C was probably deposited in an estuarine to marginal-marine environment.

The surficial aquifer is typically overlain by a soft grey silty clay typically 3-6 m thick. The sediments of the surficial aquifer in the Cluster 11 area are dominantly fine grained sands (occasional gravel) with minor clay.

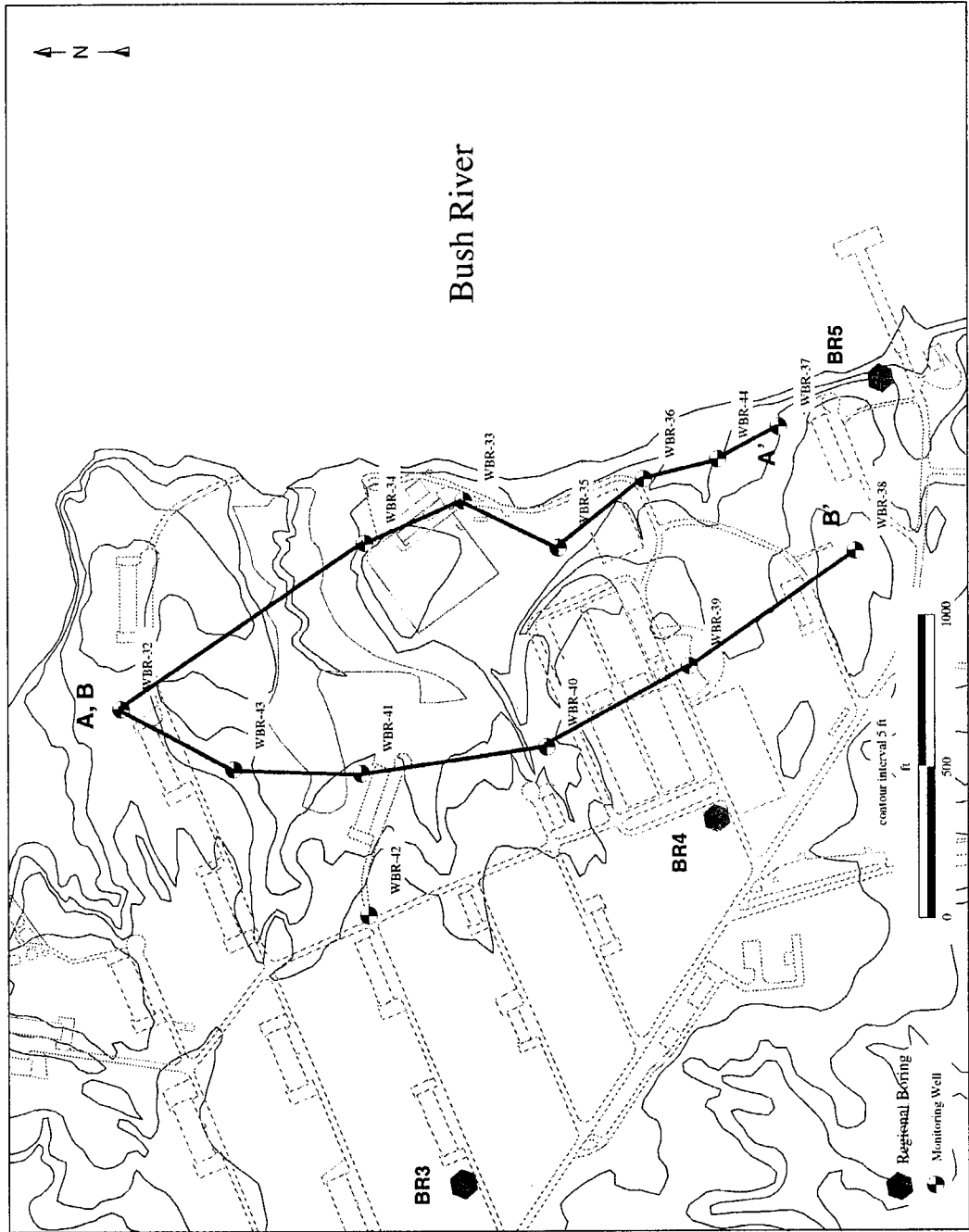


Figure 3. Location of regional borings and monitoring wells relative to the Cluster 11 area. Metric scale:
1 cm = 60 m

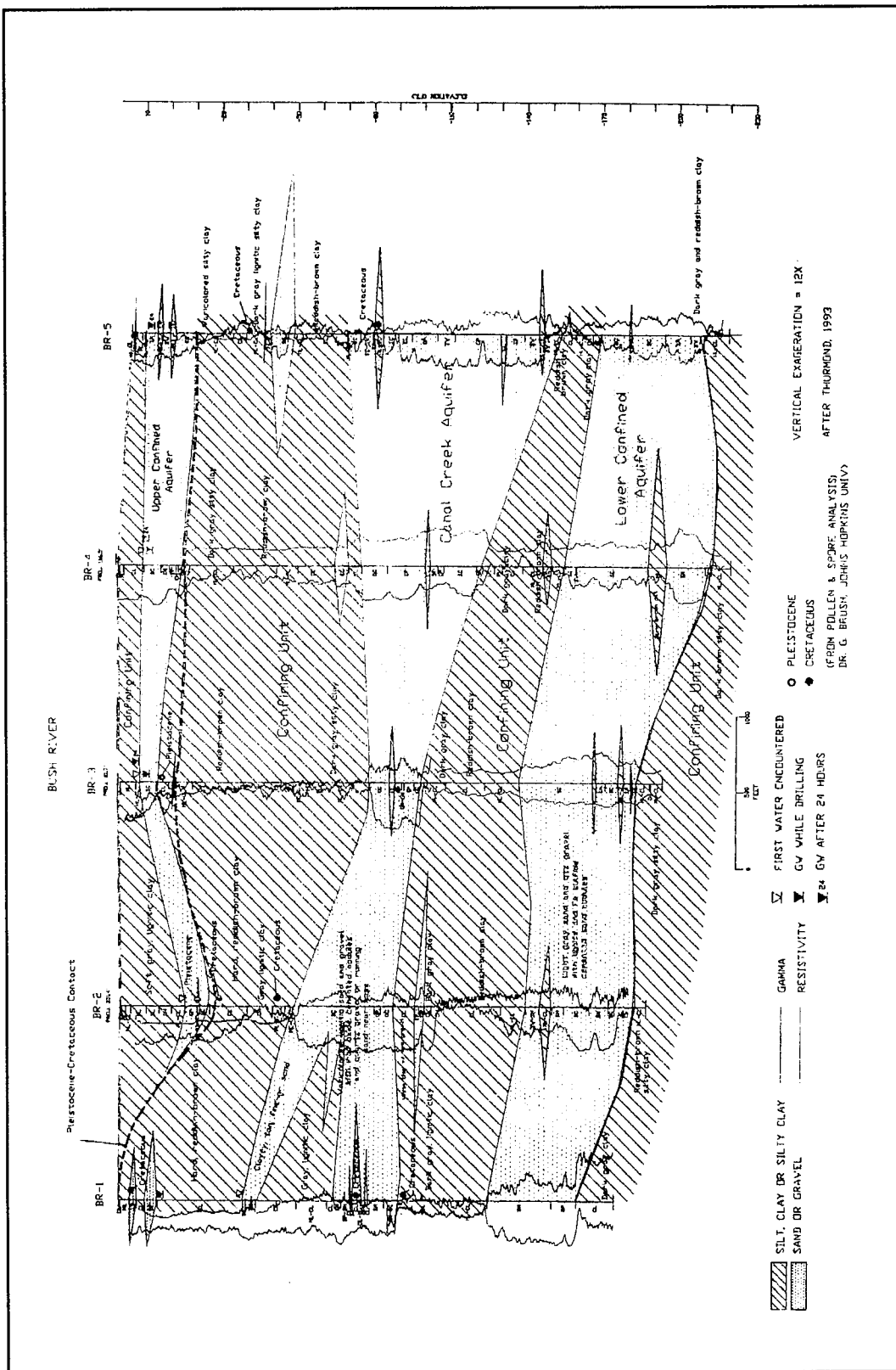


Figure 4. Stratigraphic cross section from regional borings BR-1 through BR-5, Bush River area (from Thurmond 1993). Metric horizontal scale: 1 cm = 96 m

3 Geophysical Test Principles and Field Procedures

Geophysical Test Principles

Electromagnetic surveys

The frequency EM technique is used to measure differences in terrain conductivity. Like electrical resistivity, conductivity is affected by differences in soil porosity, water content, chemical nature of the ground water and soil, and the physical nature of the soil. In fact, for a homogeneous earth, the true conductivity is the reciprocal of the true resistivity. Some advantages of using the EM over the electrical resistivity technique are (a) less sensitivity to localized resistivity heterogeneities, (b) no direct contact with the ground required, thus no current injection problems, (c) smaller crew size required, and (d) rapid measurements (McNeil 1980).

The EM equipment used in this survey consists of a transmitter and receiver coil set a fixed distance apart. The transmitter coil is energized with an alternating current at an audio frequency (kHz range) to produce a time-varying magnetic field which in turn induces small eddy currents in the ground. These currents then generate secondary magnetic fields which are sensed together with the primary field by the receiver coil. The units of conductivity are millisiemens per meter (mS/m). The EM data are then presented in profile plots or as isoconductivity contours, if data are obtained in a grid form. A more thorough discussion on EM theory and field procedures is given by Butler (1986), Telford et al. (1973) and Nabighian (1988).

There are two components of the induced magnetic field measured by the EM equipment. The first is the quadrature phase component, which gives the ground conductivity measurement. The second is the inphase component, which is used primarily for calibration purposes. However, the inphase component is significantly more sensitive to large metallic objects and hence very useful when looking for buried metal containers (Geonics, Ltd. 1984). When measuring the inphase component, the true zero level is not known since the reference level is arbitrarily set by the operator. Therefore, measurements collected in this mode are relative to a reference level and have arbitrary units of parts per thousand (ppt).

Geonics model EM-31 ground conductivity meter was used to survey the site. The EM-31 has an intercoil spacing of 3.66 m and an effective depth of exploration of about 6.1 m (Geonics, Ltd. 1984). The EM-31 meter reading is a weighted average of the earth's conductivity as a function of depth. A thorough investigation to a depth of 4.57 m is usually possible, but below that depth the effect of conductive anomalies becomes more difficult to distinguish. The EM-31, when carried at a usual height of approximately 1 m, is most sensitive to features at a depth of about 0.3 m. Half of the instrument's readings result from features shallower than about 2.74 m, and the remaining half from below that depth (Bevan 1983). The instrument can be operated in both a horizontal and vertical dipole orientation with correspondingly different effective depths of exploration. The instrument is normally operated with the dipoles vertically oriented (coils oriented horizontally and co-planar) which gives the maximum depth of penetration. The instrument can be operated in a continuous or discrete mode.

A second EM device used at the site is termed the EM-61 which is a time-domain system. The EM-61 is a high sensitivity high resolution time-domain metal detector which is used to detect both ferrous and non-ferrous metallic objects. It consists of a powerful transmitter that generates a pulsed primary magnetic field, which induces eddy currents in nearby metallic objects. The decay of these currents is measured by two receiver coils. By making the measurement at a relatively long time after termination of the primary pulse, the response is practically independent of the electrical conductivity of the ground.

Magnetic surveys

The magnetic method of surveying is based on the ability to measure local disturbances of the earth's magnetic field. Magnetic anomalies are caused by two different types of magnetism: induced and remanent magnetization. Remanent magnetization is a permanent magnetic moment per unit volume whereas induced magnetization is temporary magnetization that disappears if the material is removed from a magnetic field. Generally, the induced magnetization is parallel with and proportional to the inducing field (Barrows and Rocchio 1990). The remanent magnetism of a material depends on the thermal and magnetic history of the body and is independent of the field in which it is measured (Breiner 1973).

A GEM Systems GSM-19 'walking' magnetometer was used to measure the total field intensity of the local magnetic field. The magnetic unit of measurement is the nanotesla (nT) or gamma. One nanotesla is equivalent to one gamma. The local magnetic field is the vector sum of the field of the local magnetized materials (local disturbance) and the ambient (undisturbed) magnetic field.

The magnetometer was used with dual sensors thereby allowing the vertical gradient of the total magnetic field (TMF) to be measured. The gradient is taken by measuring the total field at a survey point using two sensors which

are fixed a small vertical distance apart (for this survey 56 cm). The difference in values between the two sensors divided by their separation approximates the gradient measured at the midpoint of the sensor spacing. Two advantages of using the magnetic gradient are that (a) the regional magnetic gradient is filtered out thus local anomalies are better defined and (2) since the two readings are taken simultaneously magnetic storm effects and diurnal magnetic variations are essentially removed (Breiner 1973). The magnetometers used in this survey have an absolute accuracy of approximately ± 1 gamma (± 1 nT). For reference, the earth's magnetic field varies from approximately 60,000 gammas at the poles to 30,000 gammas at the equator (the nominal field strength at the site is approximately 53,000 gammas).

A magnetic anomaly represents a local disturbance in the earth's magnetic field which arises from a localized change in magnetization, or magnetization contrast. The observed anomaly expresses the net effect of the induced and remanent magnetization and the earth's ambient magnetic field. Depth of detection of a localized subsurface feature depends on its mass, magnetization, shape and orientation, and state of deterioration.

Ground penetrating radar surveys

Ground penetrating radar (GPR) is a geophysical subsurface exploration method using high frequency EM waves. The GPR system consists of a transmitting and a receiving antenna. The transmitting electronics generate a very short duration high voltage EM pulse which is radiated into the ground by the transmitting antenna. The signal is reflected by materials having contrasting electrical properties back to the receiving antenna. The magnitude of the received signal as a function of time after the transmitter has been initiated is measured. The signals are then amplified, processed and recorded to provide a 'continuous' profile of the subsurface.

The transmitted EM waves respond to changes in soil and rock conditions having sufficiently different electrical properties such as those caused by clay content, soil moisture or ground water, water salinity, cementation, man-made objects, voids, etc. The depth of exploration is determined by the electrical properties of the soil or rock as well as by the power of the transmitting antenna. The primary disadvantage to GPR is its extremely site specific applicability; the presence of high-clay content soils in the shallow subsurface will generally defeat the application of GPR (Olhoeft 1984). High water contents in the shallow subsurface and shallow water tables can also limit the applicability of GPR at some sites. A general rule is that GPR should not be applied to projects in which the mapping objective is greater than 15 m in depth. For shallow mapping applications at sites with low clay content soils, GPR will generally have the best vertical and horizontal resolution of any geophysical method (Butler and Llopis 1990).

A Sensors and Software Inc. Pulse Echo IV GPR system with a center frequency antenna of 100 mHz was used to conduct the GPR surveys. The pulseEKKO antennas are resistivity damped dipolar antennas. The antenna

radiation patterns are the pattern of a half wavelength dipole. When the ground conditions are suitable, the great majority of the radiated signal is transmitted into the ground (typically 90 percent). Each antenna pair is designed to have a bandwidth to center frequency ratio of one, which implies that the antennas have useable energy over the frequency range of 50 to 150 mHz. The transmitter has a peak voltage of 400 volts with a rise time of 2.5 ns. The power radiated is very dependent on the soil conditions around the radiating antenna. From a specification point of view, the 400V transmitter delivers a peak power of 3.2 kilowatts into a 50 ohm load. The receiver electronics module digitizes the voltage at the receiver antenna connector to 16-bit resolution. The receiver electronics clip the incoming voltage at a 50 mV level. The receiver noise level is nominally around 200 microvolts for a single stack. The present receiver resolution for a single bit after A/D conversion is 1.5 microvolt. The received signal was displayed on a laptop computer screen during the survey to allow the operator to check data quality. The received signal was also recorded on the computer's hard disk for future processing. By recording a vertical intensity modulated scan for every 0.3 m of antenna travel, a continuous profile is developed showing reflections from subsurface strata and anomalies within the strata. A near-horizontal geologic interface, for example, will appear as a near horizontal line or band on the GPR record. A small localized object, such as a buried metallic object will appear as a hyperbolic-shaped event centered over the object's location.

Electrical resistivity surveys

The electrical resistivity survey method allows for the investigation of the electrical properties of subsurface materials from the ground surface. When a current is introduced into a homogeneous earth through a pair of electrodes, the current radiates out through the ground from one electrode and current paths converge on the second electrode through which current leaves the ground. In a homogeneous earth model, the potential drop will be equal for all points equidistant from the point of current entry or exit. Differences in the electrical properties of the underlying materials perturb the distribution of the equipotential surface. In the resistivity method a known current is introduced in the ground by means of two electrodes emplaced in the ground and a potential difference is measured at two other electrodes. Earth resistivity is calculated from the current (known) and the potential difference (measured) using Ohm's Law. The objective of the electrical resistivity surveys is the determination of the electrical resistivity or variations in resistivity of subsurface geological materials.

One type of resistivity survey was conducted at the site, vertical electrical sounding. In the vertical electrical sounding technique the resistivity of the material as a function of depth is obtained below a given point on the earth's surface. In conducting a sounding, four electrodes are implanted at a fixed distance with the inner electrodes spacing termed "m" and the outer electrode spacing termed "n". Current is injected into the ground through the outer electrodes and read at the inner electrodes. The outer electrodes are advanced

in a logarithmic fashion while the inner electrodes remain constant thereby increasing the "n" spacing. Eventually a point is reached where the inner electrode "m" spacing is increased. By steadily increasing the "m" and "n" spacing, deeper and deeper depths of investigation can be obtained.

Surface seismic surveys

A sudden disturbance, or displacement, occurring at a small localized region in the earth will propagate outward from its origin. This displacement propagates as a spherical wavefront and eventually arrives at distant points where it can be recognized by the motion it induces in the materials present. This is the basis for seismic exploration. This disturbance in the earth can occur on the surface (an object impacting the ground) or in the subsurface (an earthquake). It is possible for two types of waves to be transmitted by this mechanism. One type of wave is transmitted by particle movements back and forth along the direction of propagation of the wave and is referred to as a longitudinal wave. The other type is termed a transverse wave, because particle motions are transverse to the direction of movement of the wavefront, or perpendicular to the ray. The particle motions that transmit longitudinal waves consist of a series of compressions and dilations. These waves are usually termed P-waves for compression or primary, since they are the fastest waves and the first to arrive at a specific location. As a transverse wave is moving through material, particles are subjected to shearing stresses as adjacent points move in a plane at right angles to the direction of propagation of the wave. These waves are termed S-waves for shear or secondary waves (they arrive after the P-waves).

Seismic waves will reflect and refract as they travel through sediment or rock and encounter surfaces bounding materials with different elastic coefficients and densities. This gives rise to two types of surface seismic surveys, seismic refraction and seismic reflection. In this report we will be concerned with the seismic reflection technique. When a wavefront traveling with velocity V_1 strikes an interface, it creates a disturbance that spreads outward both into the upper and lower materials. The disturbances into the upper material are the seismic reflections.

In conducting a seismic reflection survey, energy is imparted at or near the ground surface. This energy is usually produced by a small explosive source such as a shotgun shell, or by impacting the ground with a hammer blow or drop weight. The resulting waves activate sensors, termed geophones, placed at intervals along the surface. These waves arriving at the sensors are recorded as a function of time from energy source.

Field Procedures

Land surveys

The area to be investigated was initially established and subdivided into smaller areas based upon physical constraints. The Cluster 11 area was divided into six sites, shown in Figure 2. Site 1 was the wooded area just west of the 22nd street landfill and north of Building E2314. The site is approximately 122 m by 46 m in size and was gridded with stakes placed throughout the area on 6.1 m centers. Figure 5 is a map of the site showing the locations of the grid and locations where data were obtained. Although the grid was established on 6.1 m centers, data were obtained on 3.05 m centers. The grid stations were marked by implanting polyvinyl chloride (PVC) stakes into the ground. PVC stakes were used to prevent any possible interference with the geophysical tests conducted at the site. This gridding and data collection method was used for all the sites at Cluster 11.

Site 2 was the large open area where the major portion of landfilling activity supposedly occurred. The gridded site is shown in Figure 6 and is approximately 265 m by 187 m in size. A thick coverage of phragmites had to be removed from part of the area before surveying could be accomplished.

Site 3 is located west of the rad yard in a large open field. This site may have also been part of the landfilling activity associated with 22nd street. The gridded site, shown in Figure 7, is approximately 122 m by 91 m in size. There is a meteorological station located in the approximate center of the site with three associated support wires and anchors.

Site 4 consists of the area associated with the radioactive material disposal facility. The gridded site is shown in Figure 8. Overall area is approximately 152 m by 100 m. There are five buildings in the surveyed area in addition to two areas which contain railroad lines. These two areas were not gridded or surveyed. The entire area is surrounded by a chain link fence. The area also contains a metal vault of unknown origin or contents.

Site 5 is located southeast of Site 4 and is also surrounded by a chain link fence. The gridded site, shown in Figure 9, is approximately 76 m by 92 m in size. The site contains two small buildings, a concrete catch basin, an underground storage tank, and a gravel road extending the total length of the site.

Site 6 is located just north of the old power plant building that is now abandoned. The gridded site, shown in Figure 10, is approximately 76 m by 107 m in size. The site is bounded to the west by an earthen berm that stands approximately 6.1 m high. The north and east sides of the site are bounded by a chain link fence.

Each site was investigated based on the objective for that particular area. Since one of the objectives was to determine the presence of man-made

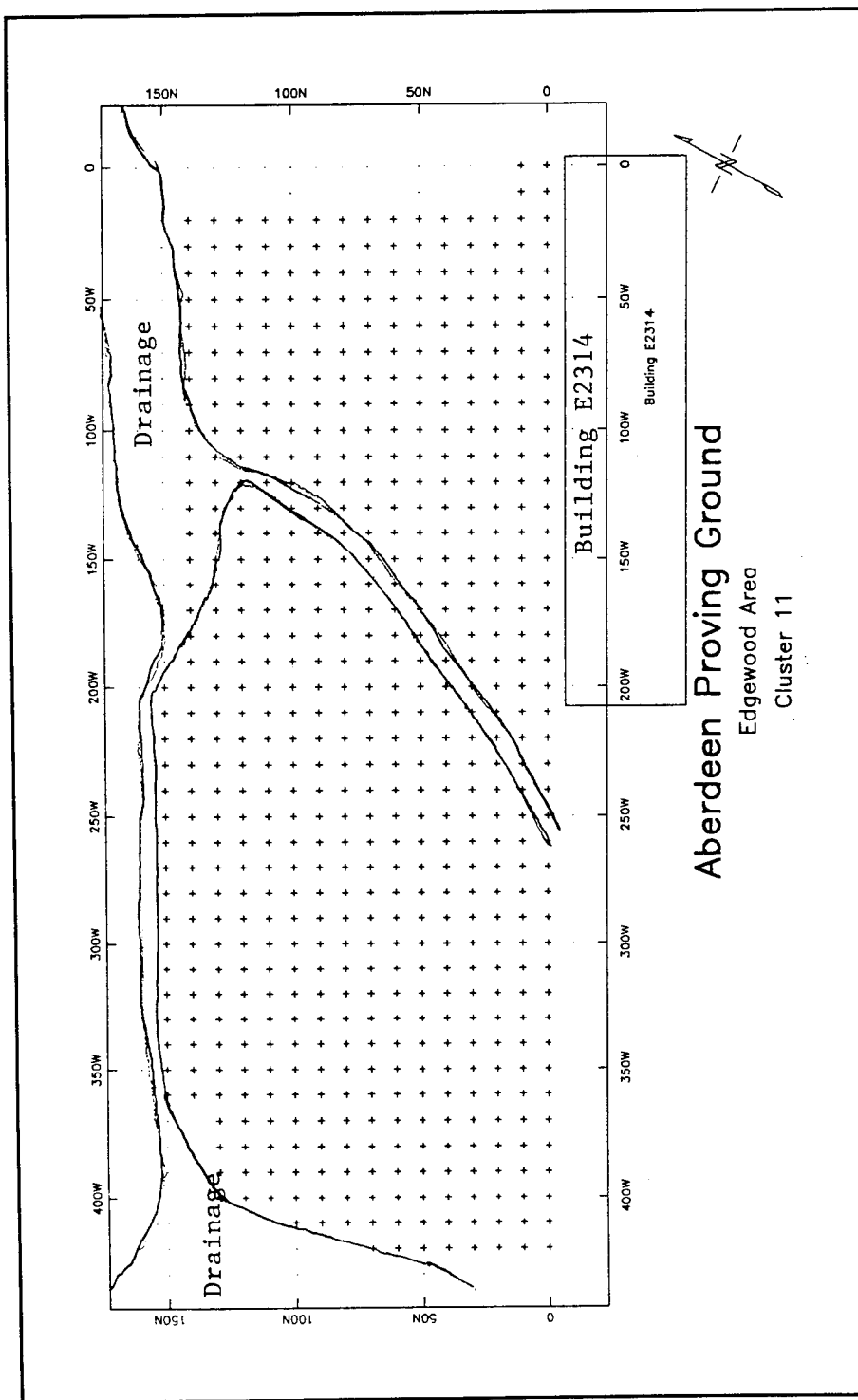


Figure 5. Grid map for Site 1 geophysical investigation. Stations are gridded at 10 ft (3 m) intervals

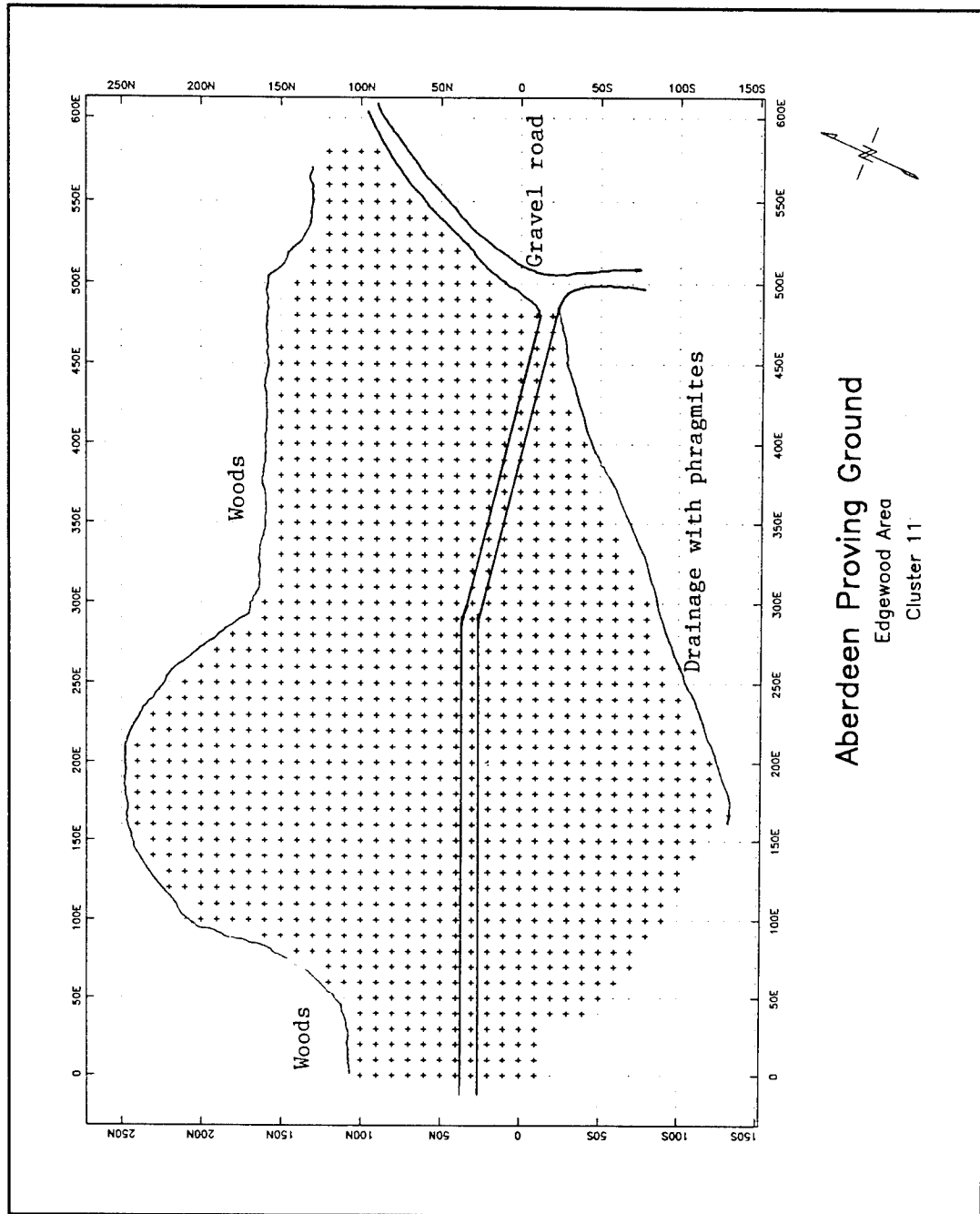


Figure 6. Grid map for Site 2 geophysical investigation. Stations are gridded at 10 ft (3 m) intervals

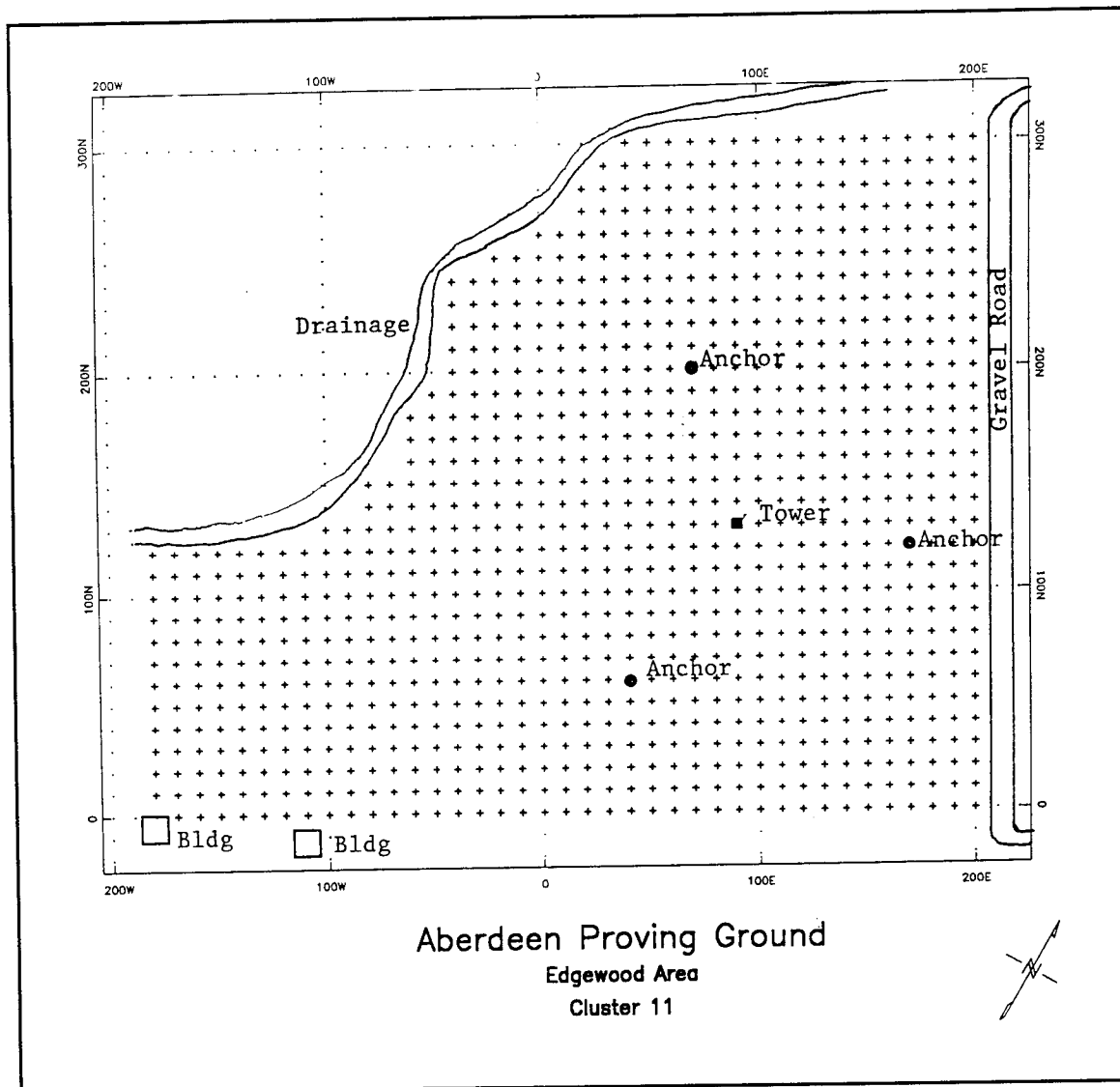


Figure 7. Grid map for Site 3 geophysical investigation. Stations are gridded at 10 ft (3 m) intervals

materials that may have been buried at the sites, all six sites were investigated with the magnetometer and EM-31. These instruments combined give an indication of subsurface materials that would show a metallic or conductivity contrast to the insitu materials. Sites 2, 3, and 6 were also surveyed with the EM-61, which would aid in the determination of subsurface metallic and non-metallic objects. Sites 1, 4, and 5 were not surveyed with the EM-61 due to the physical constraints associated with them (trees, buildings, railroad lines, fences, etc.). Sites 2, 3, and 6 were also surveyed with the seismic reflection and GPR methods to aid in the determination of geological conditions. Site 2 had a limited amount of resistivity soundings performed, to aid in geological characterization.

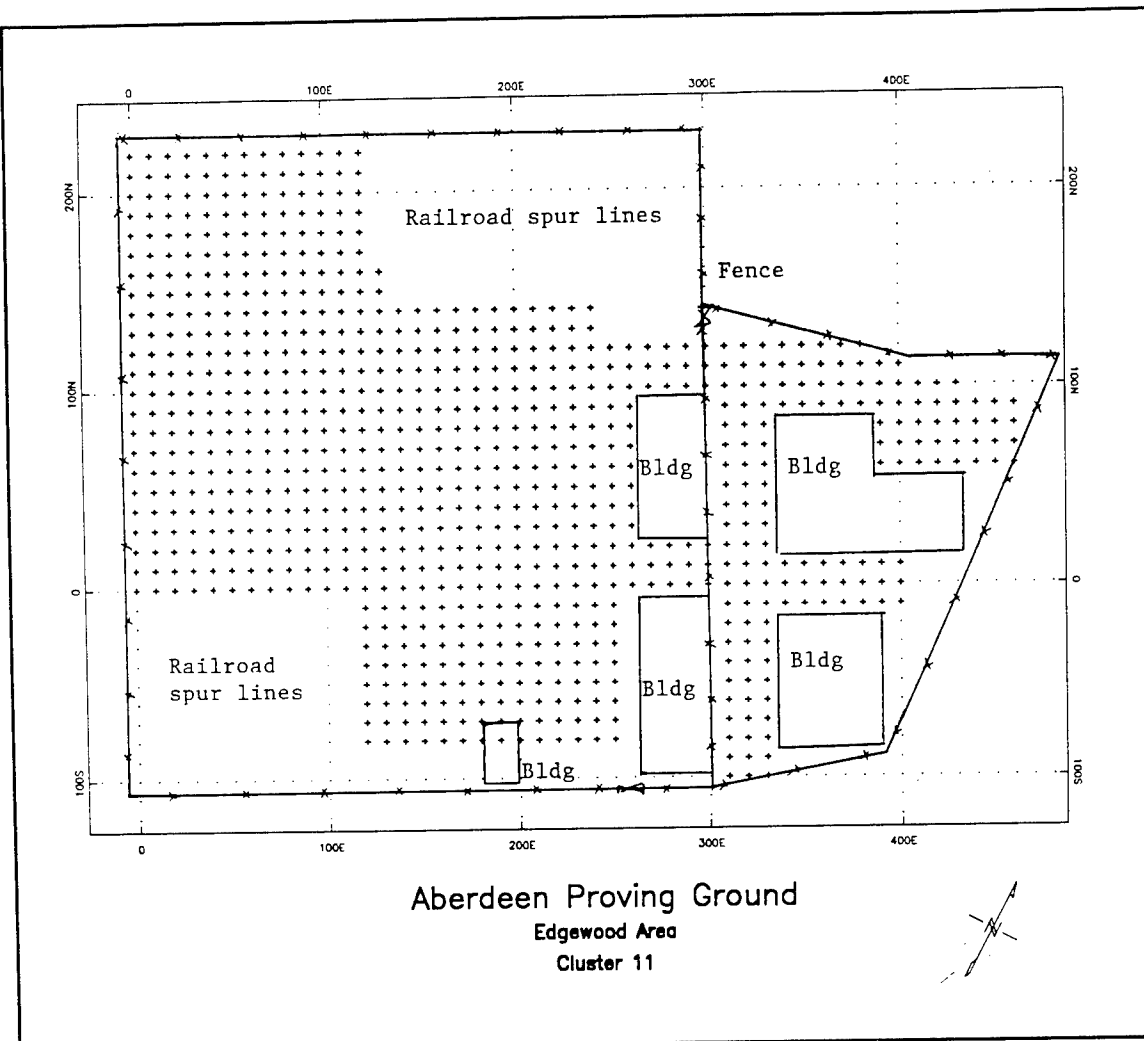
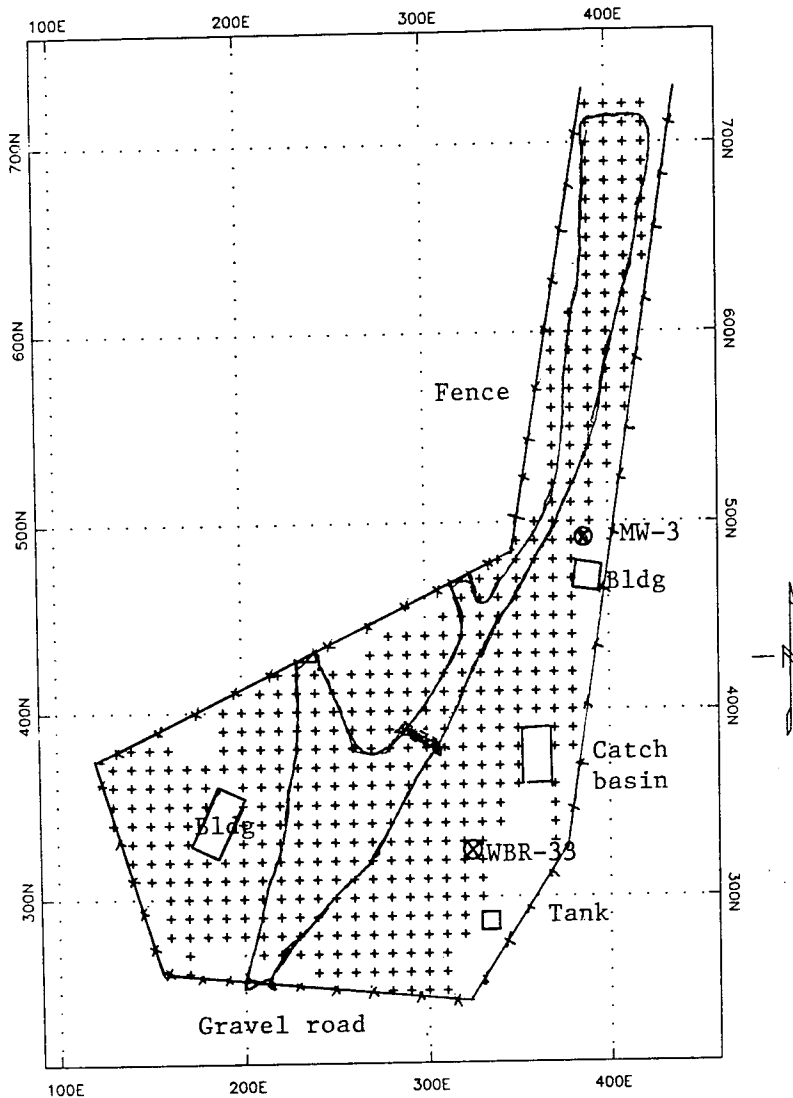


Figure 8. Grid map for Site 4 geophysical investigation. Stations are gridded at 10 ft (3 m) intervals

Offshore surveys

The area along the shoreline from the old WWII pier to Eagle point was also surveyed, utilizing a small nonmetal boat. The grid for this area is shown in Figure 2. The grid was established on 30.5 m centers using small diameter PVC pipe for station markers. The survey was designed to stay as close to shore as possible and extend out from the shoreline 61 m. The area was divided into two grids based on the orientation of the shoreline. The first grid extended from the WWII pier to the pier associated with the old power plant building. This grid was 61 m wide and 274 m long. This area was surveyed with the EM-31 and cesium magnetometer. The cesium magnetometer is very similar to the magnetometer discussed in the magnetic survey, geophysical test principles section of this report. The major difference being the source that excites the sensors in the magnetometer. The second grid extended from the old power plant building pier to just south of Eagle point.



Aberdeen Proving Ground

Edgewood Area

Cluster 11

Figure 9. Grid map for Site 5 geophysical investigation. Stations are gridded at 10 ft (3 m) intervals

The grid was 61 m wide by 396 m long. This area was also surveyed with the EM-31 and cesium magnetometer.

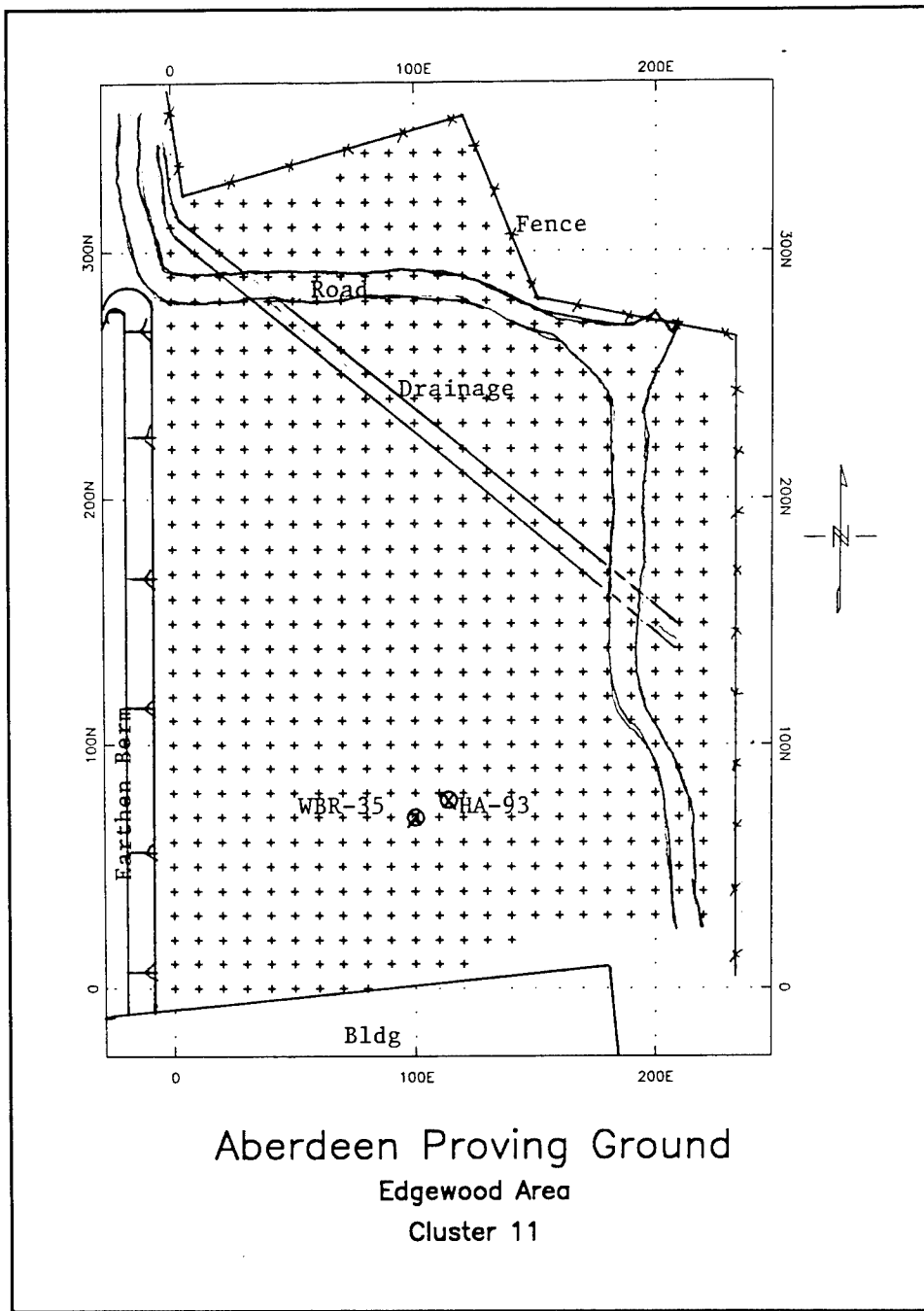


Figure 10. Grid map for Site 6 geophysical investigation. Stations are gridded at 10 ft (3 m) intervals

4 Test Results and Interpretation

In deciding what constitutes significant anomalies for a particular site several factors must be weighed. Anomaly detection is limited by instrument accuracy and local "noise" or variations in the measurements caused by factors not associated with the anomalies of interest such as fences, power lines, steel rails, etc. (cultural noise). For the anomaly to be discernible or detectable, the measurement attributed to the anomaly must have a response greater than that caused by the interfering cultural noise. Since the anomaly amplitude, spatial extent, and wavelength are the keys to detection, the size and depth of the feature causing the anomaly are important factors in determining detectability and resolution. The intensity of the anomaly is also a function of the degree of contrast in material properties between the anomaly and the surrounding material.

The results of the TMF, magnetic gradient, EM-31 conductivity, EM-31 in-phase, and EM-61 data collected for each site are presented as contour maps of the measured parameter. The color coded contour maps show a two-dimensional representation of the data with hot colors (reds) indicating areas with relatively high values and cold colors (blues) showing areas with relatively low values. The electrical resistivity data are presented as profile plots. The GPR data and seismic reflection data are presented as depth sections for each line surveyed. In both cases the actual data are recorded as time sections and later converted to depth sections based on a knowledge of the subsurface velocities.

Site 1 Results

The portion of Cluster 11 designated as Site 1 was shown in Figure 5. The results of the EM-31 survey are shown in Figures 11 and 12. Figure 11 shows the results of the conductivity survey, with data contoured every 2 mS/m. Typical background values for this area are 14 to 18 mS/m. Areas that are considered as anomalous would have values that deviate significantly from the background, either high or low, and are not associated with known surface features. There is a high area in the southeast section of the grid from station 0W to 200W. This area is associated with Building E2314. There is

also a high area centered around station 150W, 140N, associated with a concrete drainage structure, and station 20W, 110N associated with a metal post. There is one area not associated with any surface feature at station 50W, 50N. The results of the inphase survey are shown in Figure 12. The data are contoured every 1 ppt. From this survey, the same areas appear anomalous as did those from the conductivity survey with the exception of station 150W, 140N and station 50W, 50N.

The results of the magnetometer survey are shown in Figures 13 and 14. Figure 13 shows the results of the total field survey, with contours every 50 gammas. Typical background values for this area are approximately 53,700 gammas. Normally, magnetic anomalies from metallic objects will have a high and associated low that align in the direction of true north. For example the area at station 20W, 110N has a high and associated low as does the anomaly at station 0W, 70N. The effect of the building is seen as a large magnetic low (0N, 0 - 225 W) with no associated high. The results from the magnetic gradient survey are shown in Figure 16, with contours every 25 gammas/m. Although it might appear as if the entire area is covered with anomalies, in actuality the yellow and green values do not deviate very much from zero and can be considered as typical background values. Careful observation of the plot will reveal the same areas as the total field survey indicated as anomalous.

Based on the findings from all the surveys conducted in this area, the following interpretation can be drawn. The building clearly affected each survey and in effect masks any other results that might have been obtained in the area near the building. The area at station 50W, 50N only appeared in the conductivity survey, which indicates that there is no metallic object associated with this area. This spot is a low area where water is collecting and therefore conductivity values are increased. The remaining anomalous areas at the site can all be attributed to surface features. The anomalies detected at this area are summarized in Table 1.

Site 2 Results

The Site 2 grid layout and surface features was shown in Figure 6. The results of the EM-31 survey are shown in Figures 15 and 16. Figure 15 shows the results of the conductivity survey, with contours every 5 mS/m. There is a stark contrast in the conductivity values between the eastern and western sections of the plot. The values in the western section range from 10 to 20 mS/m whereas those in the eastern section range from 60 to 120 mS/m. These values are much higher than would normally be associated with typical silty clay materials. The values in the western section, 10 to 20 mS/m, are more typical of expected conductivities. There is also a clear demarcation between the two sections at approximate location 150E. The eastern section of the plot also contains many isolated highs and lows. There is one clear anomaly in the western section at location 10E, 80N which corresponds to the metal post mentioned in the Site 1 results. The results of the

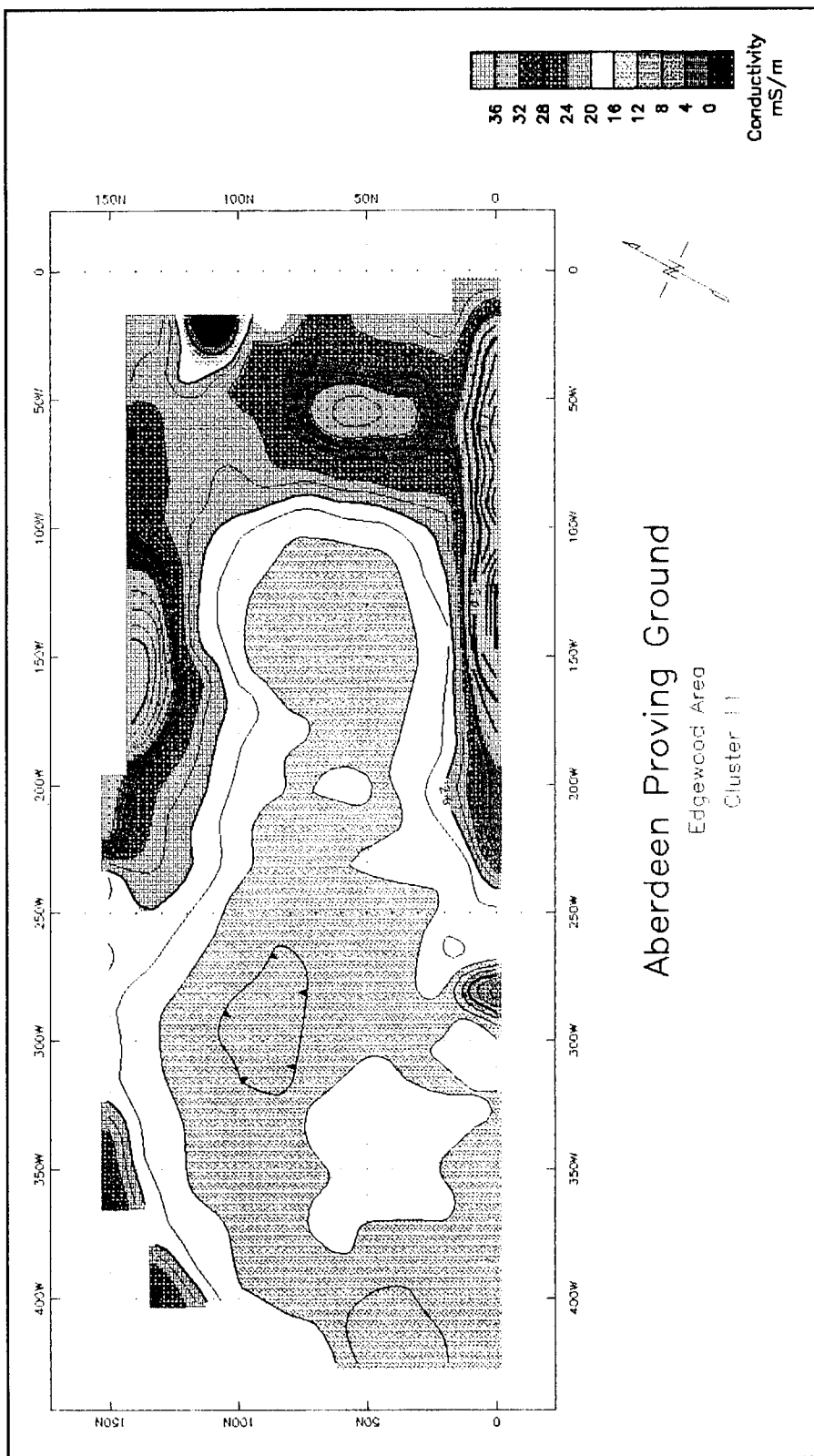


Figure 11. EM-31 conductivity survey for Site 1. Contours are 2 mS/m. Station intervals are 10 ft (3 m)

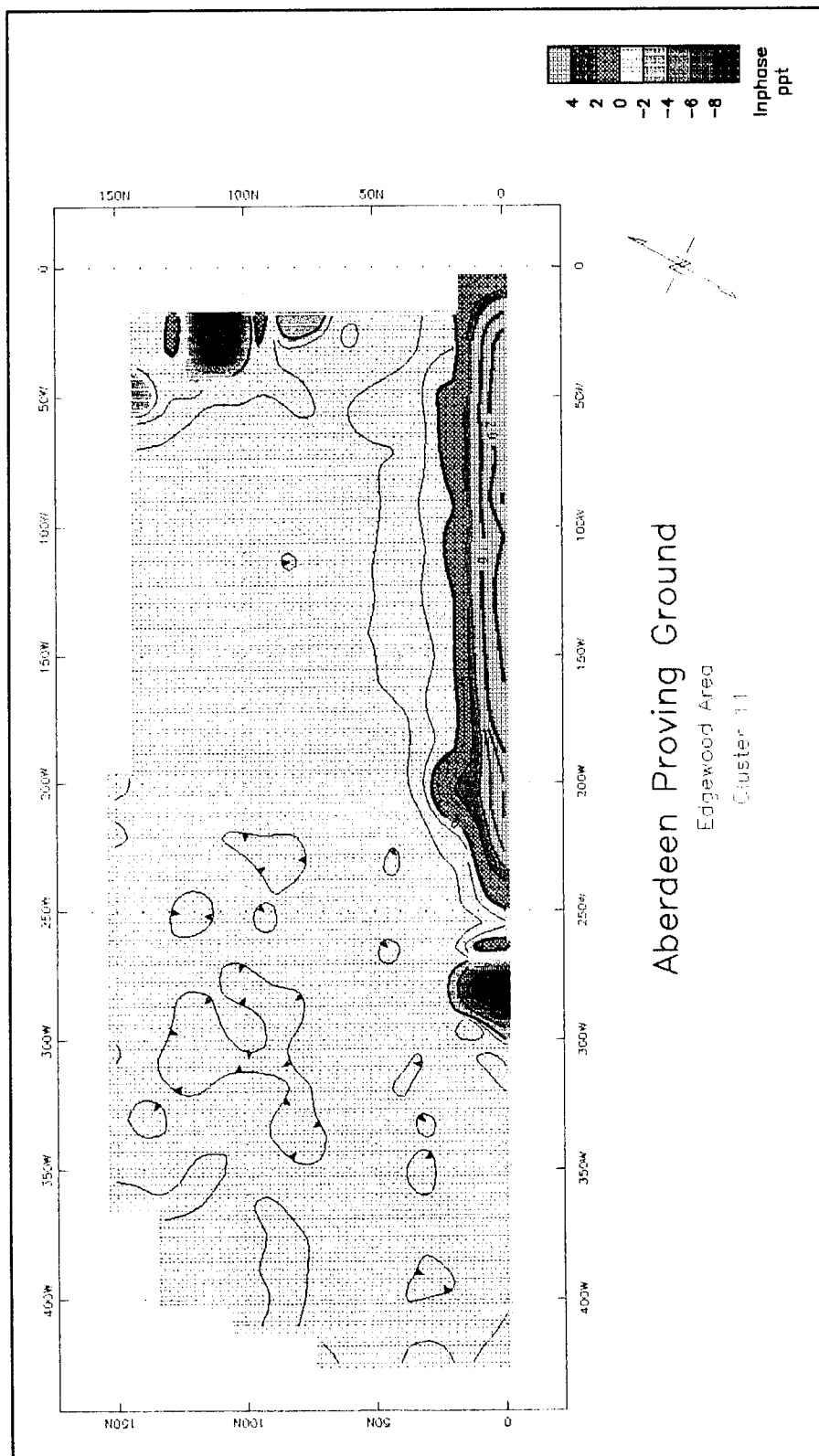


Figure 12. EM-31 inphase survey for Site 1. Contours are 1 ppt. Station intervals are 10 ft (3 m)

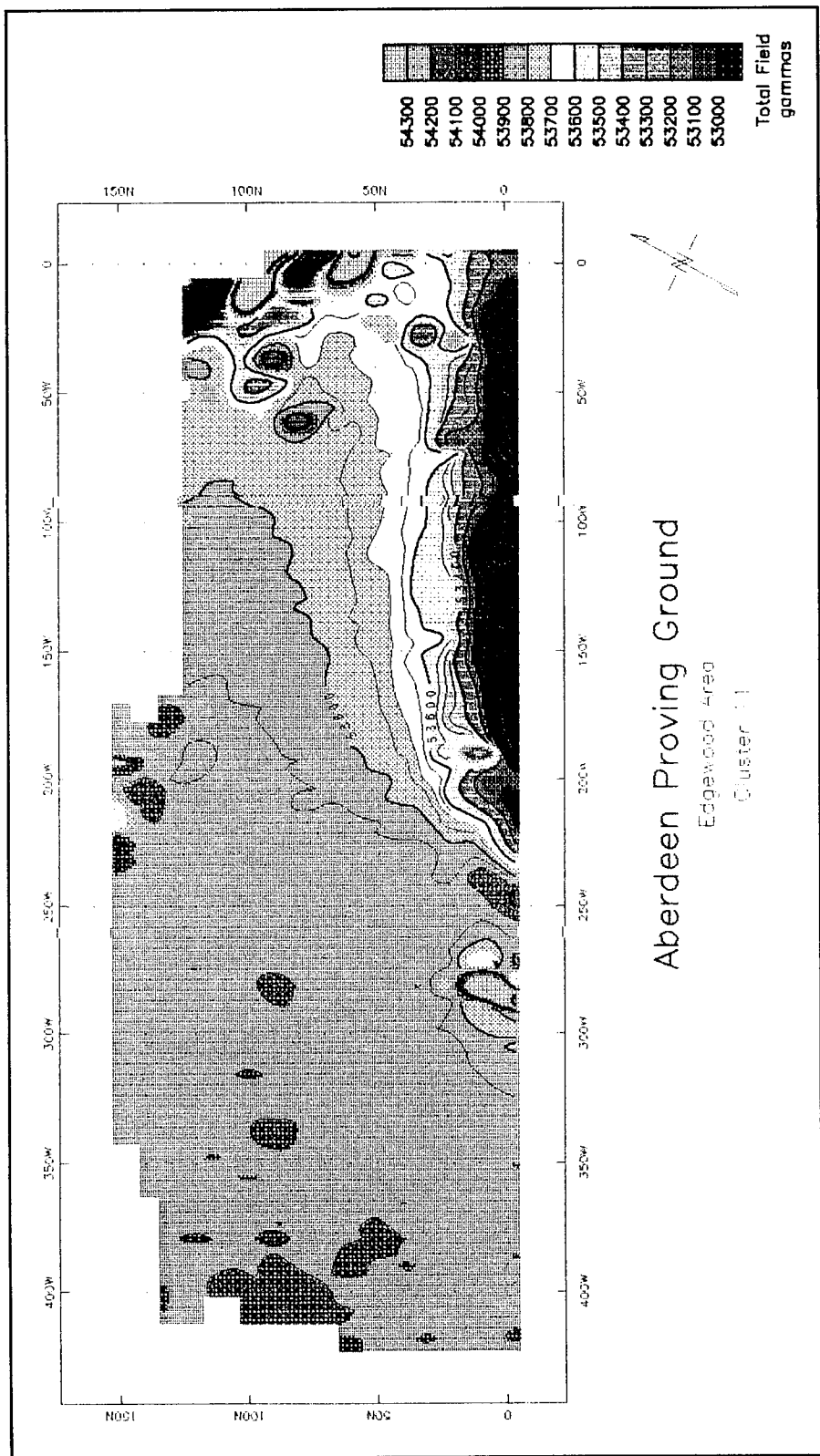


Figure 13. Magnetic total field survey for Site 1. Contour intervals are 50 gammas, and station intervals are 10 ft (3 m)

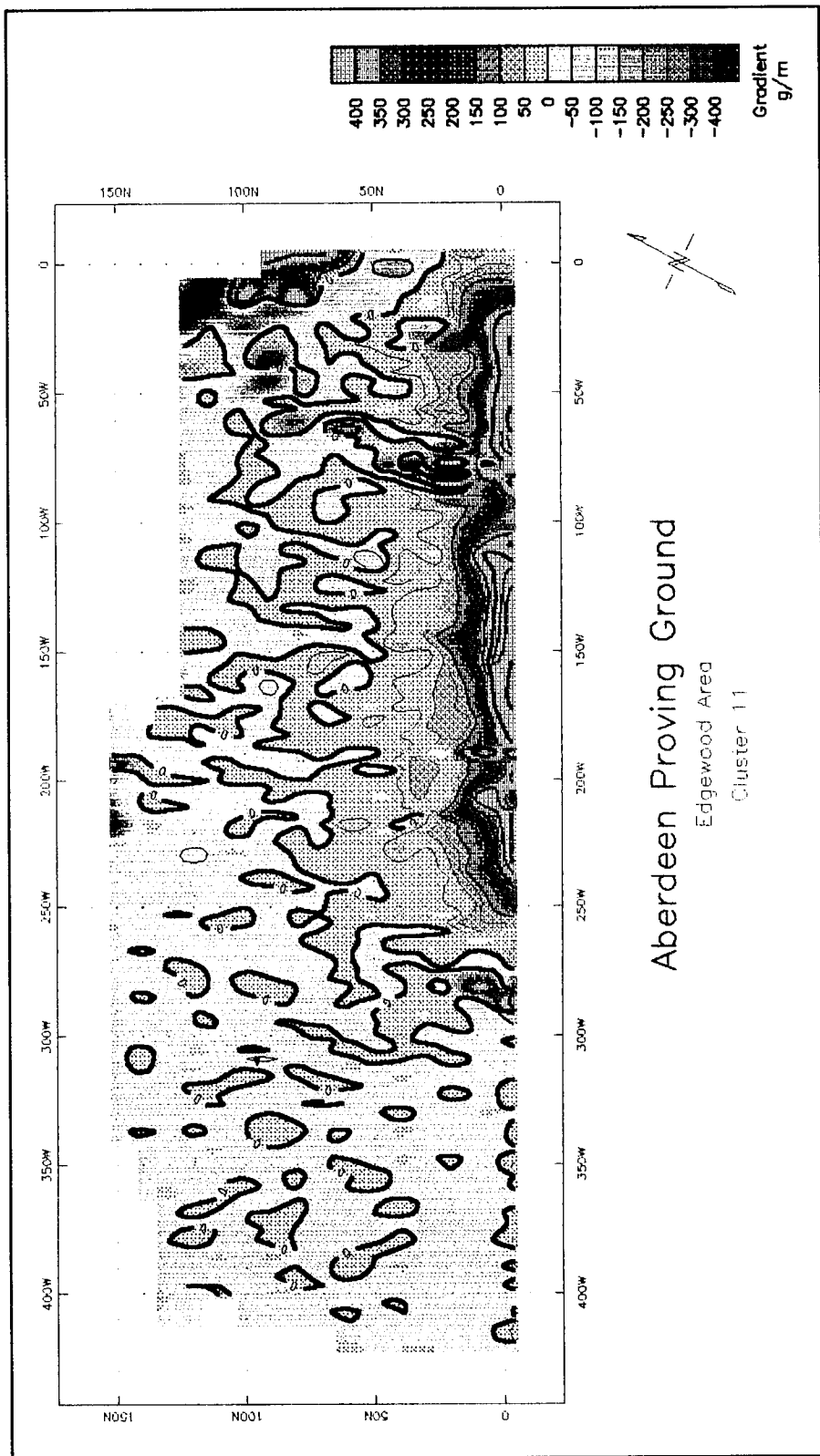


Figure 14. Magnetic gradient survey for Site 1. Contours are 25 gammas/m. Station intervals are 10 ft (3 m)

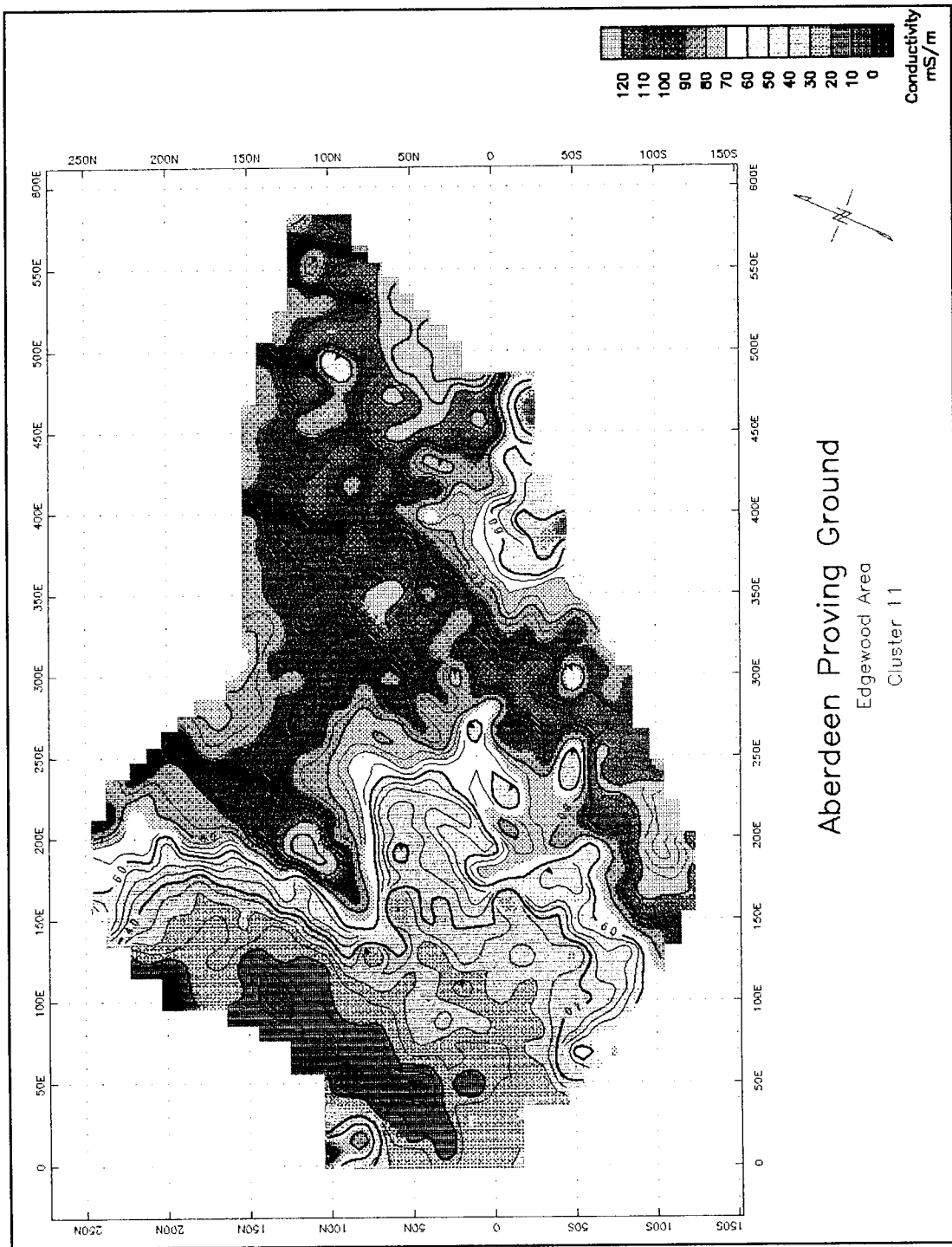


Figure 15. EM-31 conductivity survey for Site 2. Contours are 5 mS/m, and station intervals are 10 ft (3 m)

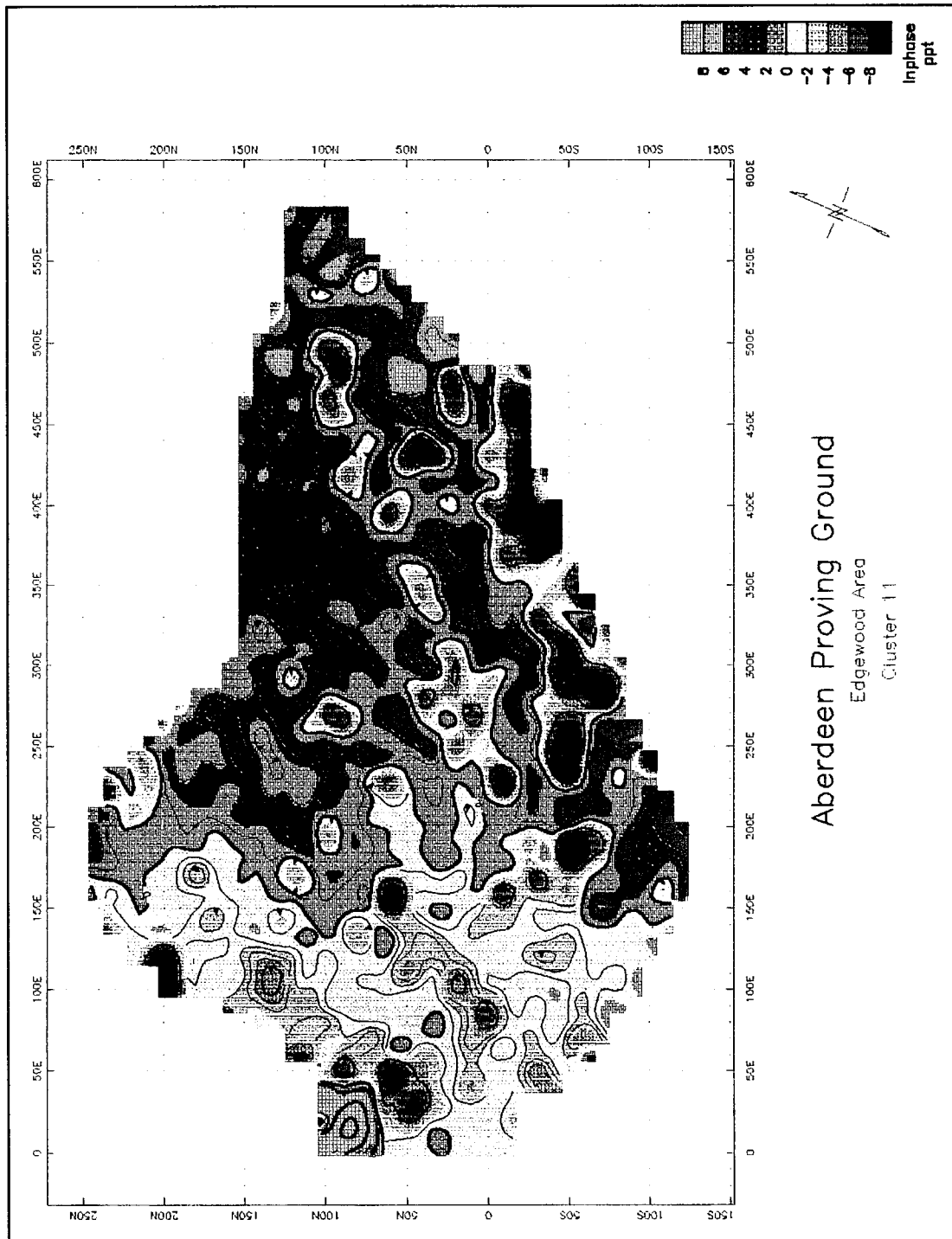


Figure 16. EM-31 inphase survey for Site 2. Contours are 1 ppt, and station intervals are 10 ft (3 m).

Table 1
Anomalies Detected at Site 1

Anomaly	Location	Type	Cause
1	25W,110N	conductive, magnetic	metal post
2	50W,50N	conductive	soil conditions
3	10-250W,0-5N	conductive, magnetic	building
4	150W,130N	conductive, magnetic	concrete
5	280W,10N	conductive, magnetic	metal sign

inphase survey are shown in Figure 16, with contours every 1 ppt. The results are exactly as stated for the conductivity survey. Although not as clear from the inphase survey as the conductivity, there is a linear trend in a north-easterly direction through the eastern section from 150E, 100S to 450E, 100N.

The results of the magnetometer survey are shown in Figures 17 and 18. Figure 17 shows the results of the total field survey, with contours every 250 gammas. Typical background values for this area probably range around 53,500 gammas. There are numerous anomalies scattered throughout the area. The anomalies are too numerous to enumerate, but can be easily recognized by the small closed contours with values greater than 54,500 gammas (purple to pink colors) or less than 52,500 gammas (blue areas). Similar results can be seen in the magnetic gradient plot shown in Figure 18.

The results of the EM-61 survey are shown in Figures 19 through 21. Figure 19 is a plot of the results from the bottom coil of the instrument. Figure 20 a plot of the results from the top coil and Figure 21 a plot of the difference between the readings of the two coils. These results also indicate the presence of many anomalies. However, this instrument tends to present a 'cleaner' picture of the anomalies. Many of the smaller more isolated targets are not seen in this plot.

Based on the findings from all the surveys conducted in this portion of the Site 2 area, the following interpretation can be drawn. The conductivity values in this area are not typical of values expected for material natural to this area. This is an indication that the material is most likely fill material. The presence of a large number of magnetic anomalies, indicated from the other surveys, serve to enhance the interpretation that the area is indeed indicative of a fill. The linear trending feature, most apparent in the conductivity survey, could either be associated with an old drainage path, or possibly a trench. The anomalies detected at this area are too numerous to put into a table.

Based on the findings from all the surveys conducted at Site 2, the interpretation that this area is almost certainly a part of a landfill area can be drawn. The high conductivity values and large number of magnetic anomalies would tend to support this conclusion.

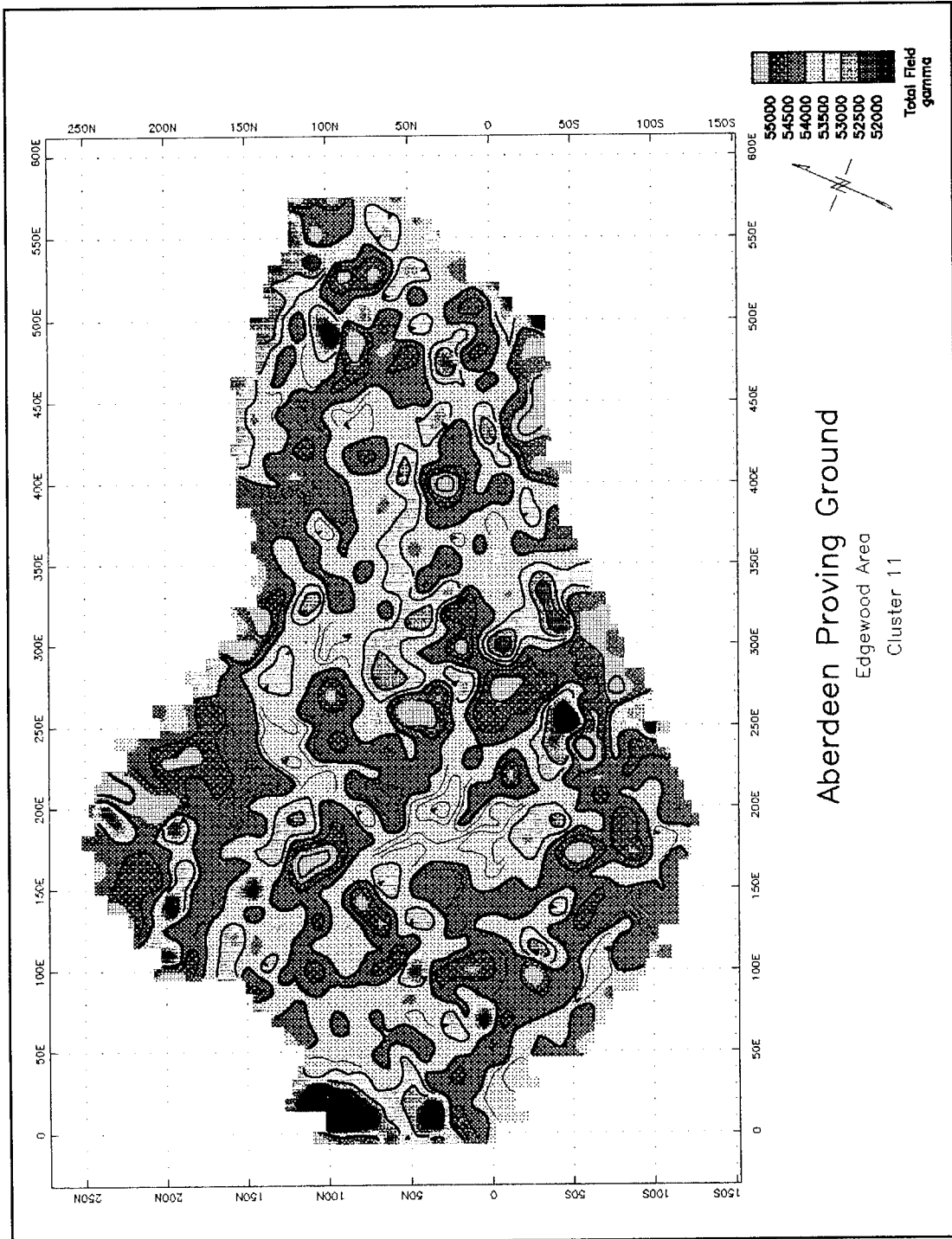


Figure 17. Magnetic total field survey for Site 2. Contours are 250 gammas, and station intervals are 10 ft (3 m)

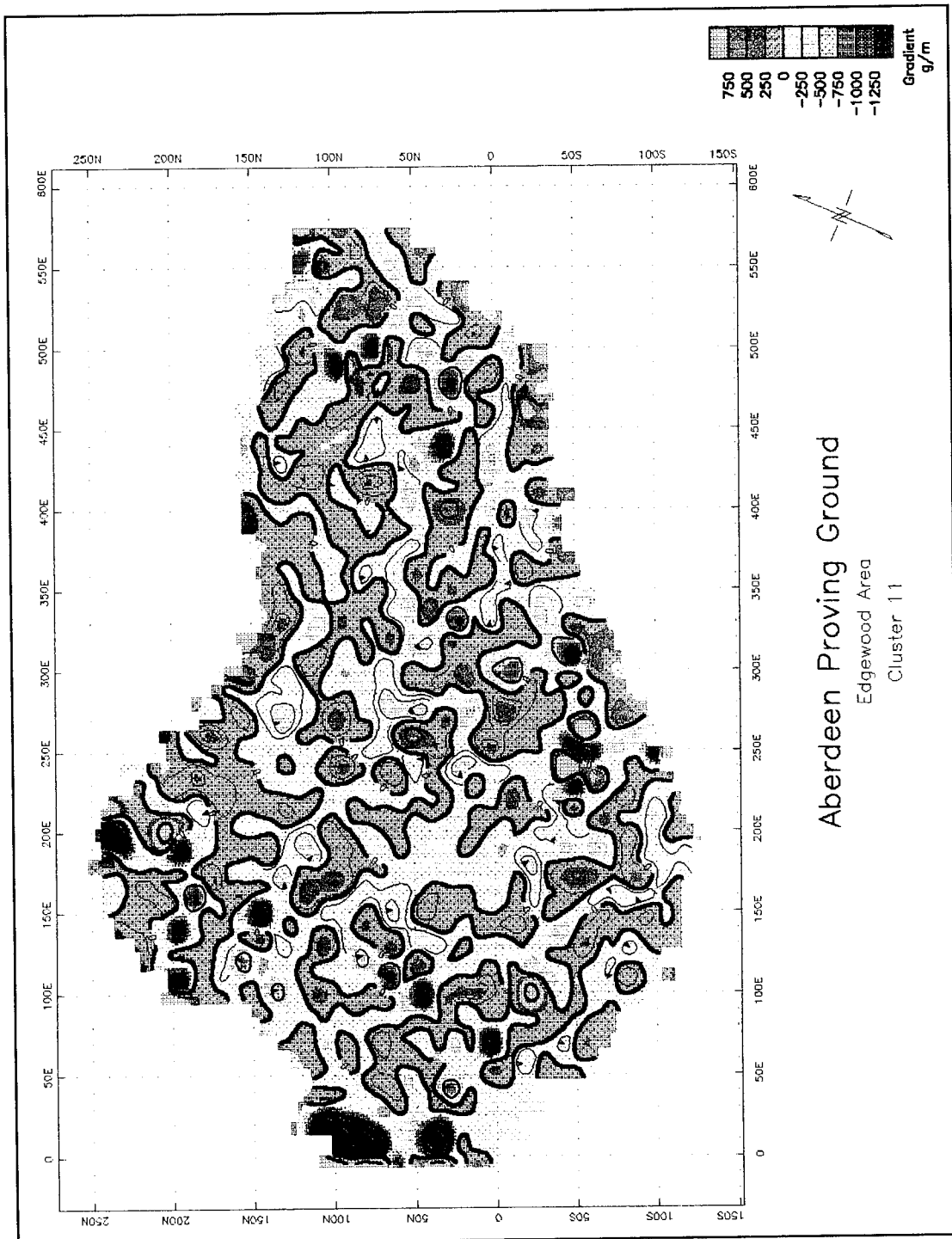


Figure 18. Magnetic gradient survey for Site 2. Contours are 125 gammas/m, and station intervals are 10 ft (3 m)

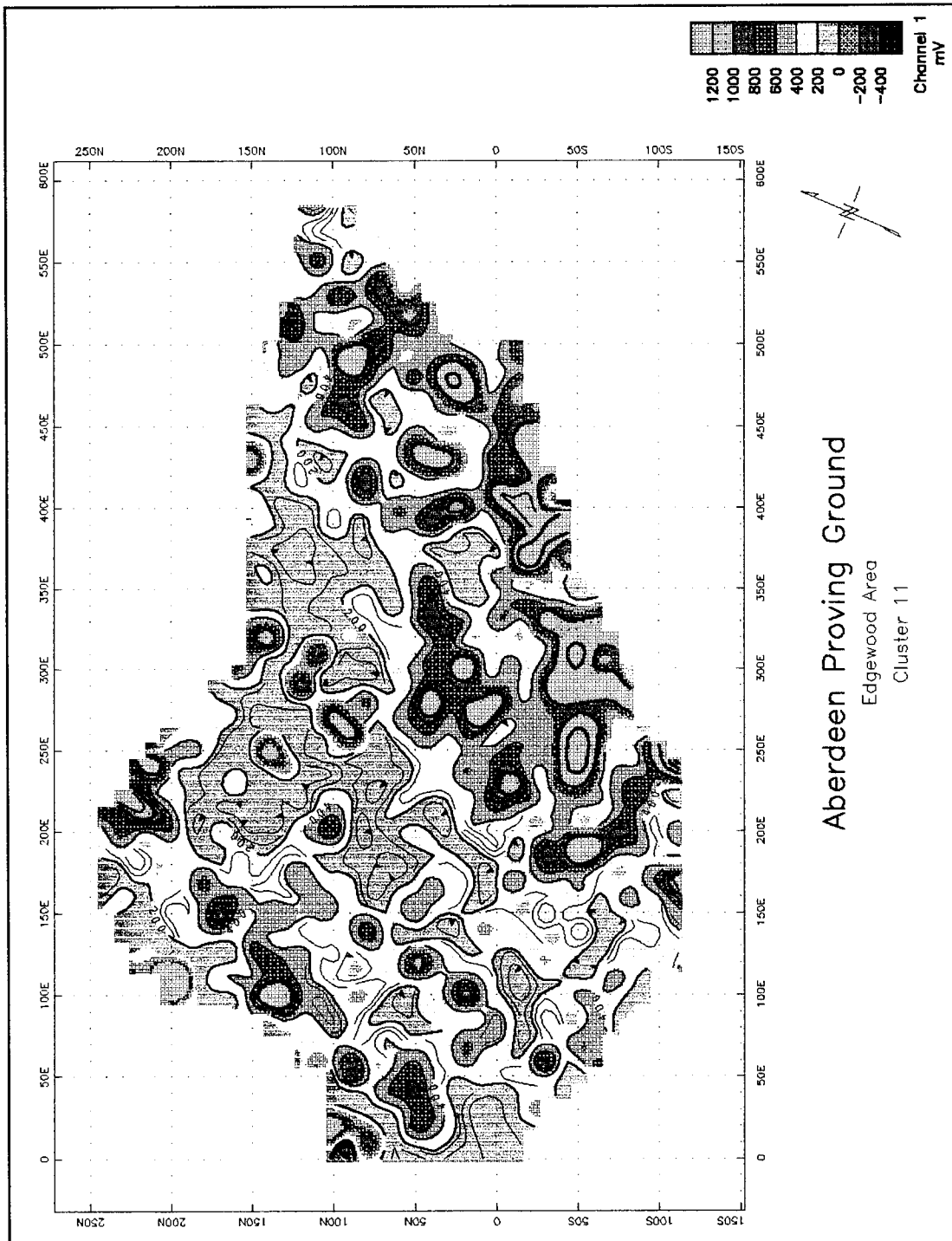


Figure 19. EM-61 bottom coil survey for Site 2. Contours are 100 mV, and station intervals are 10 ft (3 m)

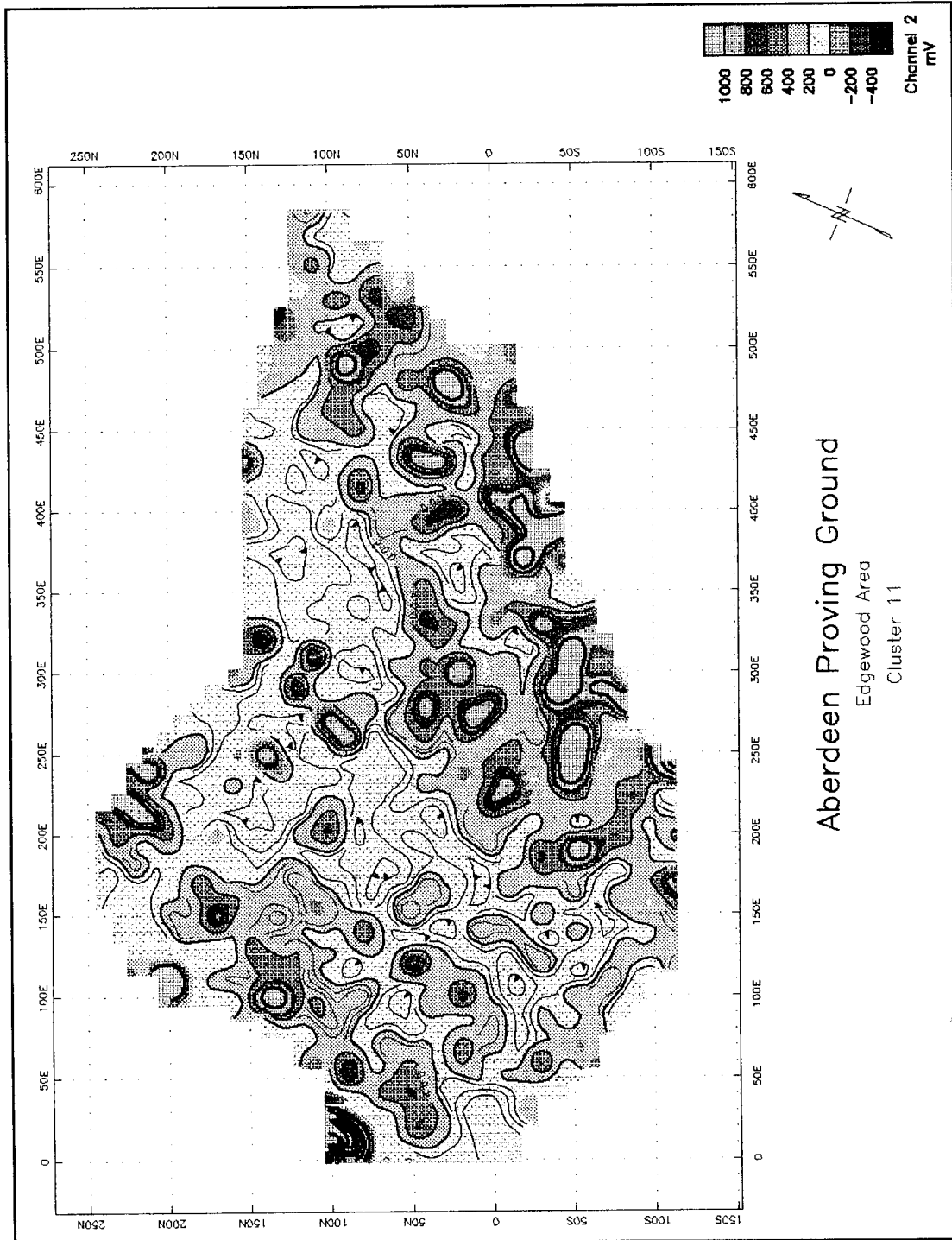


Figure 20. EM-61 top coil survey for Site 2. Contours are 100 mV, and station intervals are 10 ft (3 m)

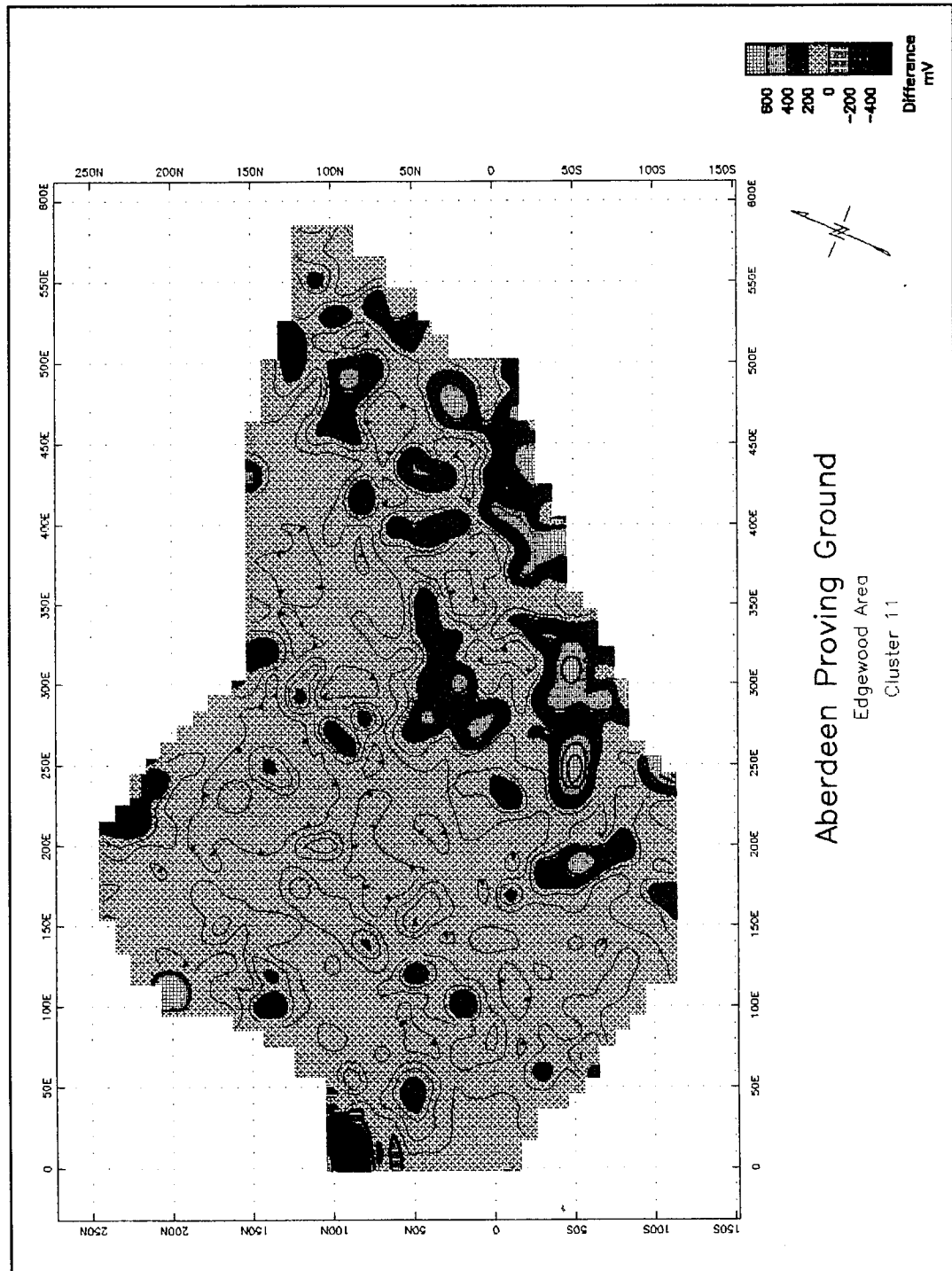


Figure 21. EM-61 difference between top and bottom coils survey for Site 2. Contours are 100 mV, and station intervals are 10 ft (3 m)

To assist in the geologic characterization of the site, seismic reflection and electrical resistivity surveys were performed in this area. A thorough description of the seismic reflection survey is given in Appendix A. One seismic reflection line, shown in Figure 22, transected the site in a near east-west orientation. The line was 180 m in length, which was the longest line attainable in the area. The results of the shear wave tests are given in Figure 23 (Appendix A as Figures 7a and 7b). Figure 23 is a portion of the converted depth reflection section, showing the raw and interpreted record. It is apparent from this line that the possible fill material has reduced the quality of the reflections, especially in the shallow regions. However, the following conclusions can be made about the geology. The interfaces above 46 m all exhibit slight dip from west to east, while the deeper interfaces show a possible reversal of dip at the western end. This appears to result in a thickening of the interpreted Canal Creek aquifer from only 6.1 m at the eastern end to about 15.25 m at the western end of the line. There is no indication of faulting or major discontinuities in any of the key horizons. Due to the poor quality of data obtained from this line, specific geologic interpretations will be discussed in the section "Site 3 Results."

Two electrical resistivity soundings were performed in this area. The location of the lines are shown in Figure 22. Line 1 was performed along grid line 0N, and centered at location 240E. The line was 160 m in length (80 m in each direction from the center point). The sounding curve and resulting interpreted model for this line are shown in Figure 24. The model reveals three layers; layer one with a thickness of 0.94 m and an apparent resistivity of 298 ohm-m, layer two with a thickness of 9.0 m and apparent resistivity of 15 ohm-m, layer three with an unknown thickness and apparent resistivity of 147 ohm-m. Performing an equivalence analysis of this data set reveals the range of resistivities and computed layer thicknesses that would also be valid models. This information is presented in Figure 25. For layer one the resistivities could range from 285 to 311 ohm-m with a layer thickness of 0.90 to 0.97 m. For layer two the resistivities could range from 14 to 16 ohm-m with a layer thickness of 7.8 to 10.4 m. For layer three the resistivities could range from 120 to 193 ohm-m with an undetermined thickness. This information reveals that the layer resistivities are modeled extremely well as is the thickness of layer one. The thickness of layer two is not as accurately modeled, in that the depth to the top of layer three (bottom of layer two) could range from 8.5 to 11.5 m.

Electrical resistivity line 2 was run along grid line 80N, and centered at location 300E. The line was 200 m in length (100 m in each direction from the center point). The sounding curve and resulting interpreted model for this line are shown in Figure 26. The model reveals four layers; layer one with a thickness of 0.58 m and an apparent resistivity of 182 ohm-m, layer two with a thickness of 3.3 m and apparent resistivity of 26 ohm-m, layer three with a thickness of 12.5 m and apparent resistivity of 11 ohm-m and layer four with an unknown thickness and apparent resistivity of 597 ohm-m. Performing an equivalence analysis of this data set reveals the range of resistivities and computed layer thicknesses that would also be valid models. This information is shown in Figure 27. For layer one the resistivities could range from 162 to

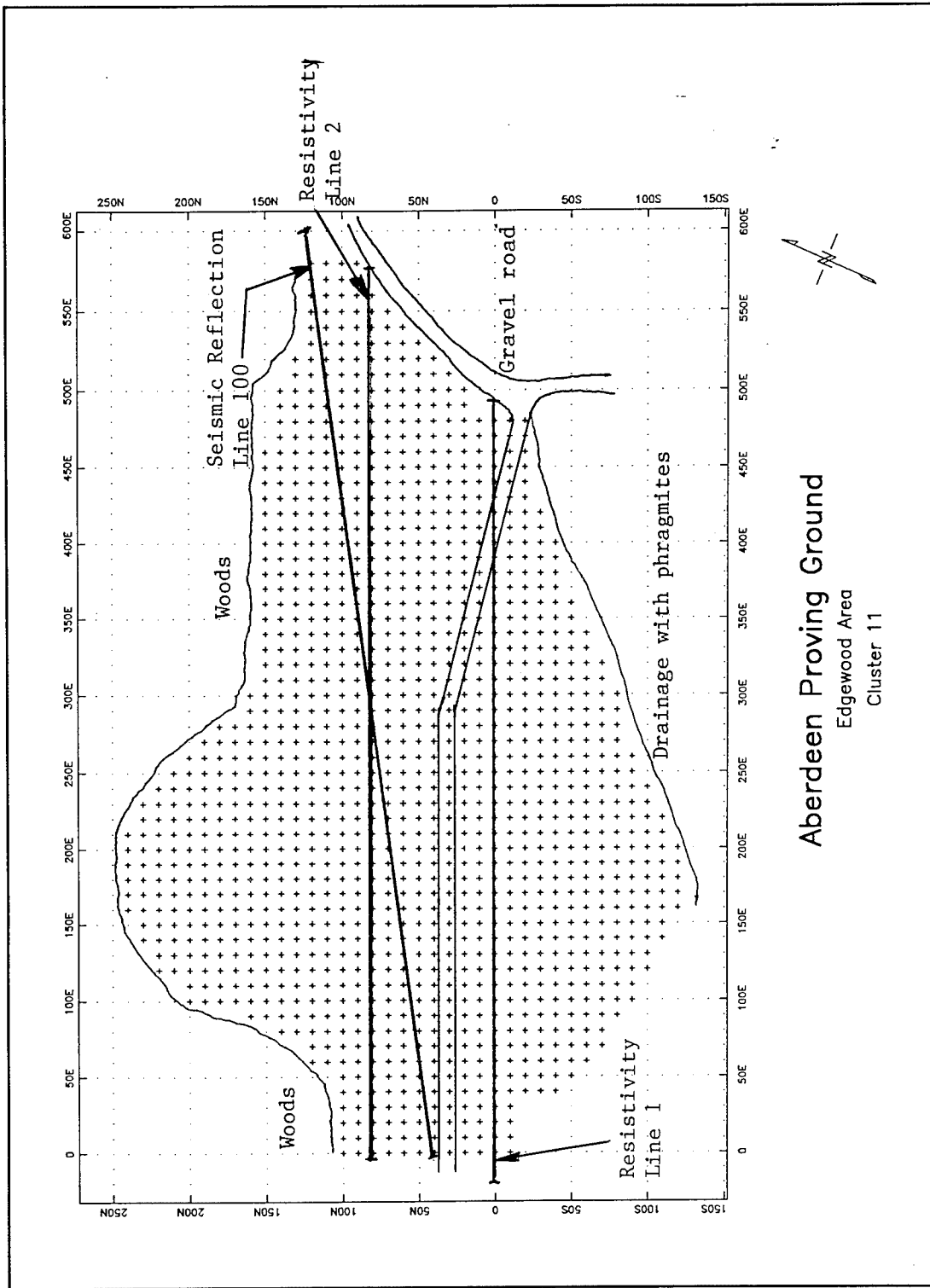


Figure 22. Seismic reflection and resistivity sounding lines at Site 2. Station intervals are 10 ft (3 m)

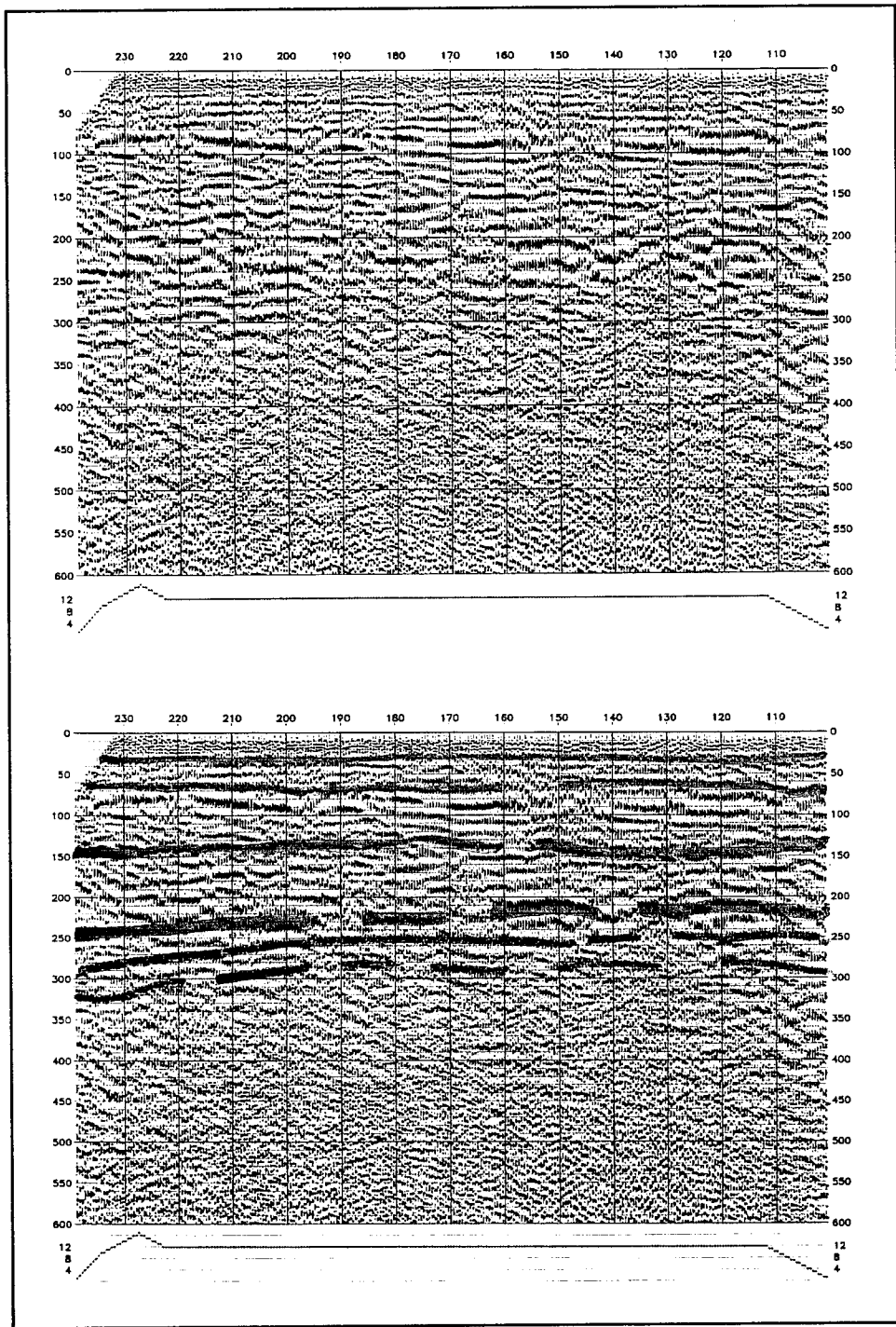


Figure 23. Seismic reflection line 100 survey results showing depth section (top) and layer interpreted depth section (bottom). Horizontal axis is station intervals of 10 ft (3 m). Vertical axis is depth intervals of 10 ft (3 m).

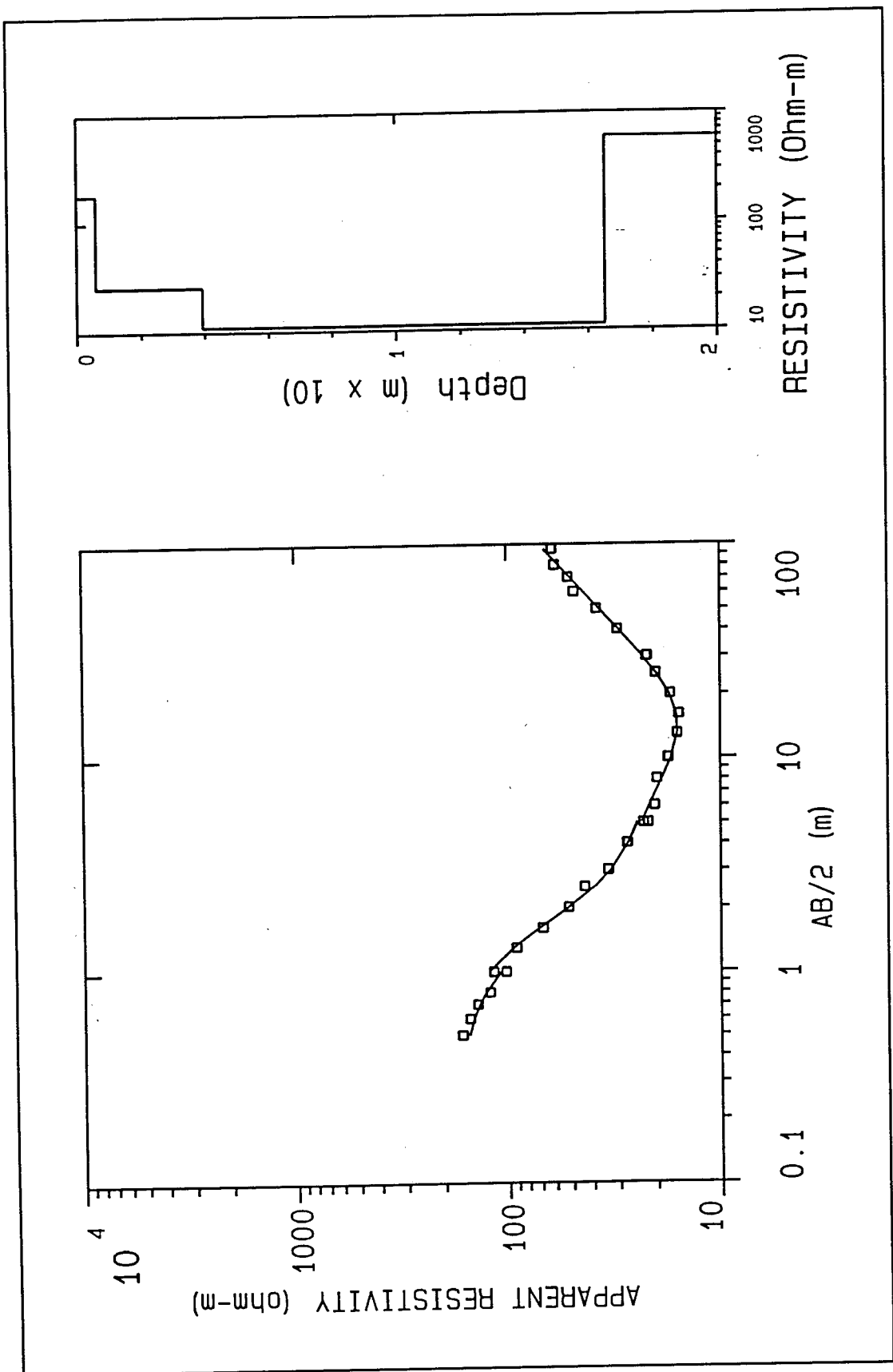


Figure 24. Resistivity sounding line 1 at Site 2, showing inversion curve (left) and interpreted layers (right)

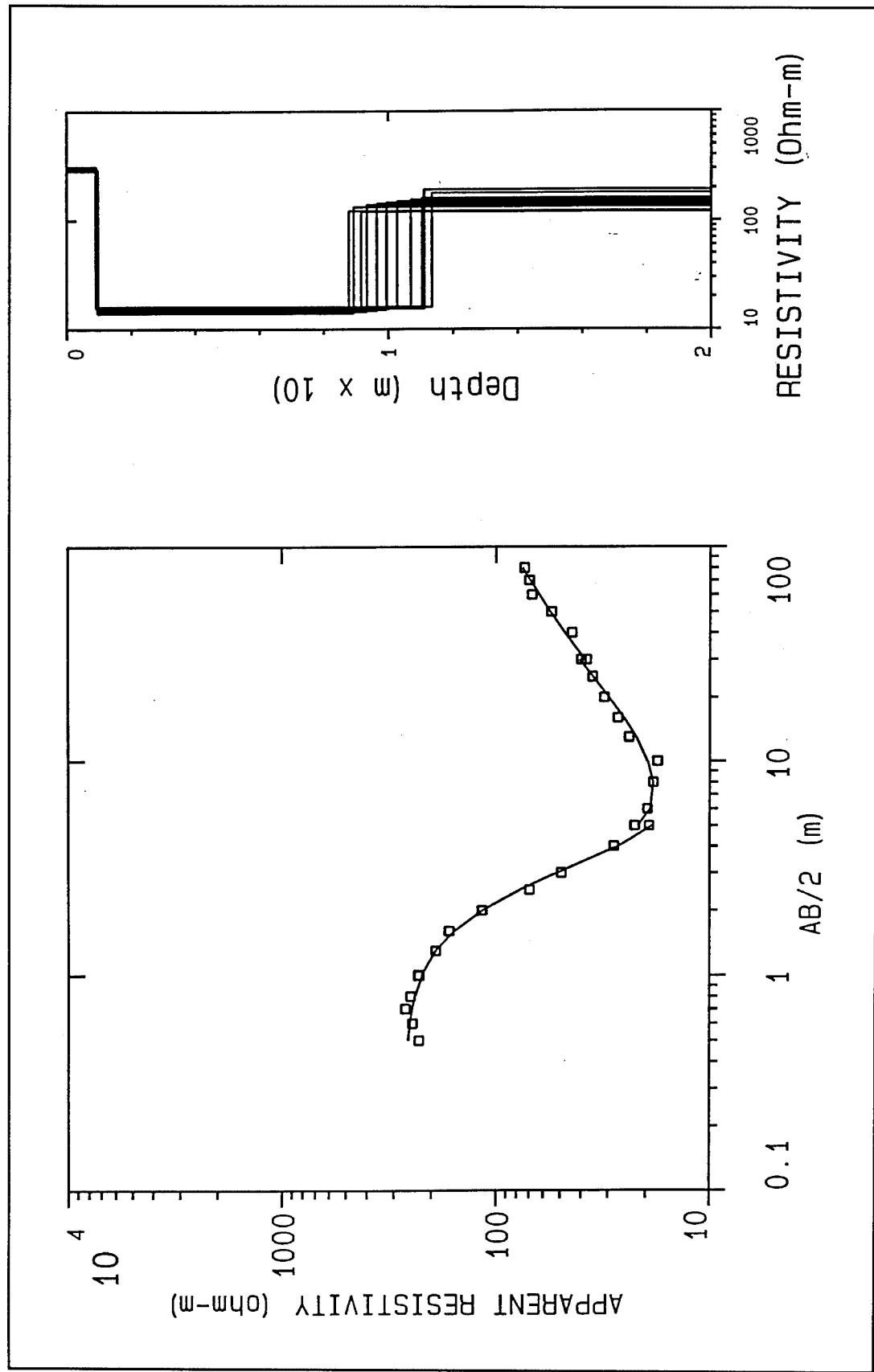


Figure 25. Inversion curve (left) and equivalence models (right) for resistivity sounding line 1 at Site 2

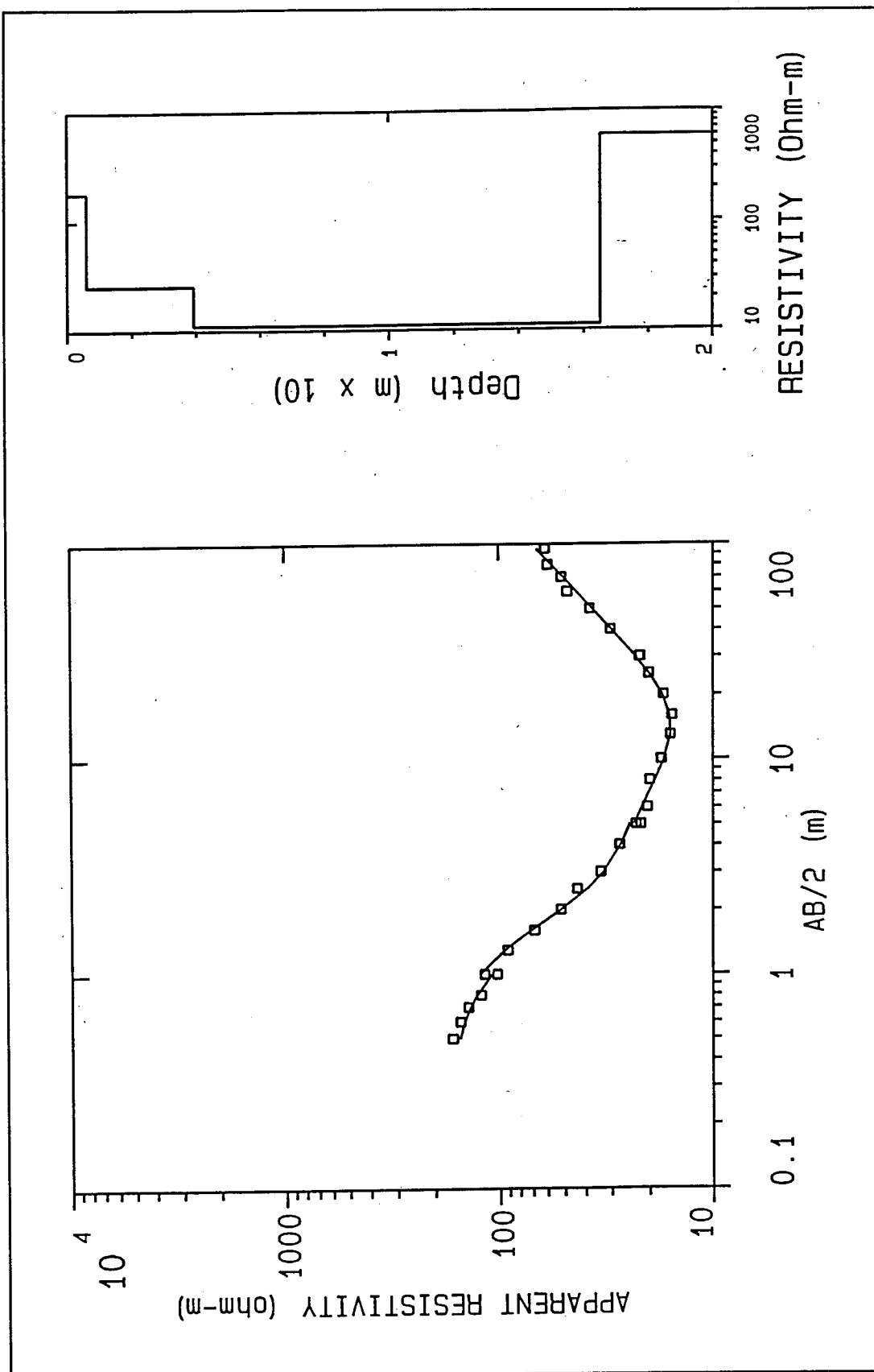


Figure 26. Resistivity sounding line 2 at Site 2, showing inversion curve (left) and interpreted layers (right)

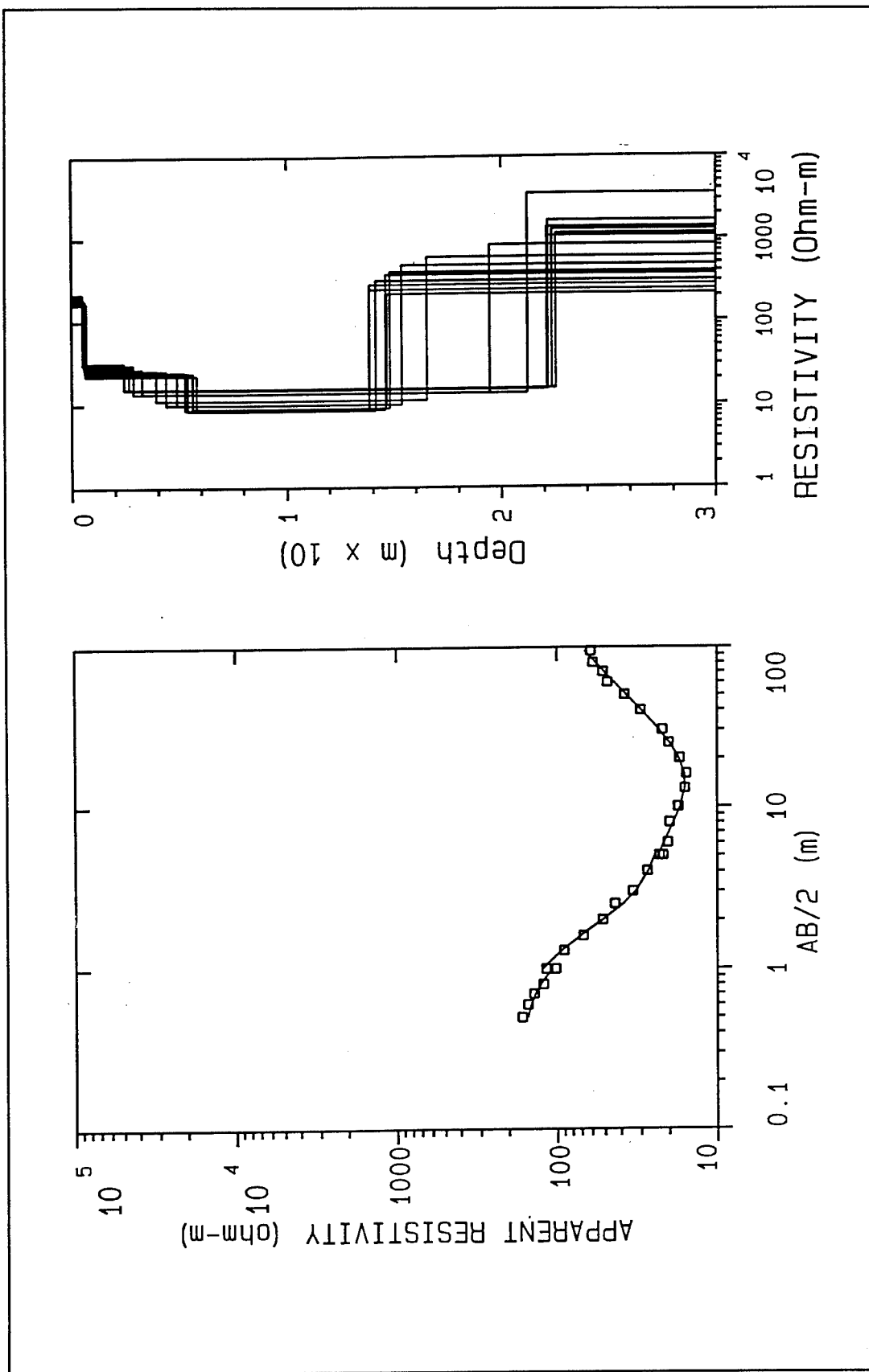


Figure 27. Inversion curve (left) and equivalence models (right) for resistivity sounding line 2 at Site 2

215 ohm-m with a layer thickness of 0.50 to 0.66 m. For layer two the resistivities could range from 22 to 32 ohm-m with a layer thickness of 1.9 to 5.2 m. For layer three the resistivities could range from 8 to 15 ohm-m with a layer thickness of 8.5 to 20.0 m. For layer four the resistivities could range from 213 to 3500 ohm-m with an undetermined thickness. This information reveals that the resistivities for layers one, two and three and the thickness of layer one are modeled extremely well. The thicknesses of layers two and three are not as accurately modeled. The depth to the top of layer two (bottom of layer one) could range from 2.5 to 5.8 m and the depth to the top of layer three (bottom of layer two) could range from 14 to 22.5 m. The inversion program also poorly modeled the resistivity of the fourth layer. This is due to the fact that insufficient data was acquired at deeper depths to accurately define this layer.

Site 3 Results

The Site 3 grid layout and surface features are shown in Figure 7. The results of the EM-31 survey are shown in Figures 28 and 29. Figure 28 shows the results of the conductivity survey, with contours every 10 mS/m. The results show a large area in the northwest corner of the grid that has very high conductivity readings. These values range from 50 to 60 mS/m whereas the background readings are approximately 15 mS/m. In addition to this area, there are a few isolated spots that have low conductivity readings (indicated by the blue). These values of zero or less, are usually indicative of surface trash (soils would not have a conductivity of zero or negative). In this area there were various spots of surface trash such as concrete rubble, asphalt rubble, shingles, etc. The results of the inphase survey are shown in Figure 29, with contours every 1 ppt. Background readings for this area are -2 to -6 ppt (whether the values are positive or negative is not important, the deviation from background is important). Most of the anomalies from this survey are located in the northwest corner of the plot. There is one anomaly at station 130W, 60N that appears to be significant. The area along line 10S illustrates a continuous line of anomalies along the paved road.

The results of the magnetometer survey are shown in Figures 30 and 31. Figure 30 is a plot of the total field survey results with contours displayed every 100 gammas. Background readings for this area are approximately 53,750 gammas. The plot reveals several anomalous areas which are small isolated spots due to surface trash. The significant anomalies are located at 130W, 60N and from 0W to 100W extending from 100N to 200N. The results of the magnetic gradient survey are shown in Figure 31, with contours every 100 gammas/m. Here again the significant anomalies are the same as discussed for the total field survey.

The results of the EM-61 survey are shown in Figures 32 through 34. Figure 32 is a plot of the results from the bottom coil of the instrument with contours every 100 mV, Figure 33 is a plot of results from the top coil of the instrument with contours every 50 mV, and Figure 34 is a plot of the

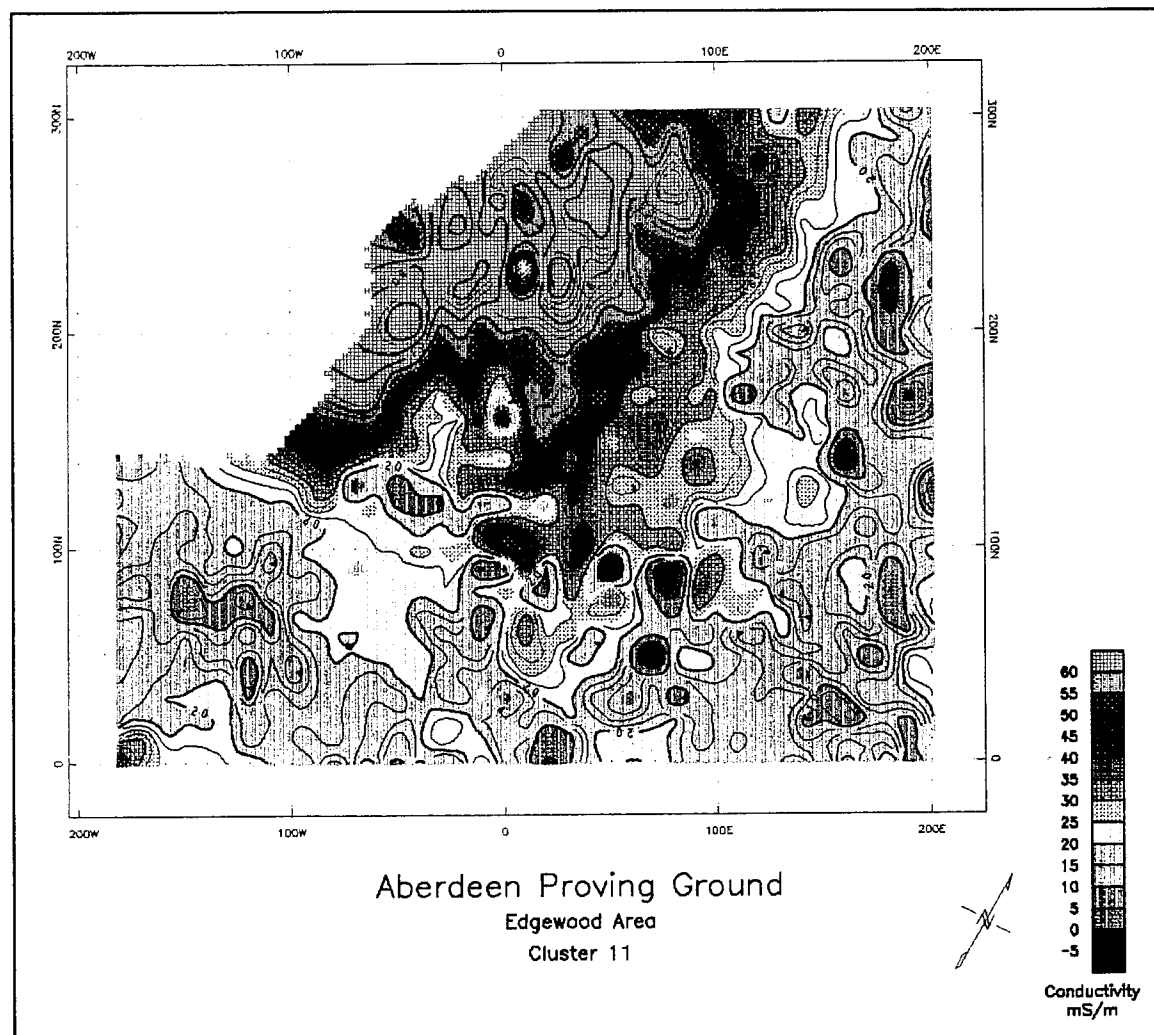


Figure 28. EM-31 conductivity survey for Site 3. Contours are 2.5 mS/m, and station intervals are 10 ft (3 m)

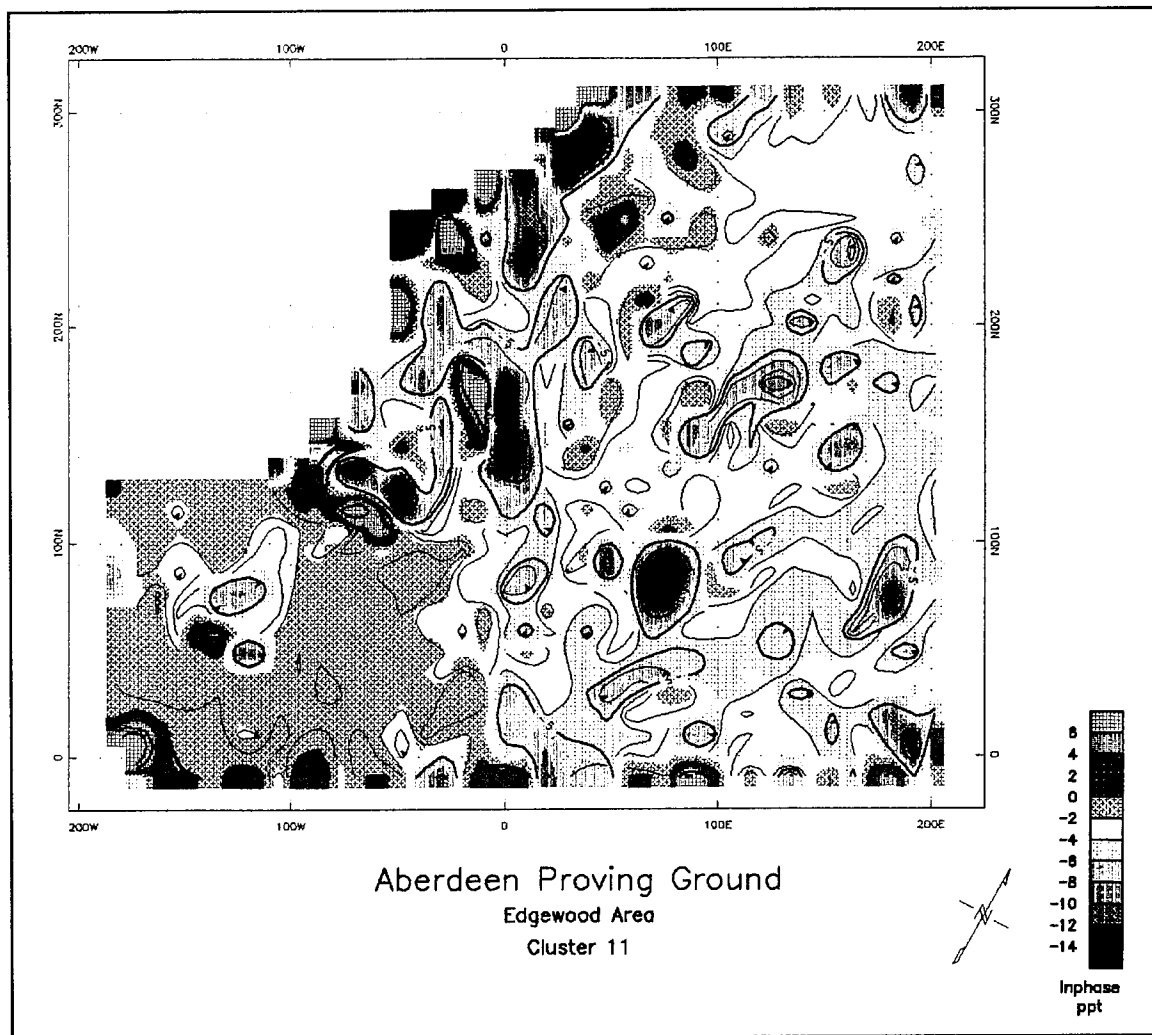


Figure 29. EM-31 inphase survey for Site 3. Contours are 1 ppt, and station intervals are 10 ft (3 m)

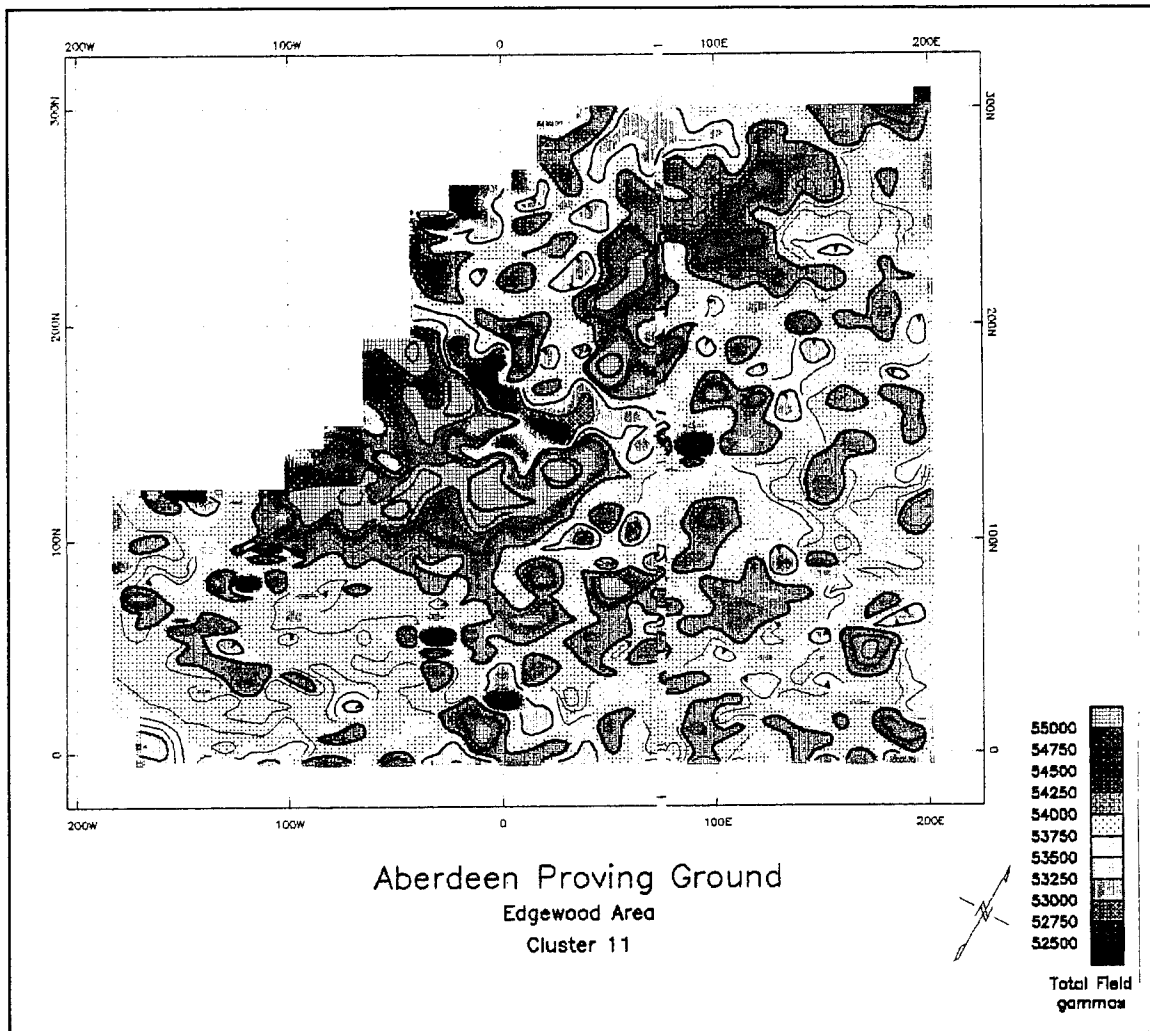


Figure 30. Magnetic total field survey for Site 3. Contours are 100 gammas, and station intervals are 10 ft (3 m)

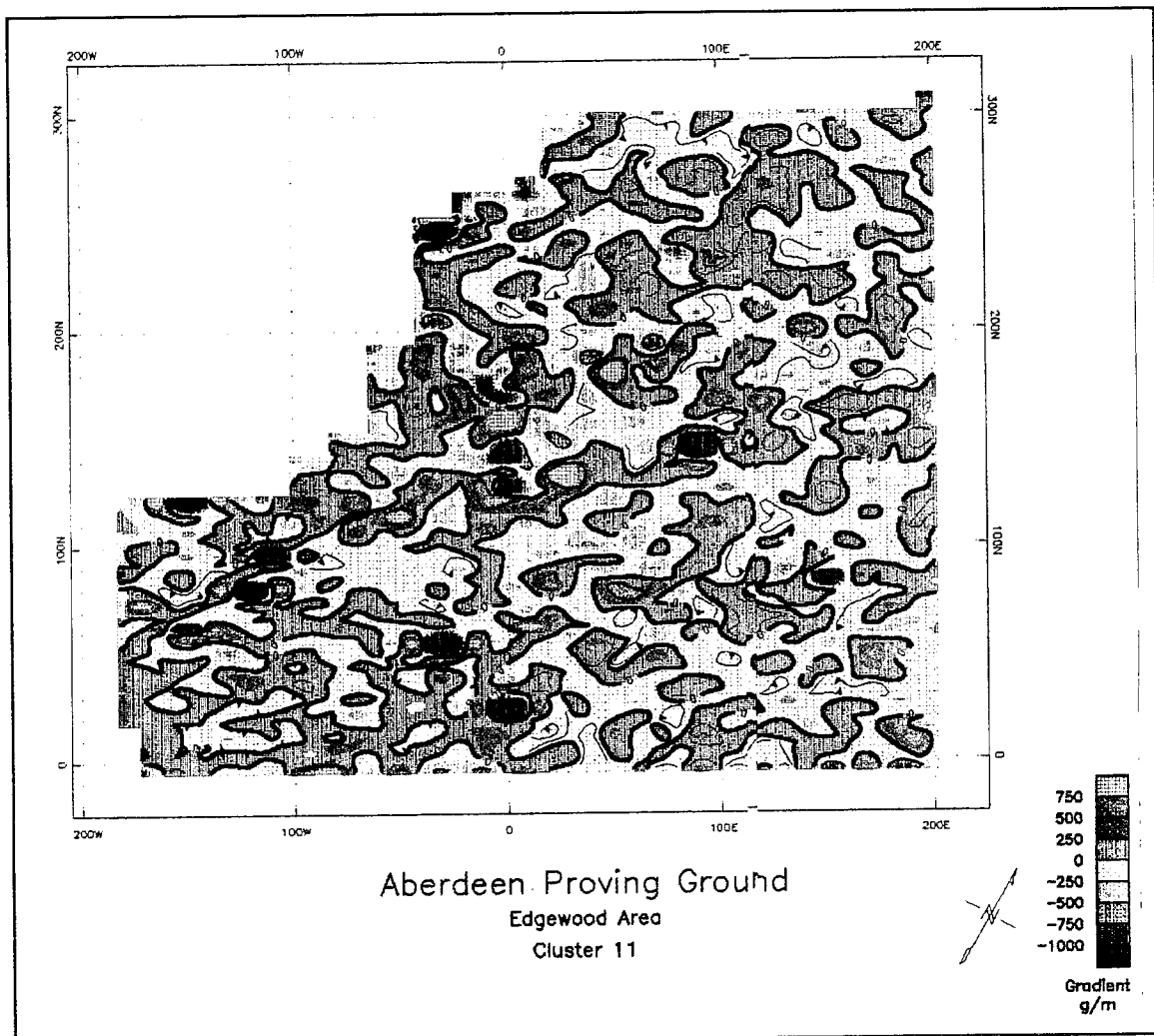


Figure 31. Magnetic gradient survey for Site 3. Contours are 100 gammas/m, and station intervals are 10 ft (3 m)

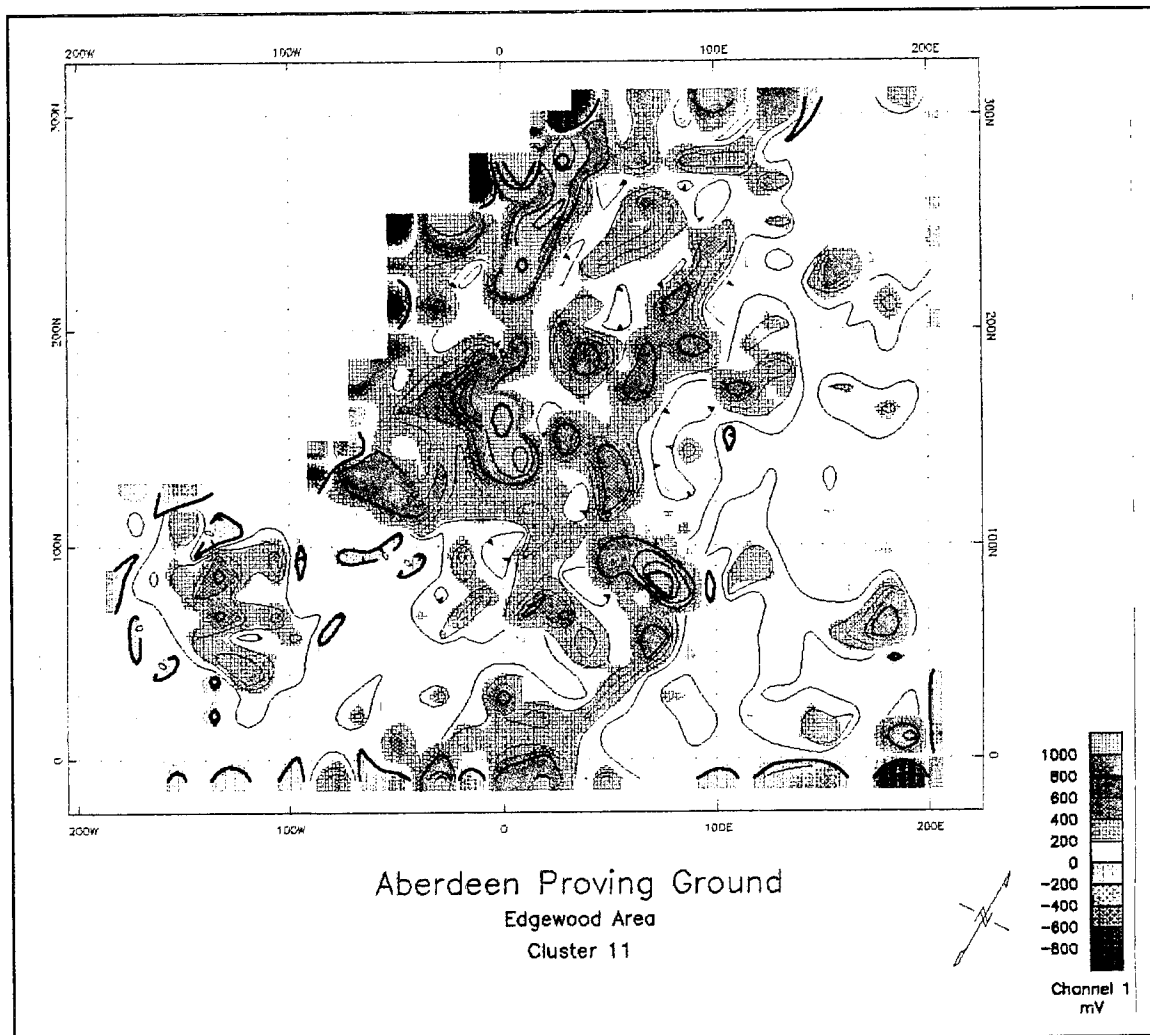


Figure 32. EM-61 bottom coil survey for Site 3. Contours are 100 mV, and station intervals are 10 ft (3 m)

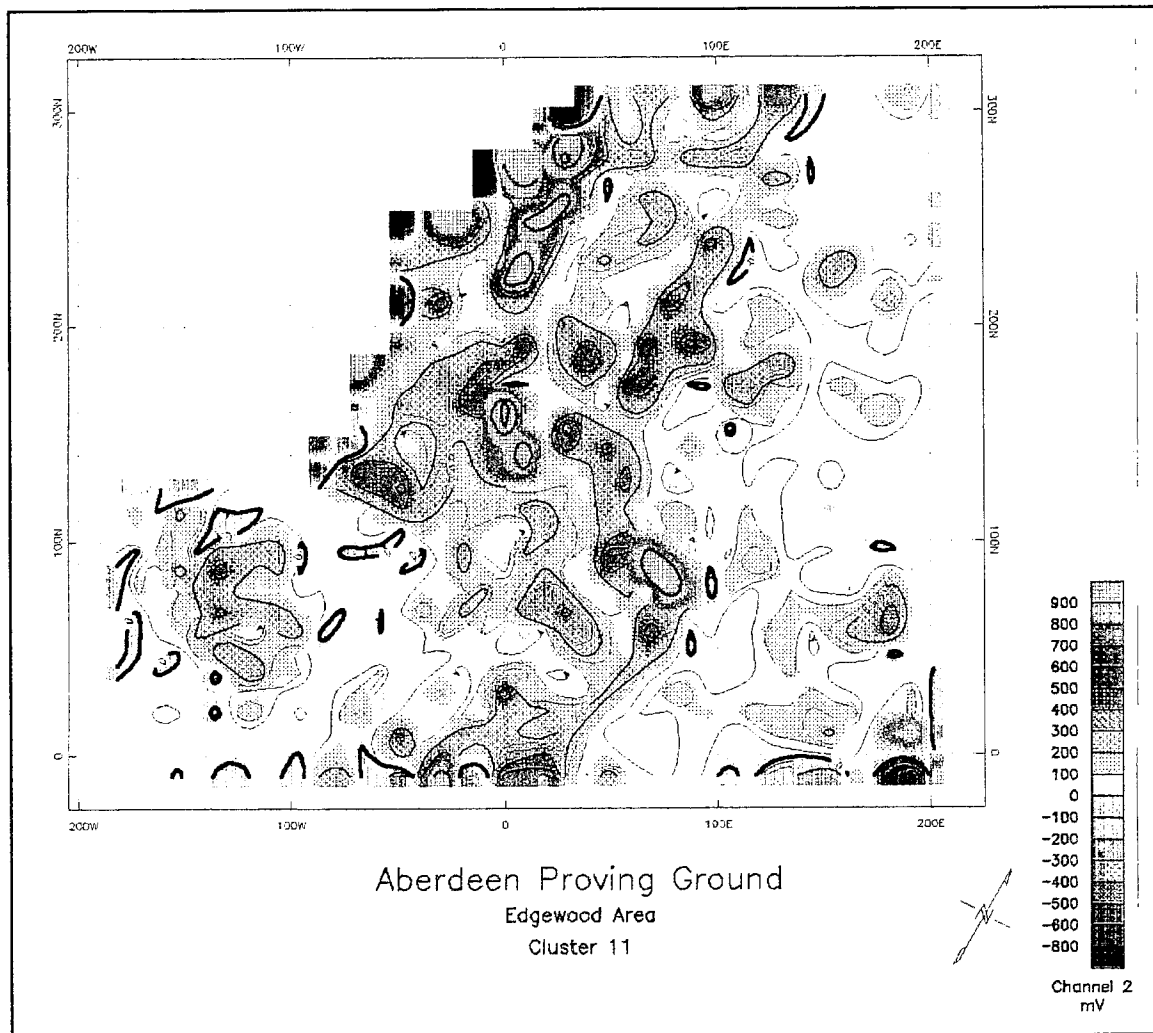


Figure 33. EM-61 top coil survey for Site 3. Contours are 100 mV, and station intervals are 10 ft (3 m)

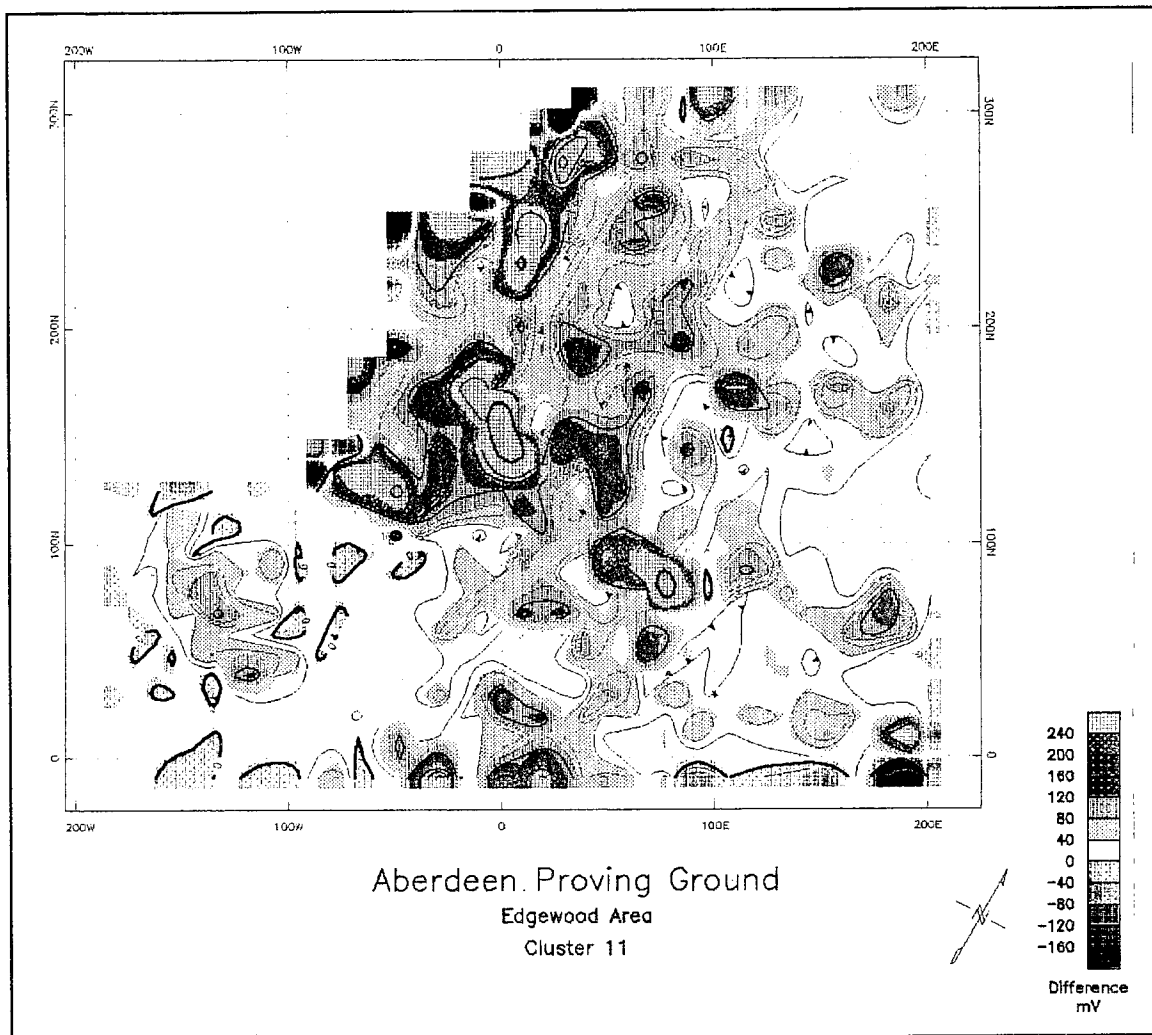


Figure 34. EM-61 difference between top and bottom coils survey for Site 3. Contours are 20 mV, and station intervals are 10 ft (3 m)

difference between the coils with contours every 20 mV. All three plots illustrate the same anomalous areas as discussed previously, namely at location 130W, 60N and the northwest corner of the grid.

Based on all the surveys performed in this area, the following interpretation can be made. The northwest corner of the grid is clearly more conductive than the rest of the site and contains many metallic anomalies. There was some amount of surface trash observed in this area which contributes to the observed readings. This area slopes toward a nearby creek draining the area, which may also contribute to the higher conductivity values. However there is clearly a large amount of metallic material in this area that must be located beneath the surface. There is also a very strong possibility that this area might be a continuation of the linear trend observed at Site 2. The other significant anomalous area is that at location 130W, 60N. This area appeared in every test and is not explained by surface features. The anomalies detected at this area are shown in Table 2.

Table 2
Anomalies Detected at Site 3

Anomaly	Location	Type	Cause
1	10S,200E-200W	conductive, magnetic	paved road
2	170E,220N	conductive, magnetic	unknown
3	180E,170N	conductive, magnetic	unknown
4	200E,120N	conductive, magnetic	unknown
5	170E,80N	conductive, magnetic	unknown
6	160E,20N	conductive, magnetic	unknown
7	150E,130N	conductive, magnetic	unknown
8	90E,40N	conductive, magnetic	tower anchor
9	140E,80N	conductive, magnetic	unknown
10	90E,100N	conductive, magnetic	unknown
11	120E,170N	conductive, magnetic	unknown
12	100E,150N	conductive, magnetic	unknown
13	100E,180N	conductive, magnetic	unknown
14	110E,190N	conductive, magnetic	unknown
15	150E,200N	conductive, magnetic	unknown
16	170E,240N	conductive, magnetic	unknown
17	110E,230N	conductive, magnetic	unknown
18	110E,280N	conductive, magnetic	unknown
19	80E,270N	conductive, magnetic	unknown
20	60E,270N	conductive, magnetic	unknown
21	70E,290N	conductive, magnetic	unknown
22	190E,290N	conductive, magnetic	unknown
23	60E,220N	conductive, magnetic	unknown
24	50E,190N	conductive, magnetic	unknown

(Continued)

Table 2 (Concluded)

Anomaly	Location	Type	Cause
25	70E,150N	conductive, magnetic	unknown
26	50E,100N	conductive, magnetic	unknown
27	80E,80N	conductive, magnetic	unknown
28	50E,80N	conductive, magnetic	unknown
29	190E,10N	conductive, magnetic	unknown
30	90E,10N	conductive, magnetic	unknown
31	50E,10N	conductive, magnetic	unknown
32	5W,20N	conductive, magnetic	unknown
33	10E,40N	conductive, magnetic	unknown
34	15E,80N	conductive, magnetic	unknown
35	20E,140N	conductive, magnetic	unknown
36	15E,180N	conductive, magnetic	unknown
37	30E,230N	conductive, magnetic	unknown
38	35E,165N	conductive, magnetic	unknown
39	40E,290N	conductive, magnetic	unknown
40	10E,250N	conductive, magnetic	unknown
41	20W,260N	conductive, magnetic	unknown
42	30W,220N	conductive, magnetic	unknown
43	5E,220N	conductive, magnetic	unknown
44	30W,190N	conductive, magnetic	unknown
45	10W,180N	conductive, magnetic	unknown
46	0W,160N	conductive, magnetic	unknown
47	0W,140N	conductive, magnetic	unknown
48	30W,50N	conductive, magnetic	unknown
49	120W,50N	conductive, magnetic	unknown
50	150W,60N	conductive, magnetic	unknown
51	20W,80N	conductive, magnetic	unknown
52	10W,100N	conductive, magnetic	unknown
53	180W,70N	conductive, magnetic	unknown
54	150W,120N	conductive, magnetic	unknown
55	50W,120N	conductive, magnetic	unknown
56	70W,120N	conductive, magnetic	unknown
57	130W,60N	conductive, magnetic	unknown

To aid in the geological interpretation, seismic reflection and GPR surveys were performed at the site. The location of the seismic reflection line is shown in Figure 35. A detailed explanation of the test procedures and results can be found in Appendix A. The line was 206 m long and extended through Site 3 and parallel to Site 6 (located west of Site 6 on the west side of the earthen berm). The results of the survey are shown in Figure 36 (Appendix A).

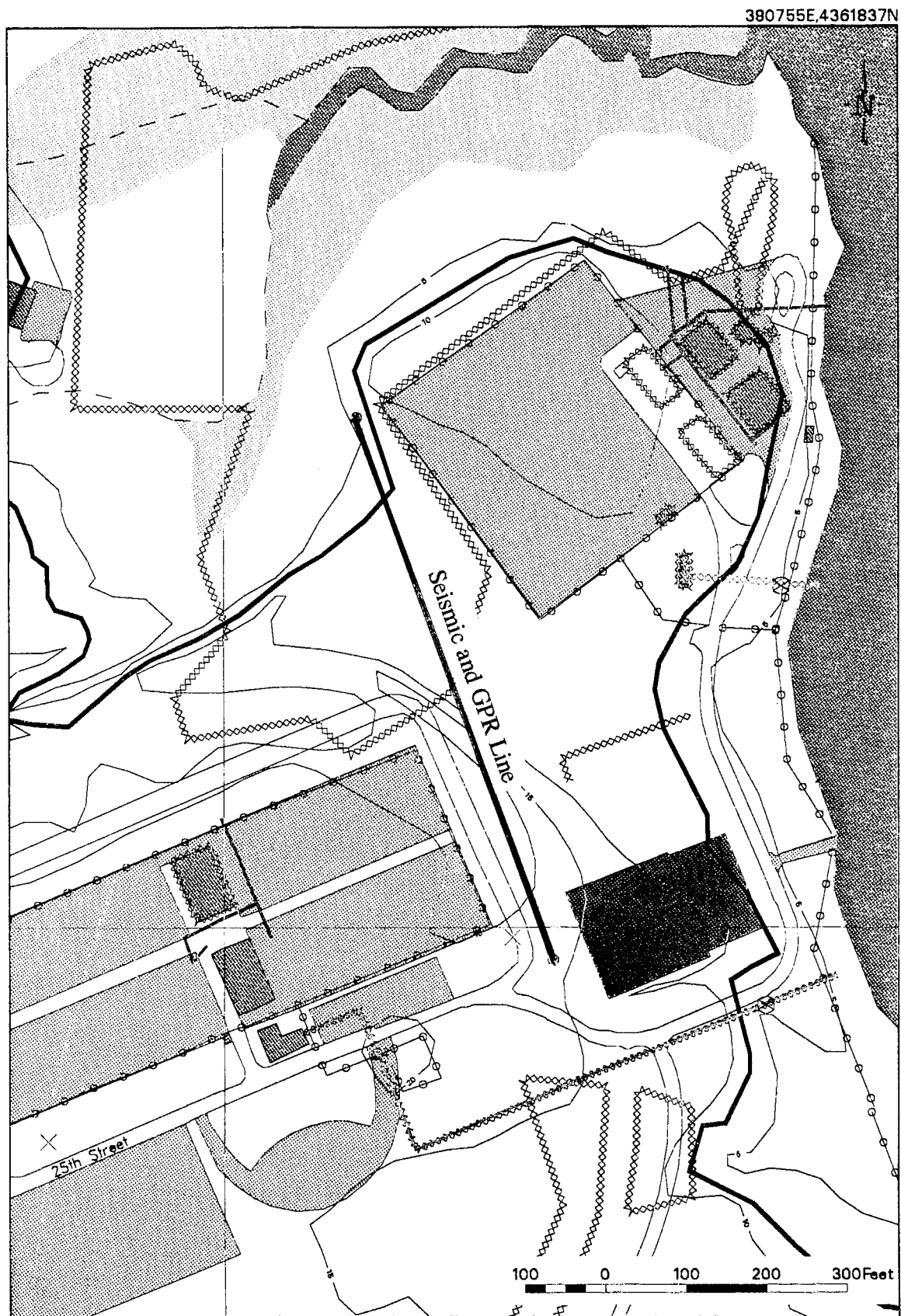


Figure 35. Seismic reflection line 200 and GPR survey lines at Site 3. Metric scale: 1 cm = 25 m

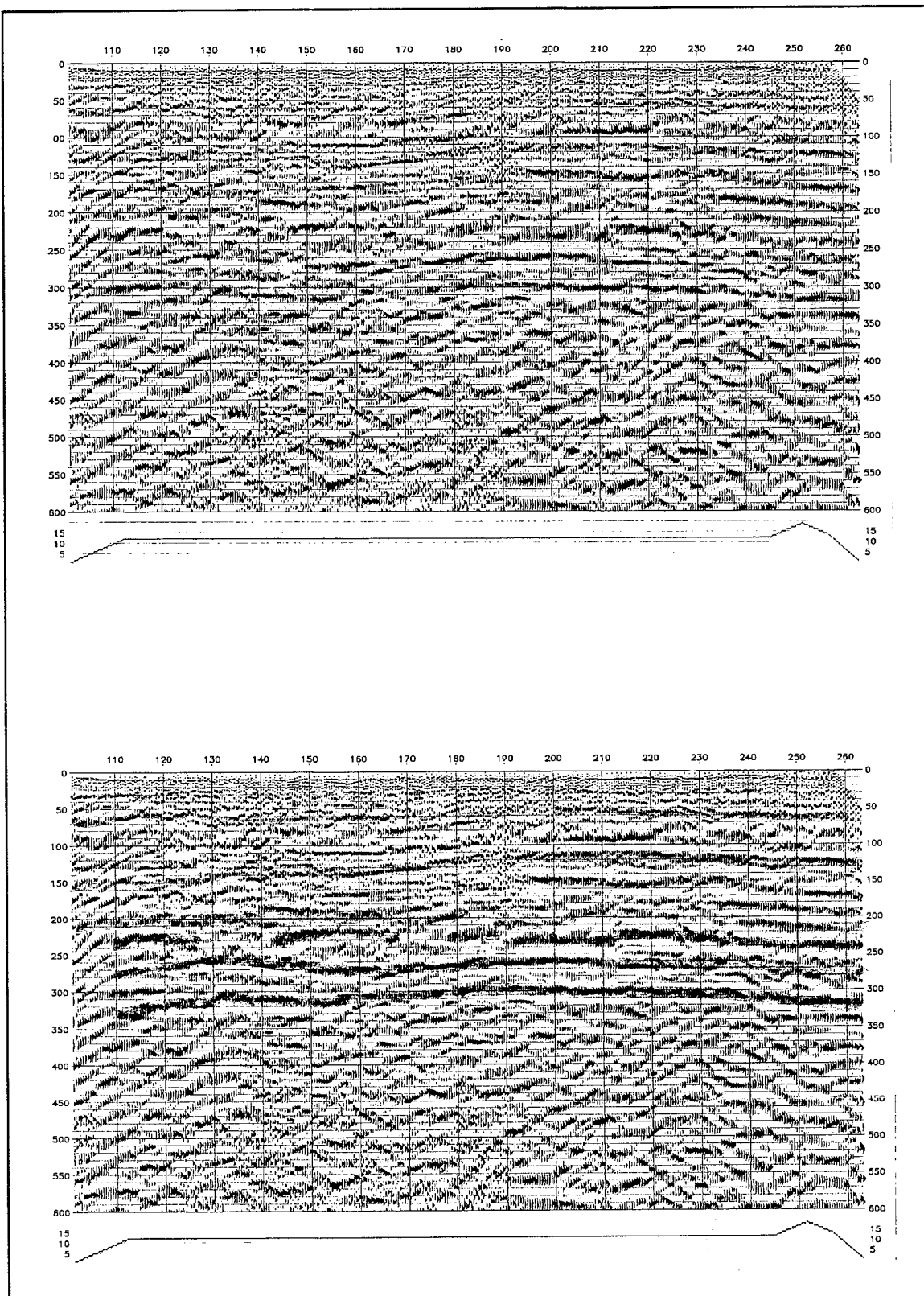


Figure 36. Seismic reflection line 200 showing depth section (top) and layer interpreted depth section (bottom). Horizontal and vertical intervals are 10 ft (3 m)

Figures 6a and 6b). Figure 36 is the depth converted section showing the raw data and interpreted interfaces. The quality of reflections obtained from this line are much better than those obtained from the line performed through Site 2. Specific to this line, the following correlations between reflections and major geologic interfaces have been determined. The reflectors are color coded to represent the top of a dominantly clay unit (blue), top of a dominantly sand unit (green) and unknown (orange). This same coloring scheme is used on the data obtained from Site 2. At a depth of 8 m Top Cretaceous/Upper Confining Unit, 30 m Top Canal Creek Aquifer, 40 m Base Canal Creek/Top Confining Unit, 49 m Top Lower Confined Aquifer, 58 m bed within Lower Confined Aquifer, 64 m Top Lowest Confining Unit. Three reflectors at 76, 82, and 91 m are apparent also but the unit producing the reflectors is unknown. From a structural sense, there is no evidence of faulting on this section, however several other features are notable. These include structural dip of the layers, pinching-out of others, and the interpretation of a channel-like feature.

The structural dip of the detected layers is not uniform. For the central portion of line 200, the layer interfaces are generally flat. There is a general increase in dip down towards the south beginning at station 230. However, there is also an increase in dip down to the north going to the north of station 180. The dip to the south is more apparent on the deeper interfaces than on the shallower interfaces. This southern dip is in general agreement with the cross sectional shown in Figure 4.

Aside from the general dip of the layers, there are also thinning of certain layers and formation of a channel-like feature. The results indicate a pinching out of a thin bed within the Cretaceous and above the interpreted Canal Creek aquifer at a depth of 15 m near station 230 which is in agreement with a possible sand lens noted on the stratigraphic cross section. Also, the Canal Creek aquifer itself shows apparent thinning from a typical 15 m thickness on the south end of the line down to a minimum thickness of 4.5-6 m near station 210. North of this area, there is downwarping and apparent thickening of the Canal Creek reflection. The overlying reflections continue across without significant downwarping, therefore this is not a general 'statics' problem. This has the appearance of a channel. It is important to note that several of the beds appear to thin at the southern end of the line and trend toward the north. The appearance of a channel is supported by two cross sections in the area based on data from monitoring wells. The two sections are shown in Figures 37 and 38 (see Figure 3 for section locations). As seen on cross section A-A' and B-B' the axial minima of this channel is near WBR-35 and WBR-43. Based on borehole and geophysical constraints, this channel may trend to the northwest/southeast.

The locations of the GPR survey lines are shown in Figure 35. The results of line 1 are shown in Figure 39 which extends from station 0 to 150 and has a maximum depth of investigation of 9 m (using a velocity of 0.23 m/sec to convert the time scale to a depth scale). The results of line 2 are shown in Figures 40 and 41. Figure 41 shows line 2 extending from station 0 to 170 with a maximum depth of investigation of 7.5 m. Figure 41 shows line 2

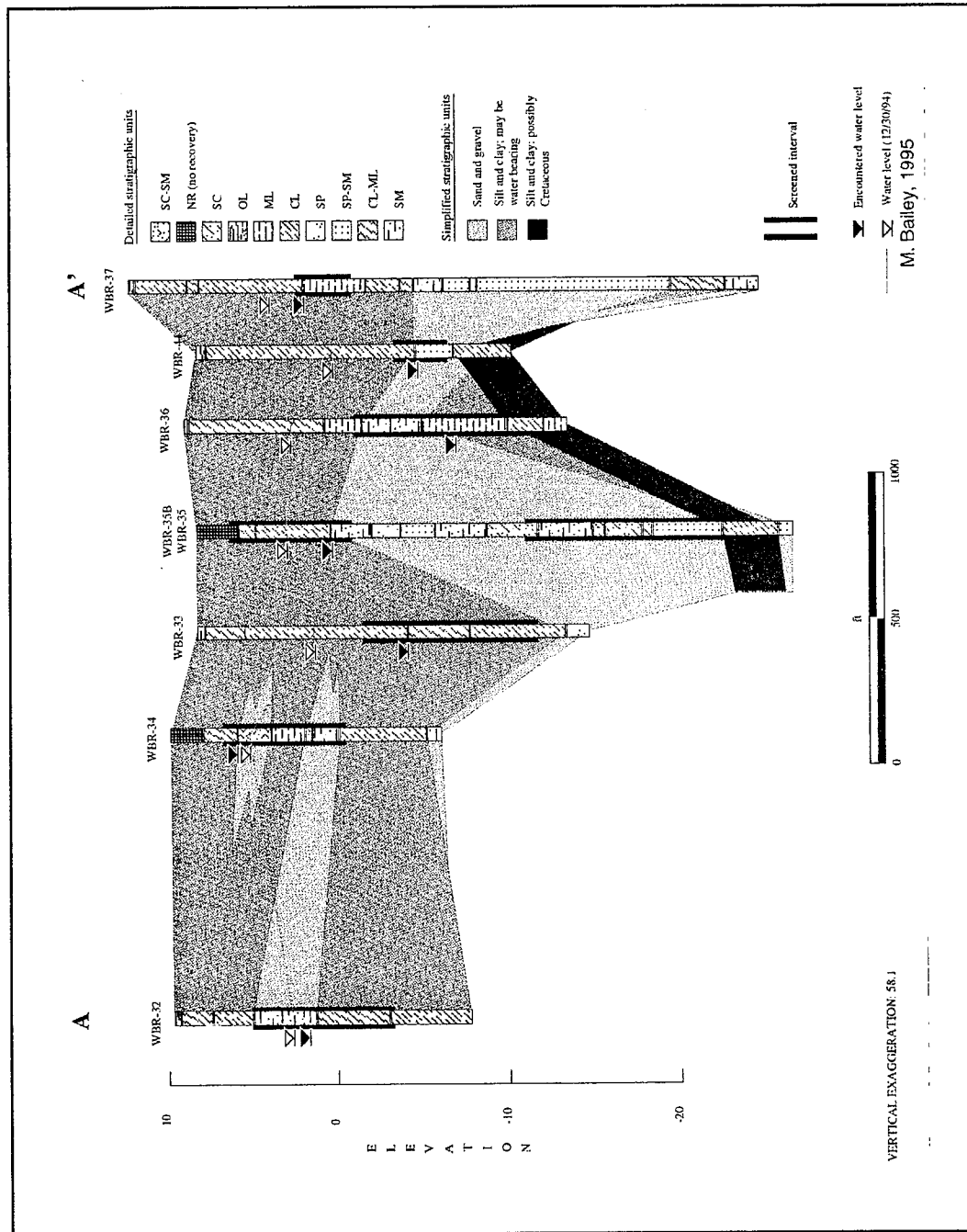


Figure 37. Geologic cross section A-A' from Bush River monitoring wells (Bailey 1995). Metric scale:
1 cm = 50 m

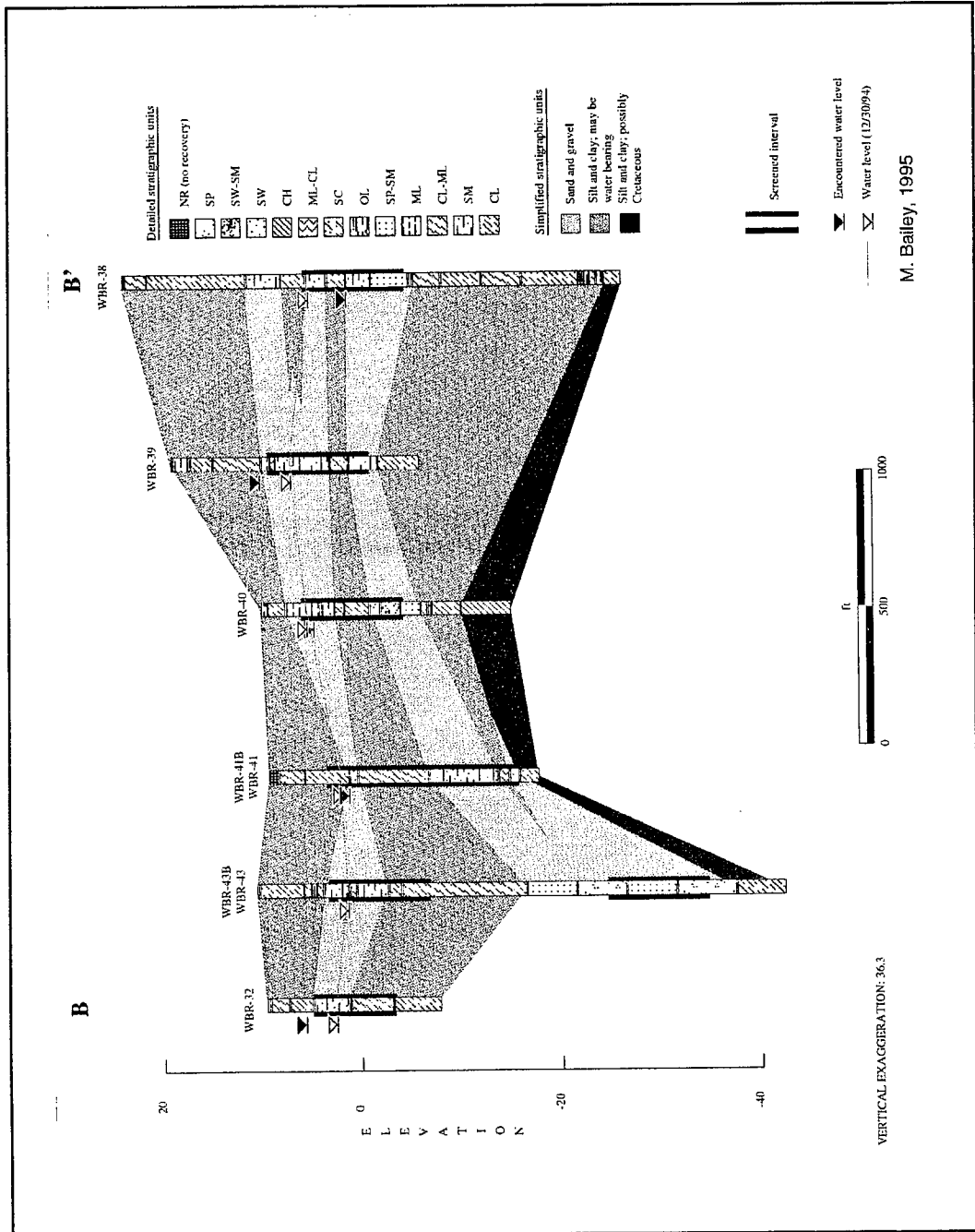


Figure 38. Geologic cross section B-B' from Bush River monitoring wells (Bailey 1995). Metric scale:
1 cm = 50 m

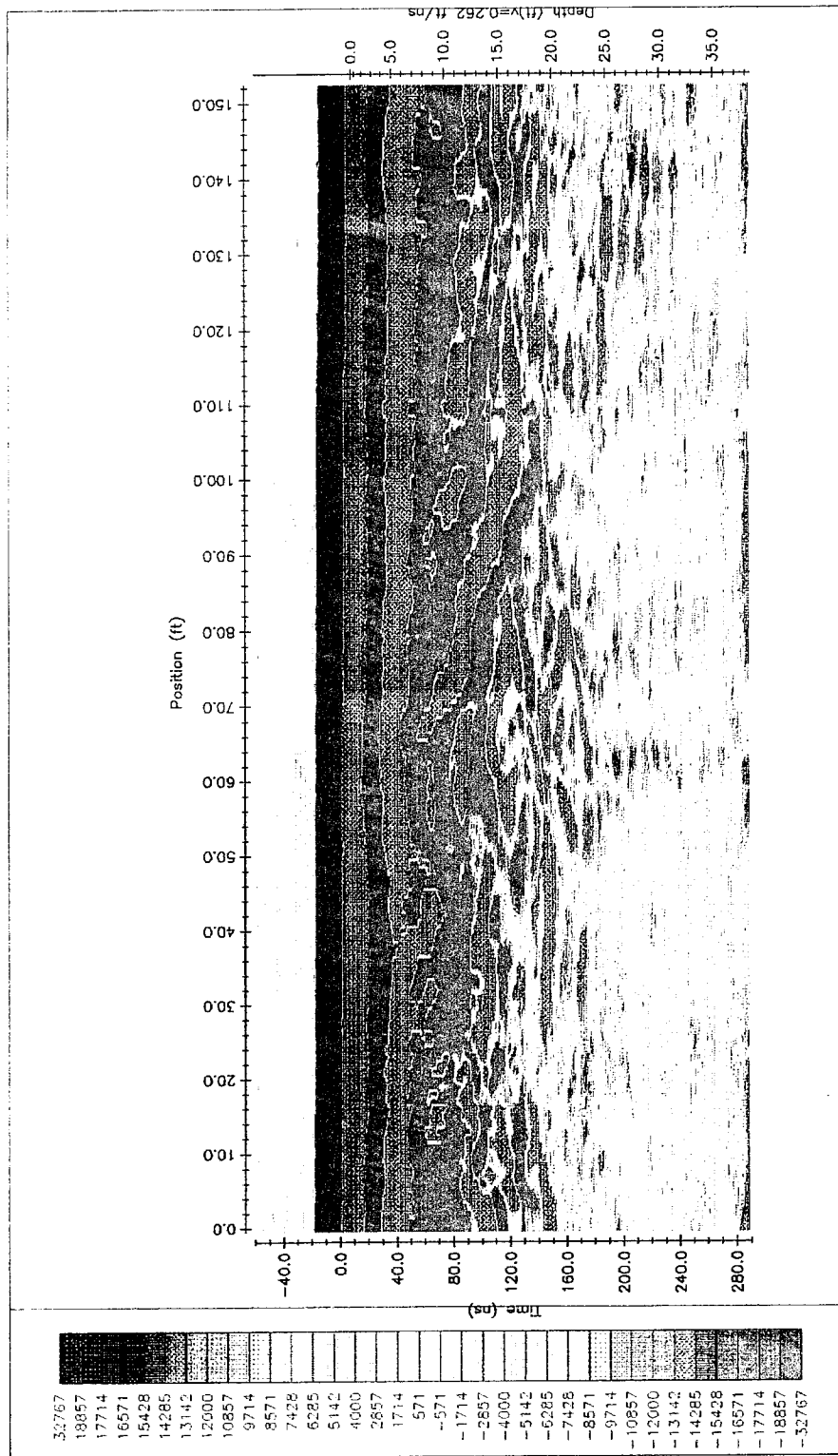


Figure 39. GPR line 1 at Site 3, stations 0 to 150, 280 nanosecond (ns) window. Station intervals are 2 ft (0.6 m).

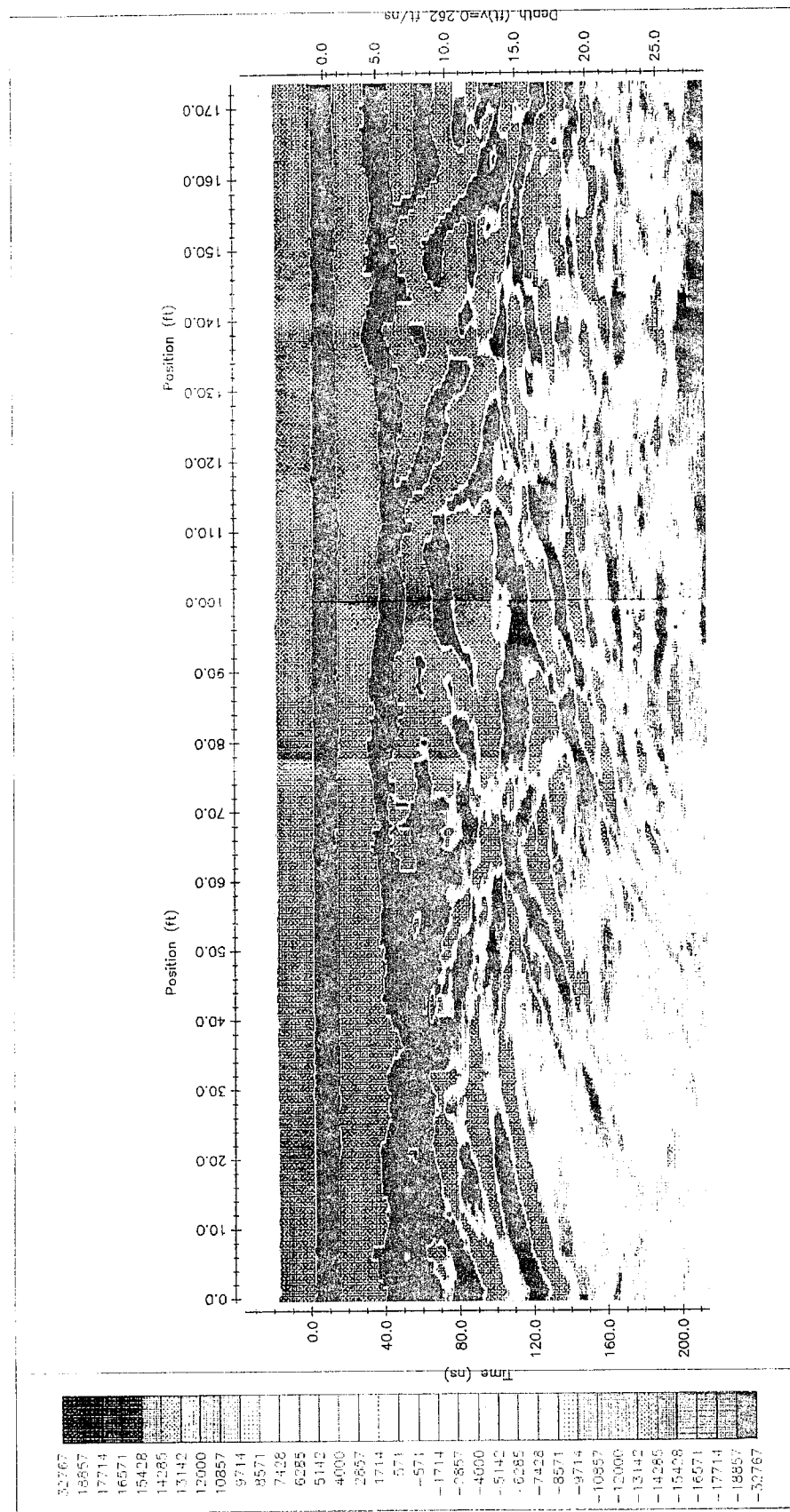


Figure 40. GPR line 2 at Site 3, stations 0 to 170, 200 nanosecond (ns) window. Station intervals are 2 ft (0.6 m).

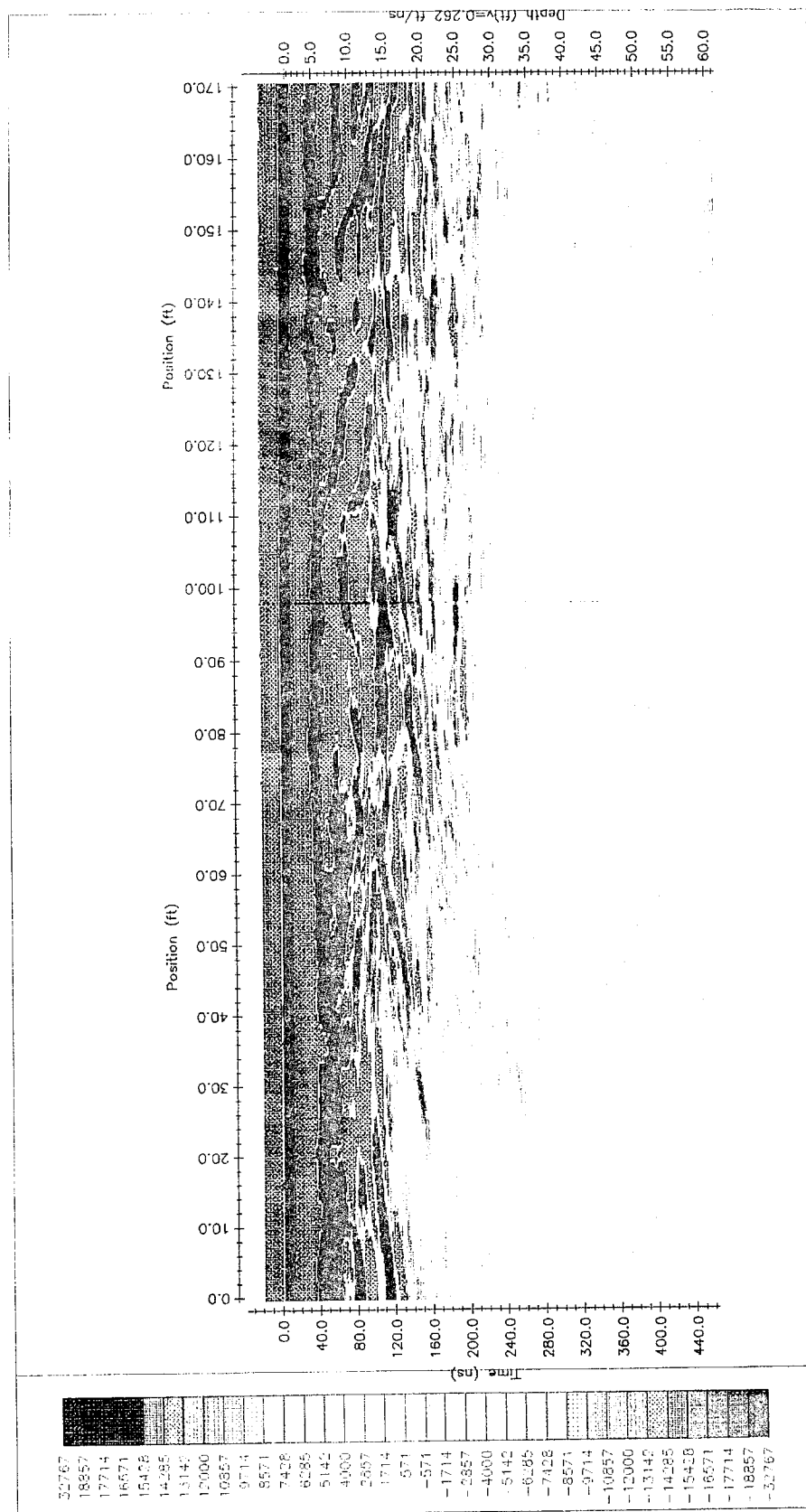


Figure 41. GPR line 2 at Site 3, stations 0 to 170, 460 nanosecond (ns) window. Station intervals are 2 ft (0.6 m).

with the time scale increased to determine if any reflectors deeper than 7.5 m were detected. It is clear from this figure that the reflectors disappear at a depth greater than 7.5 m. The reflectors visible in the radar profiles likely represent a depositional contact between a predominantly clay unit and a sandy unit. From observations at Bush River, Canal Creek and Westwood, it is evident that a Pleistocene tributary system was incised into Cretaceous sediments as a result of lowered sea level. This system has been variably filled during the late Pleistocene and Holocene transgression (Coleman et al. 1990). Figure 37 indicates a possible channel near well WBR-35 extending to the east. This feature also appears on the southern part of GPR line number 2 (Figures 40 and 41). At the lower end of resolution for this profile, the sloping reflectors appear to be truncated by a more horizontal reflector which is likely Cretaceous. The northern portion of line 1 (Figure 39) very closely mimics the geology as seen in Figure 38, in between wells WBR-41 and WBR-40. Note the pinching and swelling of individual lithofacies and the possible correlation between the inferred Cretaceous strata.

Site 4 Results

The Site 4 grid layout and surface features were shown in Figure 8. The results of the EM-31 survey are shown in Figures 42 and 43. Figure 42 shows the results of the conductivity survey with contours every 20 mS/m. The plot is relatively clear of anomalies except for the area in and around the buildings. In the area away from the buildings the only anomalies that occur are those associated with the fence (indicated around the edges of the plot). Although the buildings are affecting the area around them and effectively masking any anomalies nearby, there are indications of anomalies close to the buildings. Specifically, there is a linear northwest trending anomaly at location 240E from 20N to 100N. This may be an underground pipe associated with the nearby building. This pipe probably extends further south, in front of the next building. In addition, there is an anomalous area at location 140E, 40S. The cause of this anomaly is unknown. The high values around the western edge of the plot are associated with the chain link fence. The low at location 300E, 0N was due to construction equipment. The results of the inphase survey are shown in Figure 43 with contours every 2.5 ppt. The same features as discussed previously also apply to these data.

The results of the magnetometer survey are shown in Figures 44 and 45. Figure 44 shows the results of the total field survey with contours every 500 gammas. The only clear anomaly from this data, not associated with a surface feature, is that at location 140E, 40S. The results of the magnetic gradient survey are shown in Figure 45 with contours every 200 gammas/m. The same anomalies detected in the total field survey are also indicated in this data.

Based on the surveys performed in this portion of the Site 4 area, the following conclusions can be drawn. Although the buildings are hindering any anomaly interpretation near them, there does appear to be a pipelike

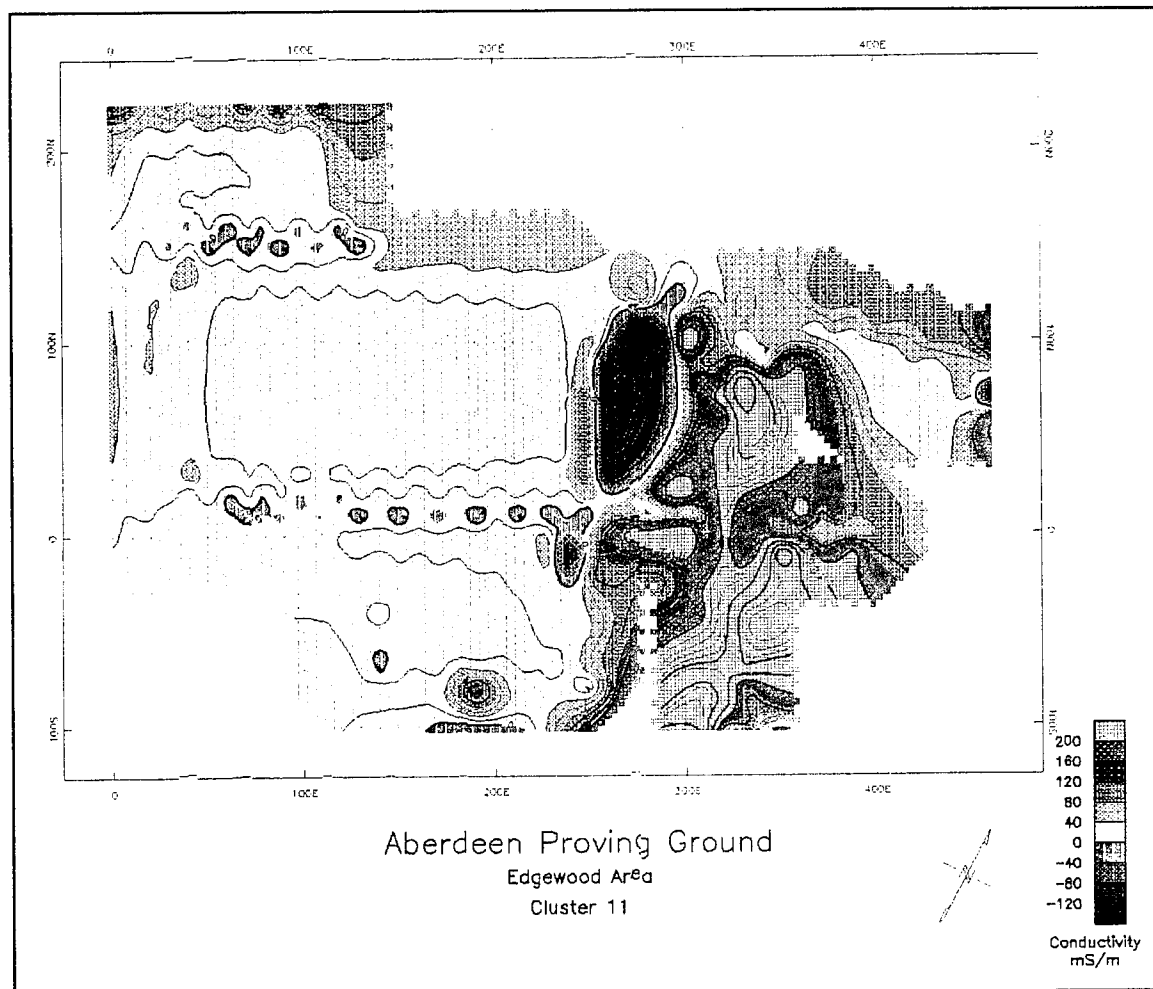


Figure 42. EM-31 conductivity survey for Site 4. Contours are 10 mS/m, and station intervals are 10 ft (3 m)

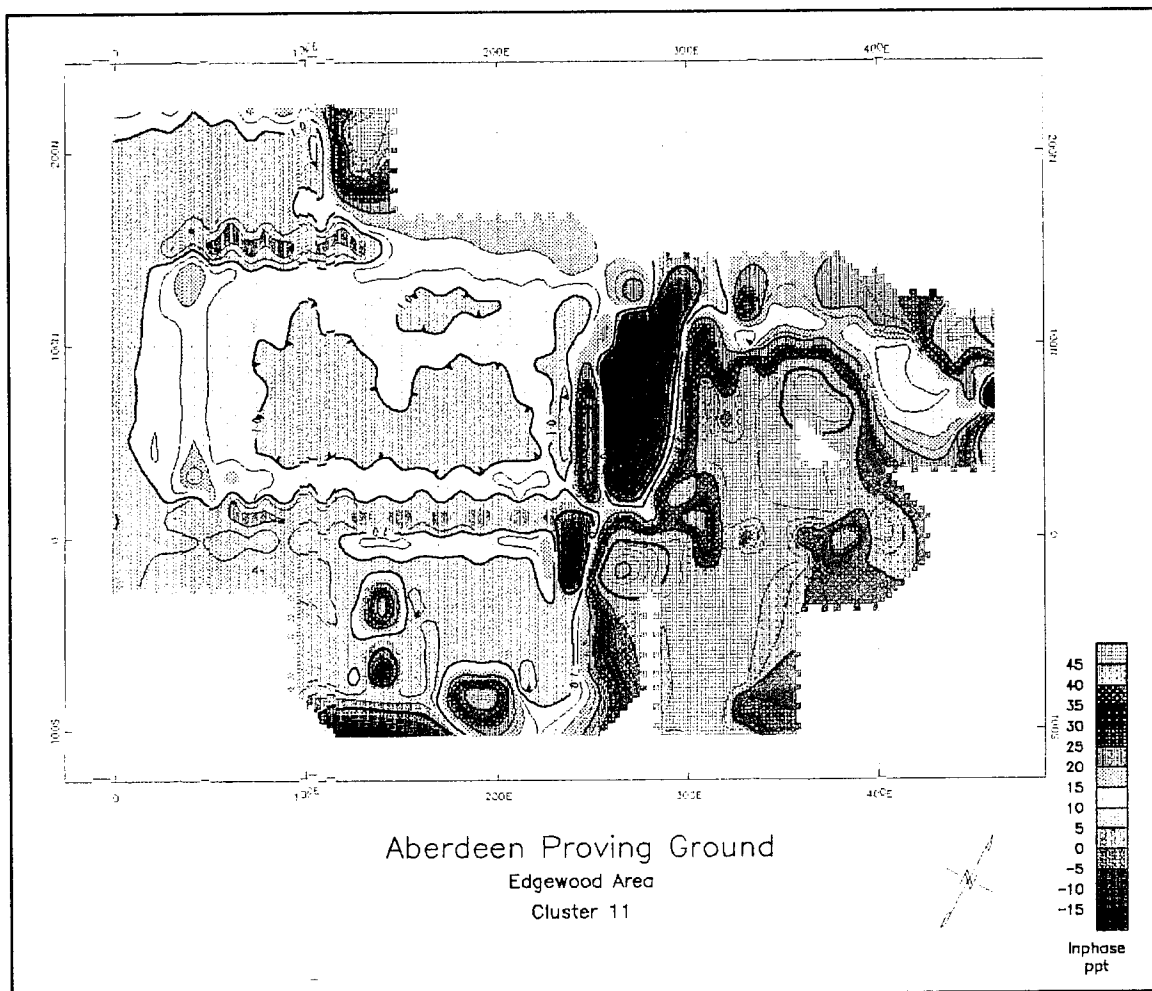


Figure 43. EM-31 inphase survey for Site 4. Contours are 2.5 ppt, and station intervals are 10 ft (3 m)

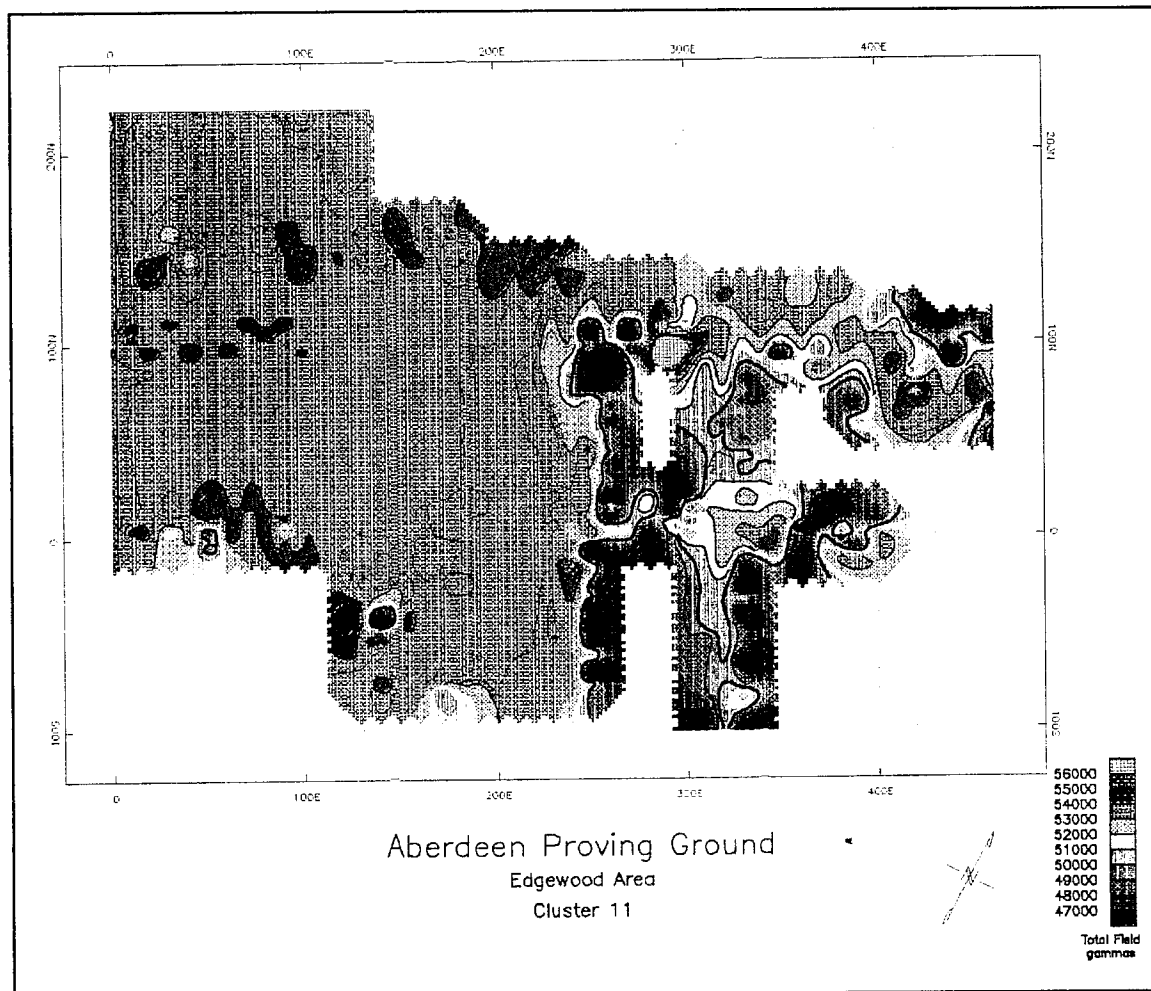


Figure 44. Magnetic total field survey for Site 4. Contours are 250 gammas, and station intervals are 10 ft (3 m)

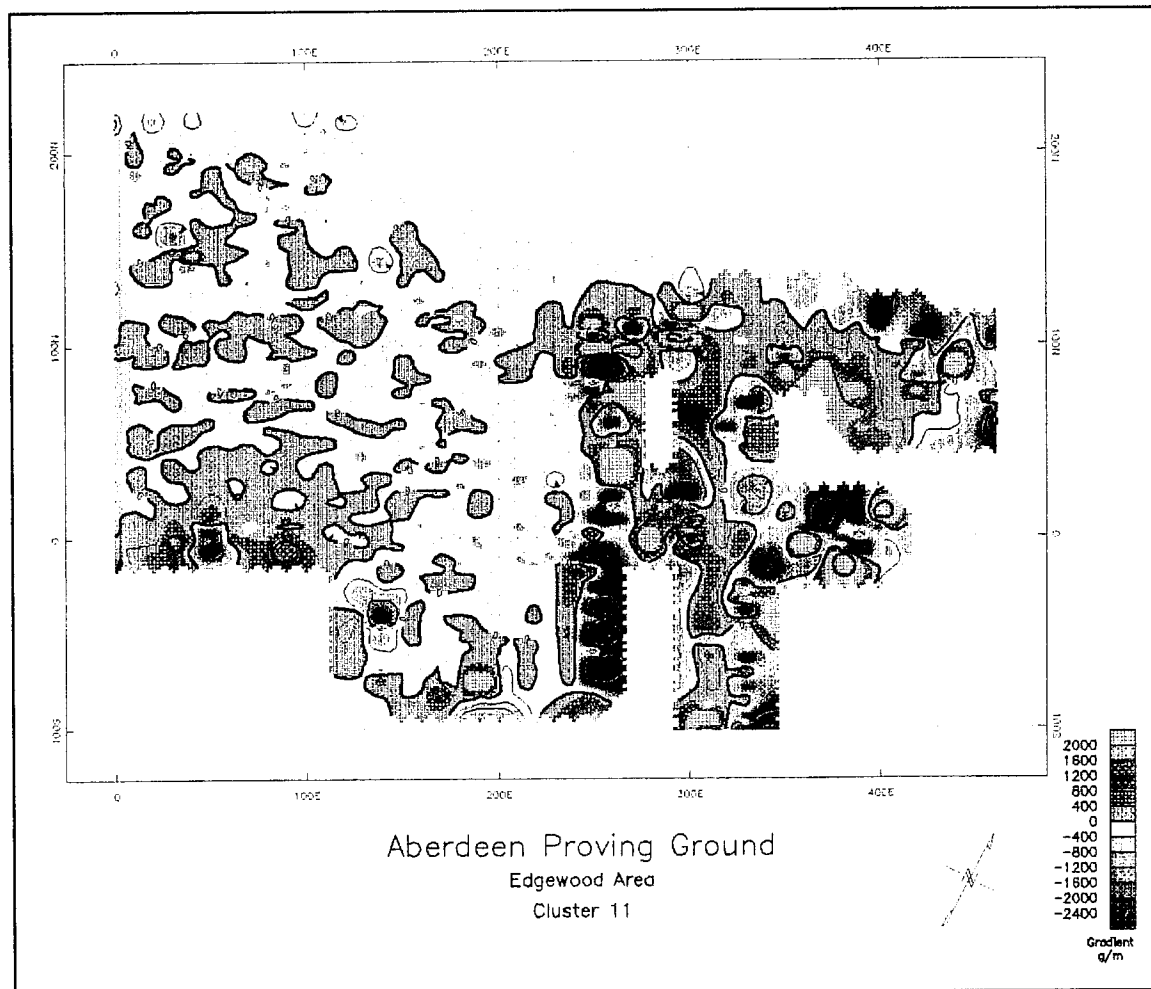


Figure 45. Magnetic gradient survey for Site 4. Contours are 200 gammas/m, and station intervals are 10 ft (3 m)

feature located beside one of the buildings at location 240E from 20N to 100N. The other anomalies unaccounted for by surface features occur at locations 140E, 40S; 230E, 0-20S; 240E, 10 -70N; and 440E, 105N. The causes of these anomalies are unknown. The anomalies detected at Site 4 are presented in Table 3.

Table 3
Anomalies Detected at Site 4

Anomaly	Location	Type	Cause
1	0-100E, 150N	conductive, magnetic	metal rails
2	50-250E, 10N	conductive, magnetic	metal rails
3	190E, 90S	conductive, magnetic	building
4	140E, 40S	conductive, magnetic	unknown
5	270E, 20-120N	conductive, magnetic	building
6	280E, 0-100S	conductive, magnetic	building
7	330E, 0-100S	conductive, magnetic	building
8	330E, 0-100N	conductive, magnetic	building
9	230E, 0-20S	conductive, magnetic	unknown
10	240E, 10-70N	conductive, magnetic	unknown
11	420E, 80N	magnetic	fence
12	440E, 105N	conductive, magnetic	unknown
13	460E, 30N	conductive, magnetic	fence
14	125E, 225N	conductive, magnetic	unknown
15	300E, 0N	conductive, magnetic	constant equipment
16	360E, 100N	conductive, magnetic	pipe
17	250E, 100N	conductive, magnetic	metal vault

Site 5 Results

The Site 5 grid layout and surface features were shown in Figure 9. The results of the EM-31 survey are shown in Figures 46 and 47. Figure 46 shows the results of the conductivity survey with contours every 20 mS/m. The site contains many surface features evidenced in the data. The road running through the site is apparent in the data and trends northeast-southwest from location 200E, 250N to 300E, 480N. Monitoring well 3 appears at location 390E, 500N and the small building just south of MW-3 at location 380E, 470N. The catch basin produces an anomaly at location 350E, 360N. Well WBR-33 and the tank located south of it in addition to a power pole all combine to produce the large anomaly at location 350E, 300N. The results of the inphase survey are shown in Figure 47 with contours every 2.5 ppt. The only apparent anomalies are from surface features.

The results of the magnetometer survey are shown in Figures 48 and 49. Figure 48 shows the results of the total field survey with contours every

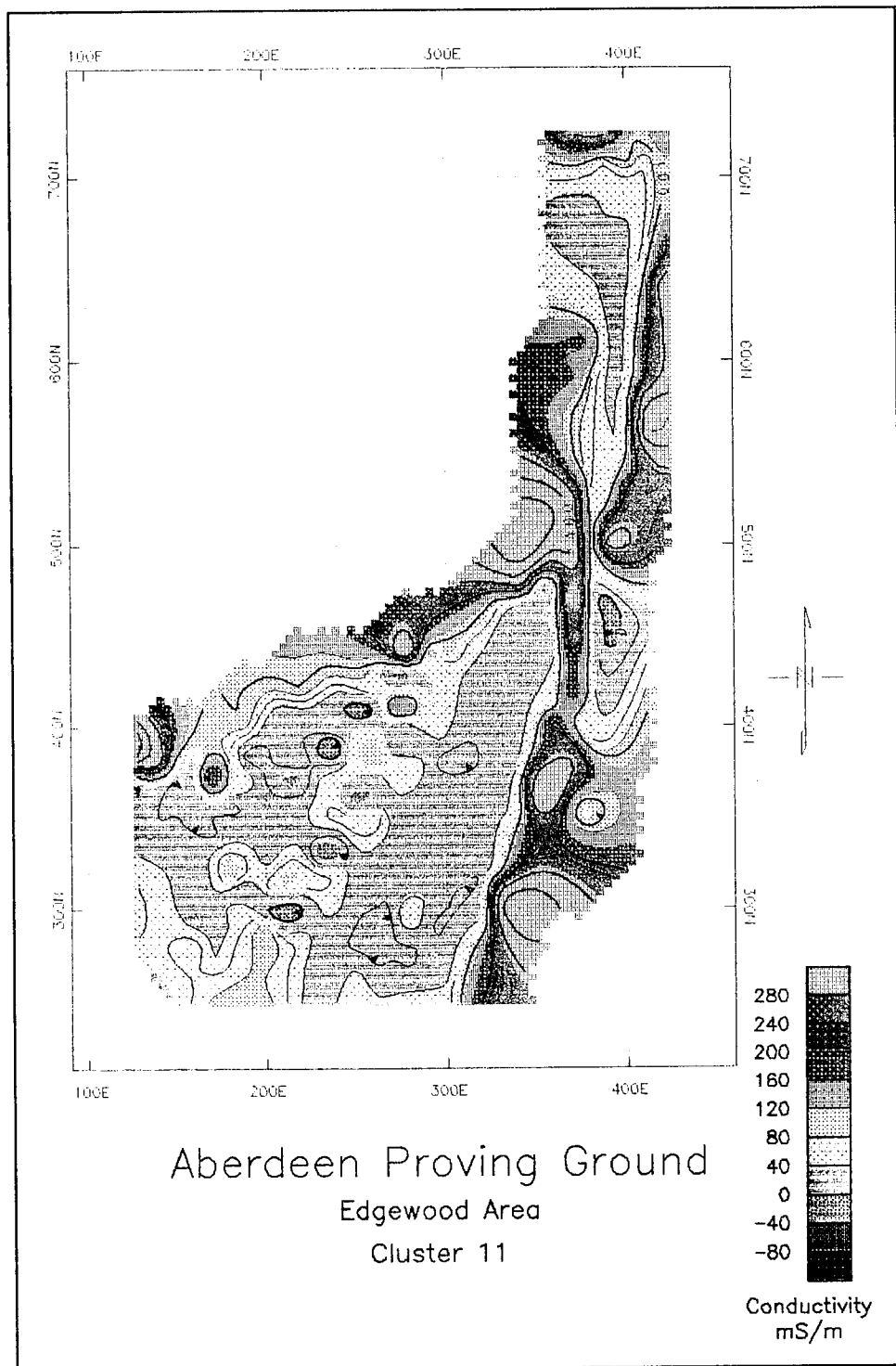


Figure 46. EM-31 conductivity survey for Site 5. Contours are 10 mS/m, and station intervals are 10 ft (3 m)

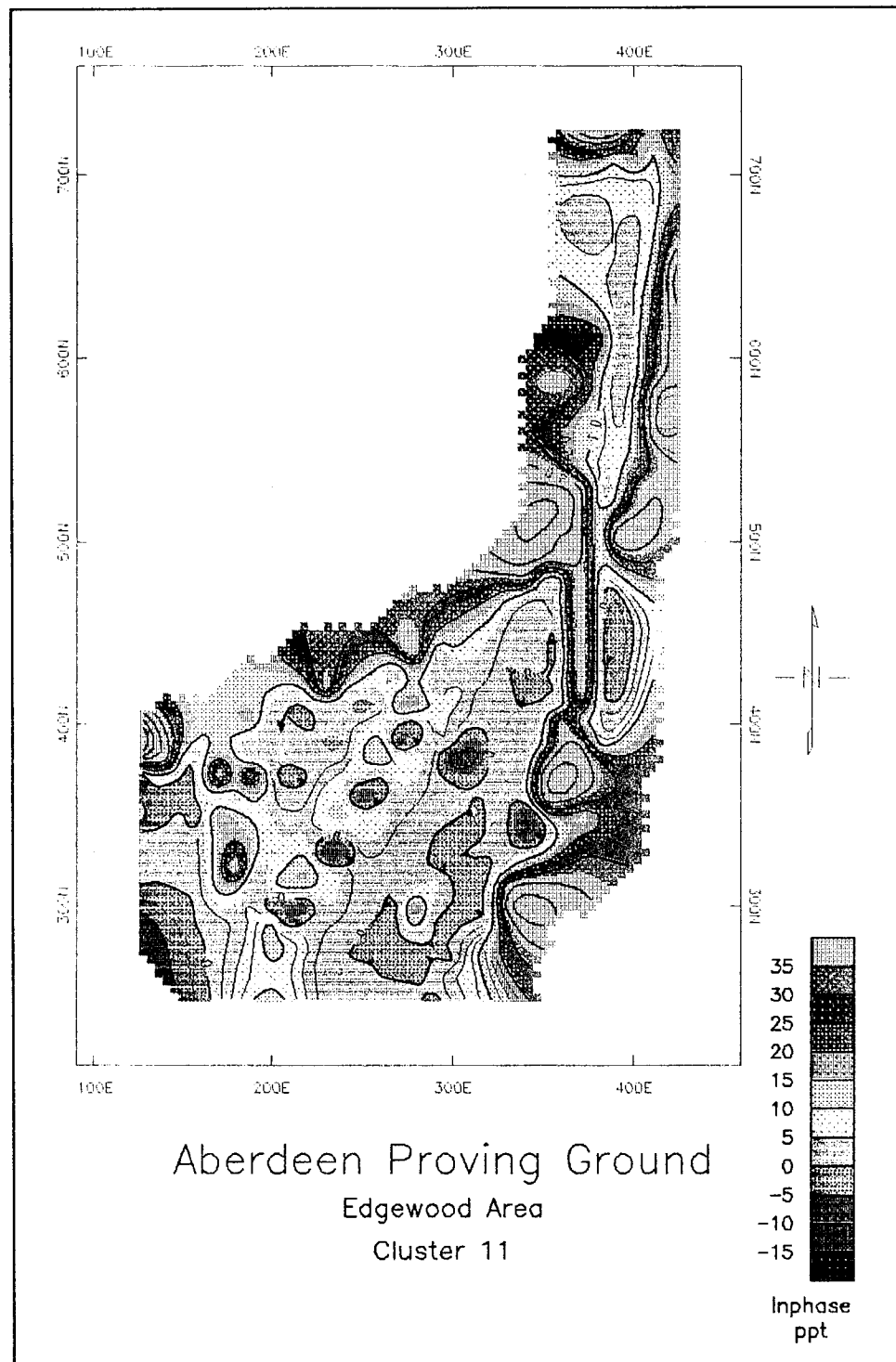


Figure 47. EM-31 inphase survey for Site 5. Contours are 2.5 ppt, and station intervals are 10 ft (3 m)

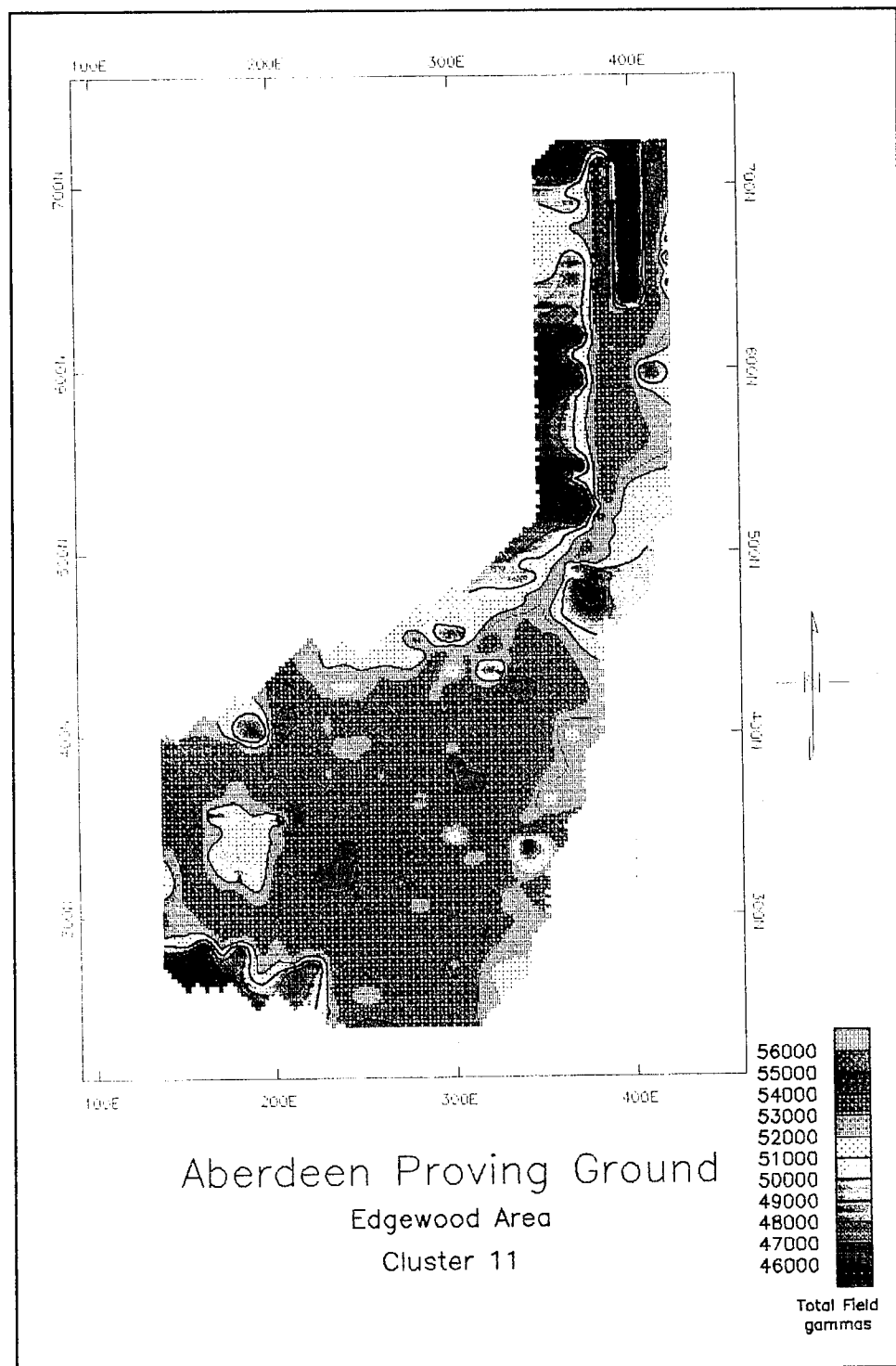


Figure 48. Magnetic total field survey for Site 5. Contours are 250 gammas, and station intervals are 10 ft (3 m)

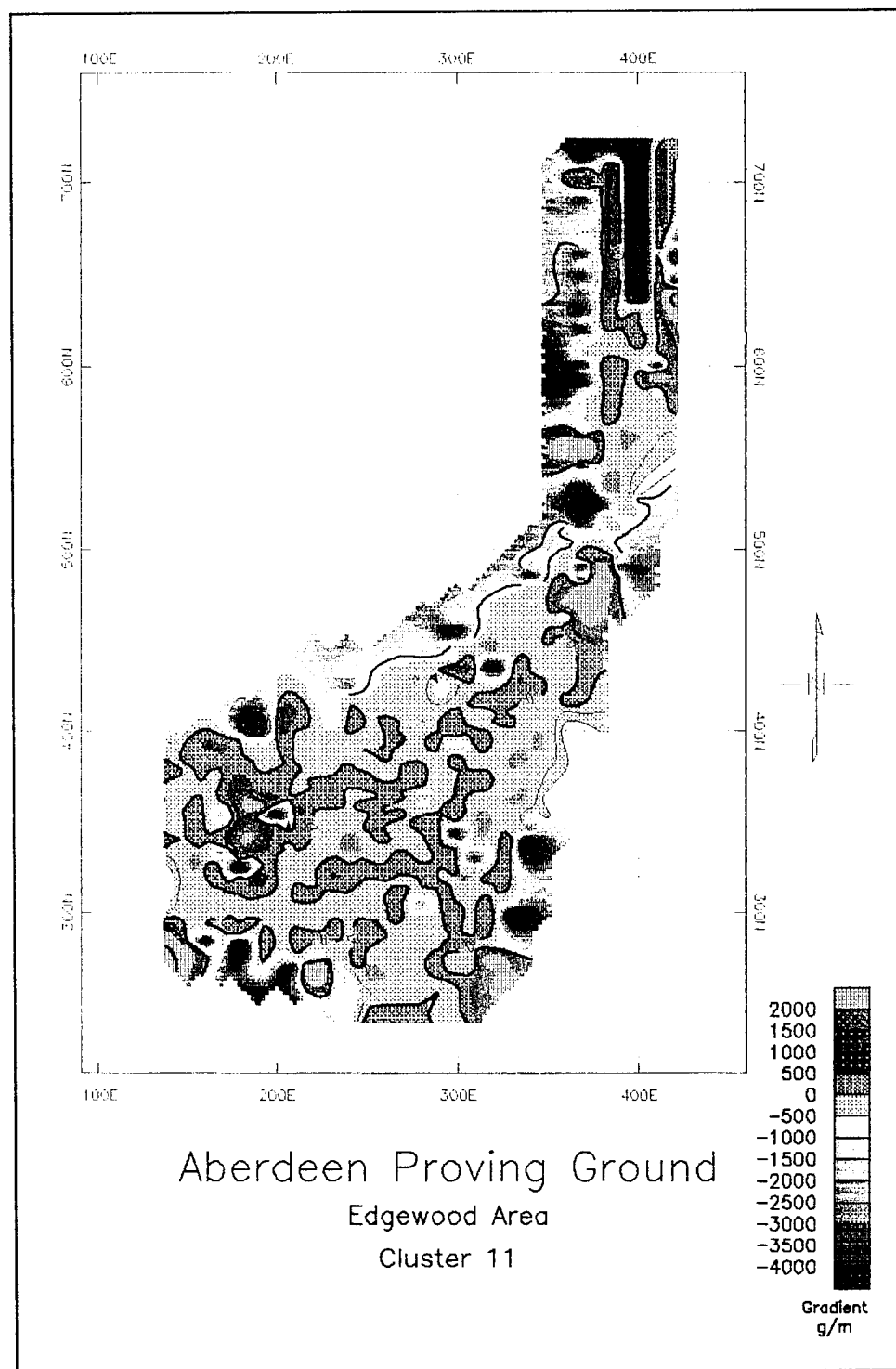


Figure 49. Magnetic gradient survey for Site 5. Contours are 250 gammas/m, and station intervals are 10 ft (3 m)

500 gammas. Figure 49 shows the results of the magnetic gradient survey with contours every 250 gammas/m. The anomalies are likely due to surface features.

Based on the surveys performed in this area, the detected anomalies are likely correlated to known surface features. The anomalies detected at this area are shown in Table 4.

Table 4
Anomalies Detected at Site 5

Anomaly	Location	Type	Cause
1	400E,600N	conductive, magnetic	unknown
2	380E,500N	conductive, magnetic	monitoring well
3	370E,480N	conductive, magnetic	building
4	330E,420N	magnetic	unknown
5	310E,380N	conductive, magnetic	culvert
6	230E,320N	conductive, magnetic	unknown
7	180E,340N	conductive, magnetic	building
8	200E,400N	conductive, magnetic	fence
9	360E,360N	conductive, magnetic	monitoring well
10	340E,300N	conductive	underground tank
11	340E,580N	conductive, magnetic	fence
12	340E,500N	conductive, magnetic	fence
13	270E,440N	conductive, magnetic	fence
14	130E,390N	conductive, magnetic	fence

Site 6 Results

The Site 6 grid layout and surface features were shown in Figure 10. The results of the EM-31 survey are shown in Figures 50 and 51. Figure 50 shows the results of the conductivity survey, with contours every 10 mS/m. An anomalous zone with a northeast-southwest trend extends across the site. No surface feature is associated with this very large anomaly. The only other anomalous areas in the survey are at locations 20E,320N (associated with the fence), and at location 100E,0N (associated with the abandoned building). The results of the inphase survey are shown in Figure 51, with contours every 1 ppt. The same results determined from the conductivity survey are apparent for the inphase survey.

The results of the magnetic survey are shown in Figures 52 and 53. Figure 52 shows the results of the total field survey with contours every 250 gammas. Although not as apparent, the same northeast-southwest trending anomaly is detected in the data. In addition to this, the paved road produces a signature trending north-south at location 190E. The magnetic effects of the building are detected in the southern portion of the plot and the chain

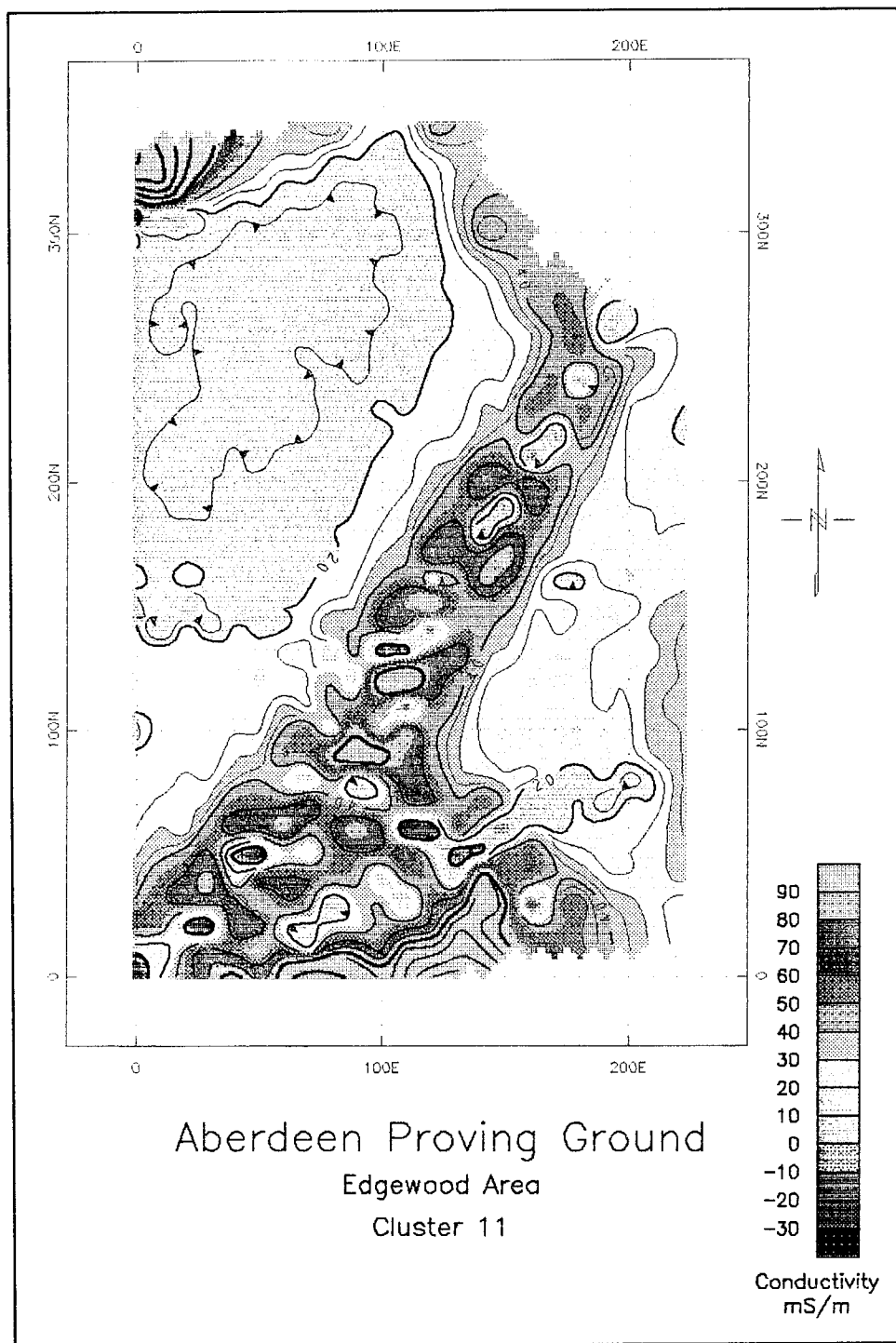


Figure 50. EM-31 conductivity survey for Site 6. Contours are 5 mS/m, and station intervals are 10 ft (3 m)

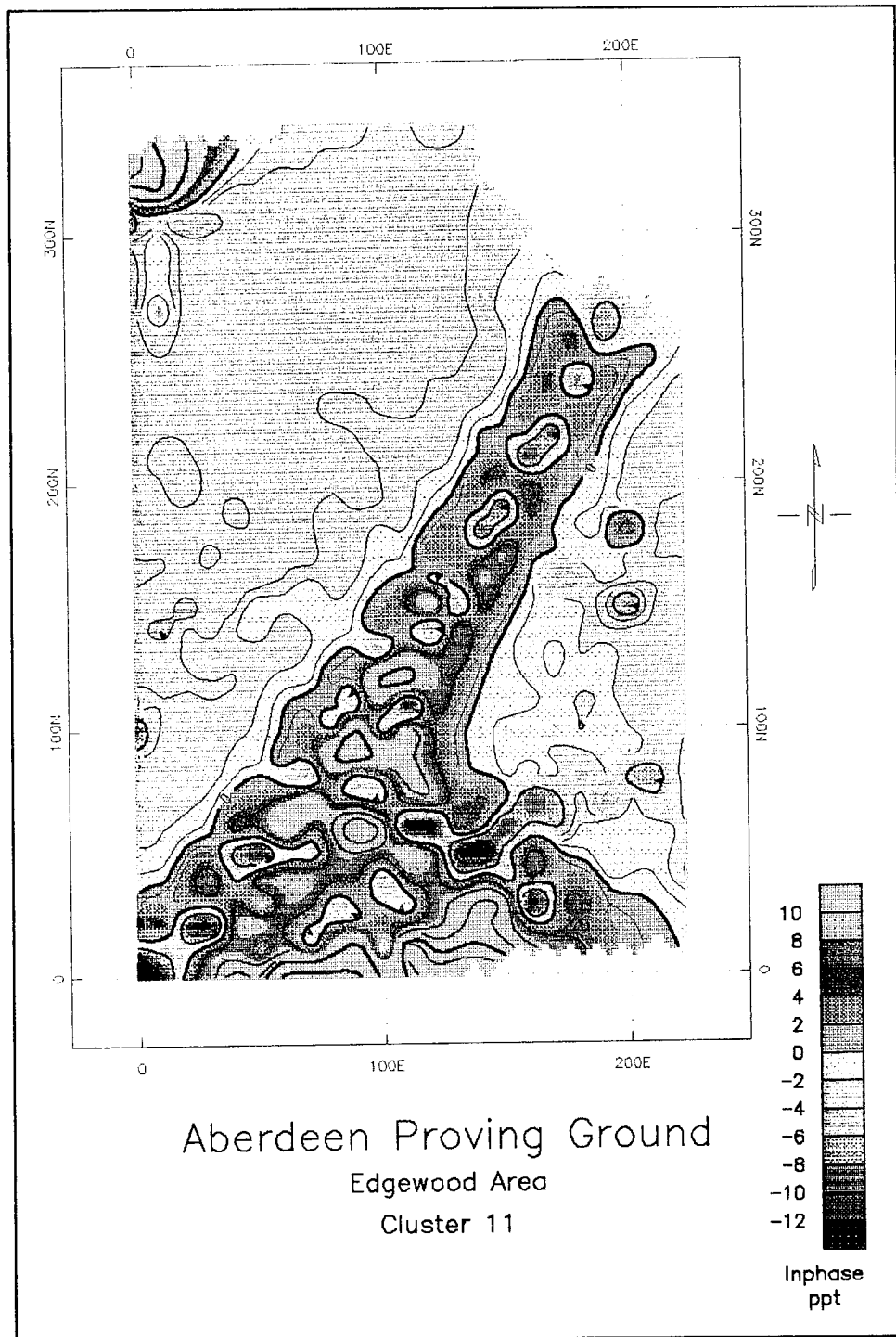


Figure 51. EM-31 inphase survey for Site 6. Contours are 1 ppt, and station intervals are 10 ft (3 m)

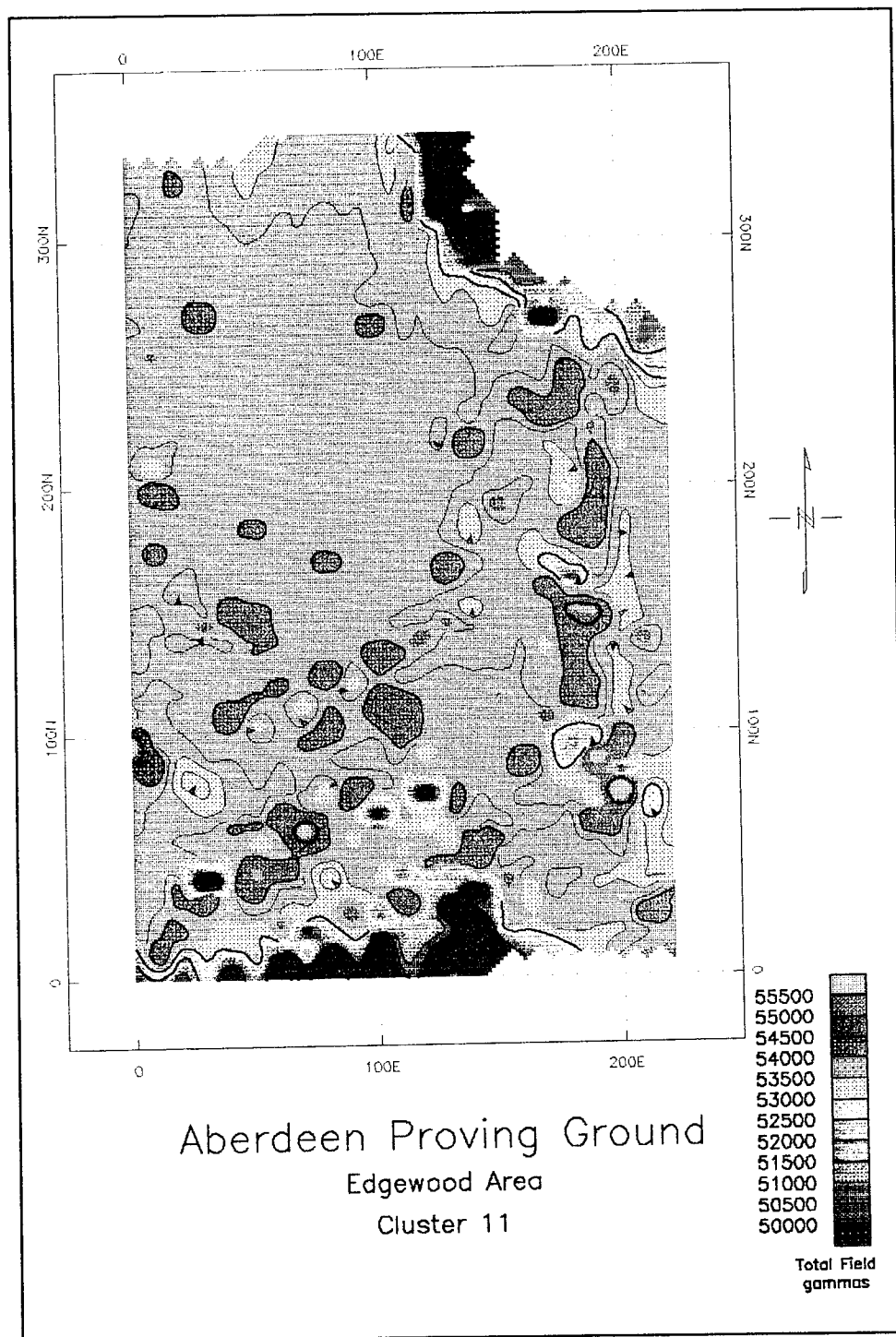


Figure 52. Magnetic total field survey for Site 6. Contours are 250 gammas, and station intervals are 10 ft (3 m)

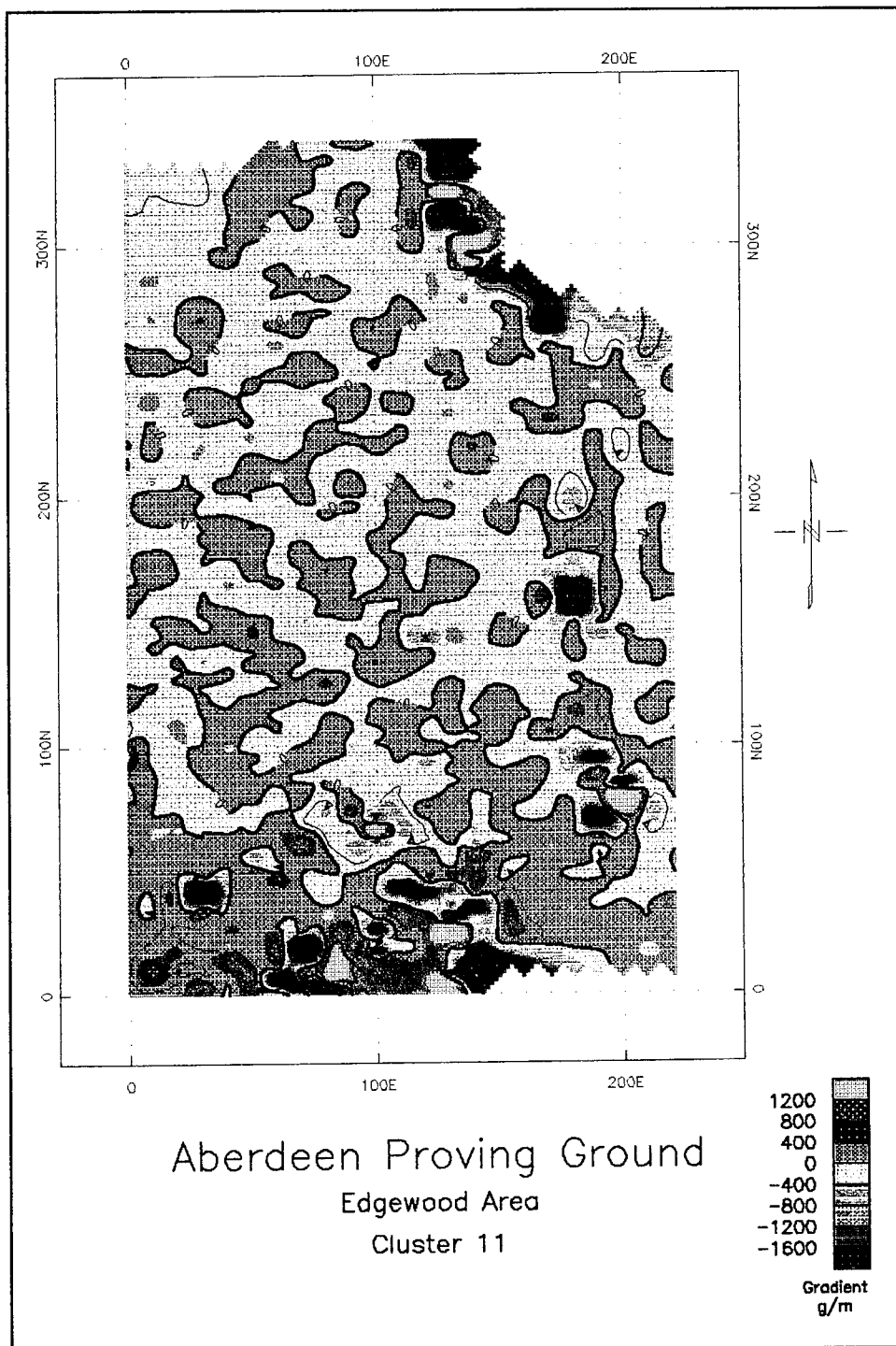


Figure 53. Magnetic gradient survey for Site 6. Contours are 200 gammas/m, and station intervals are 10 ft (3 m)

link fence in the northeast portion of the plot. The results of the magnetic gradient survey are shown in Figure 53, with contours every 200 gammas/m. The results from this survey are not nearly as conclusive as the others, although a very slight indication of the paved road can be seen.

The results of the EM-61 survey are shown in Figures 54 through 56. Figure 54 is a plot of the results from the bottom coil of the instrument, with contours every 50 mV. The northeast-southwest trending anomaly is apparent, as is the building and wells that appear in the southern portion of the plot. A plot of the results from the top coil of the instrument is shown in Figure 55 with contours every 50 mV. The same anomalies are apparent in this data as discussed for the bottom coil. Figure 56 is a plot of the difference between the two coils. This figure shows the anomalies extremely well. The building and wells are apparent in the southern portion of the plot, and the northeast-southwest trending anomaly is also clearly apparent. Also apparent is an anomaly at location 190E, 160N which is associated with a concrete drainage structure passing beneath the paved road. This anomaly can also be seen in Figures 50 through 55.

Based on the surveys conducted in this area, the following conclusions can be drawn. One anomaly that is not associated with a known surface feature is the large northeast-southwest trending anomaly. This anomaly is both a conductive and magnetic (based on the EM-31) anomaly. However, the results from the magnetometer survey did not indicate a very strong anomaly which would be indicative of ferrous material. The EM-61 did show a very large response to the anomaly since it responds well to metallic and non-metallic material. The possibilities for the cause of the anomaly would be a trench or drainage system containing slightly metallic rocks, or possibly a non-ferrous pipe. A summary of anomalies detected at this site is shown in Table 5.

Offshore Results

The layout of the grid for the offshore survey was shown in Figure 2. The results of the survey for offshore Site 1 are shown in Figures 57 through 59. Figure 57 shows the results of the EM-31 conductivity survey with contours every 5 mS/m. The effects of the concrete WWII pier can be seen in the southern portion of the plot. There is a general trend of increasing conductivity values away from the shore. There is also a large area of high conductivities in a linear feature trending nearly east-west from location 100E, 660N to location 300E, 800N. The results of the inphase survey are shown in Figure 58 with contours every 0.5 ppt. The same features are apparent in this data as previously discussed. The results of the magnetometer total field survey are shown in Figure 59 with contours every 20 gammas. These results do not show the linear trend associated with the EM-31 data. There are several smaller isolated anomalies scattered throughout the data. The anomalies detected at this site are presented in Table 6.

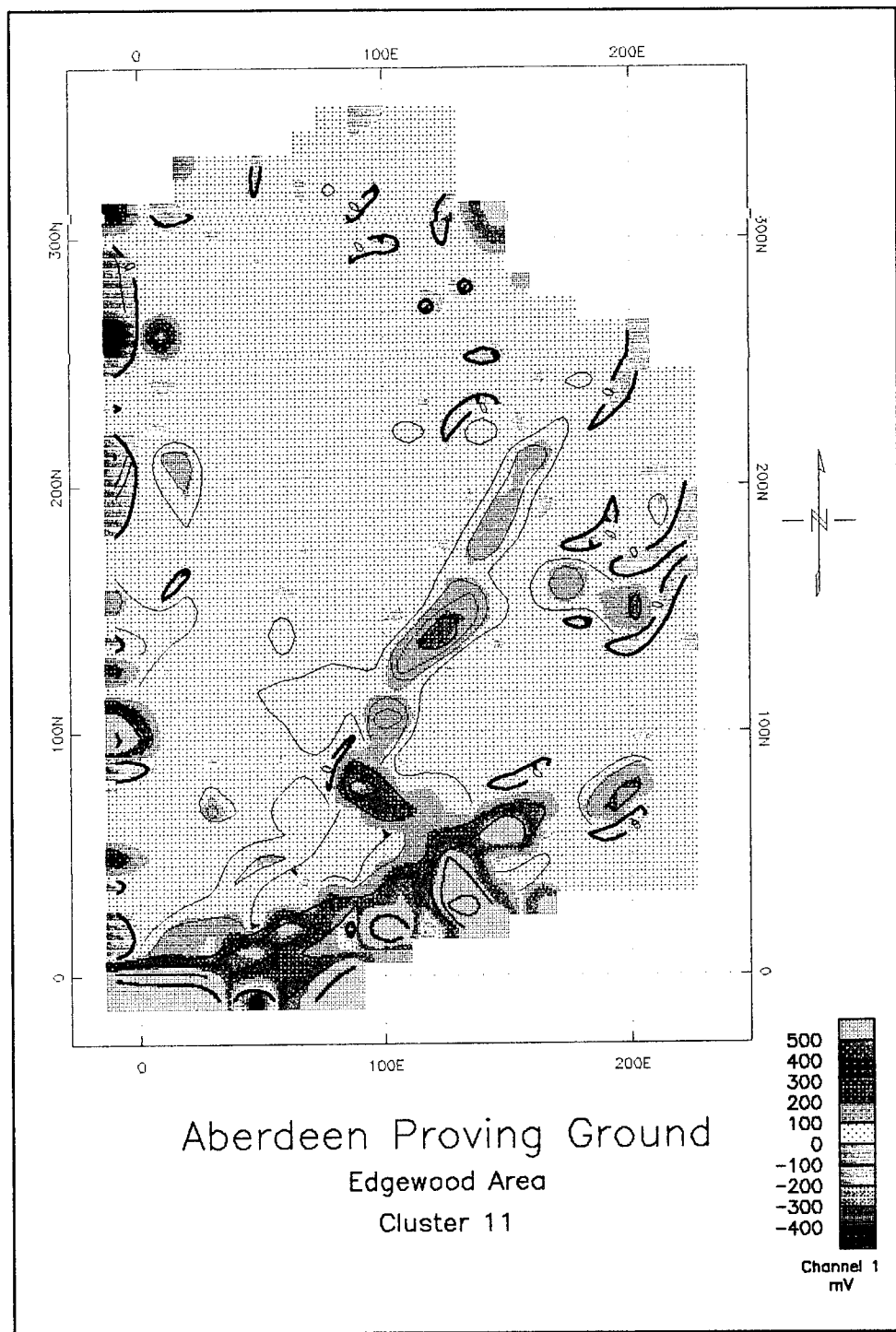


Figure 54. EM-61 bottom coil survey for Site 6. Contours are 50 mV, and station intervals are 10 ft (3 m)

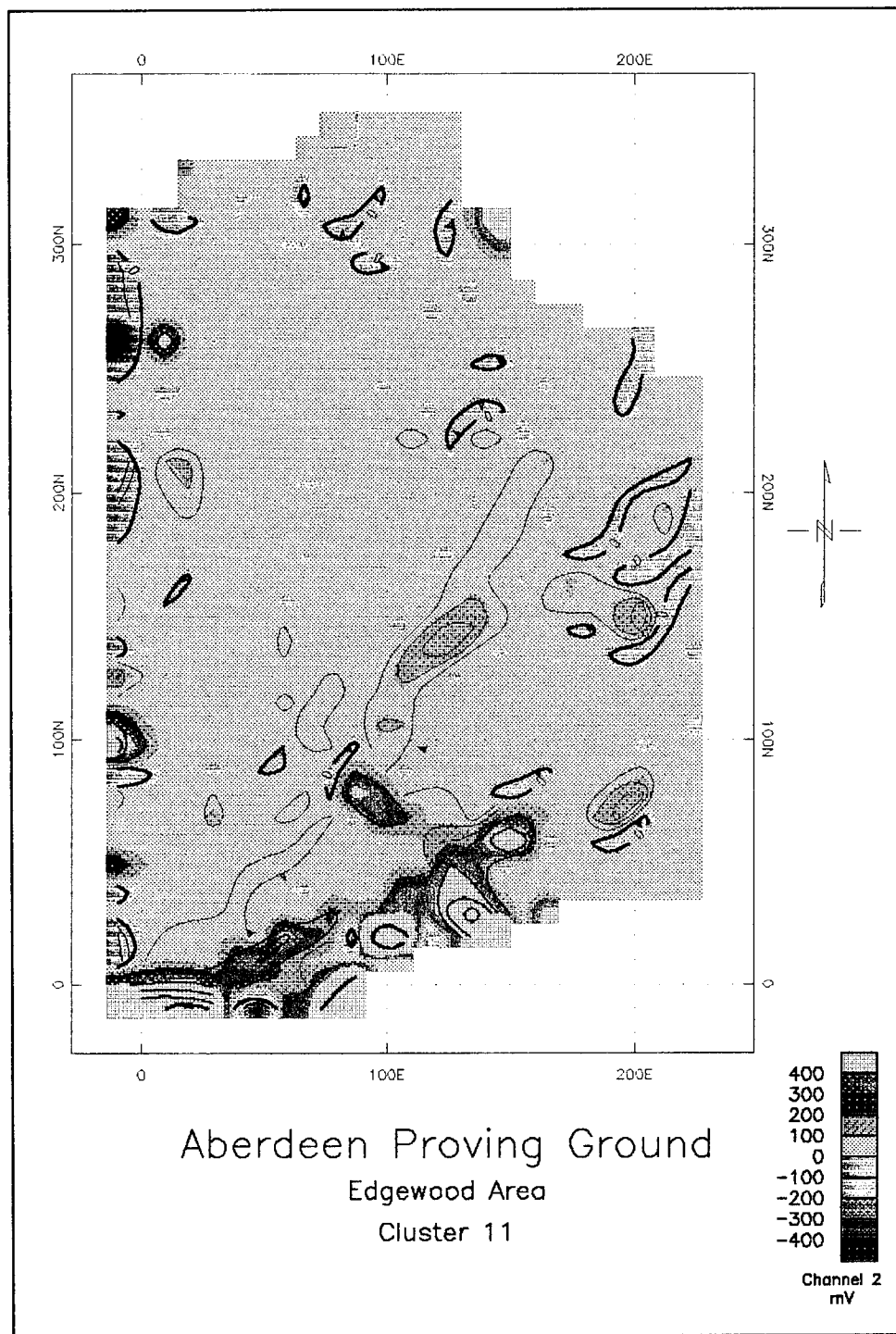


Figure 55. EM-61 top coil survey for Site 6. Contours are 50 mV, and station intervals are 10 ft (3 m)

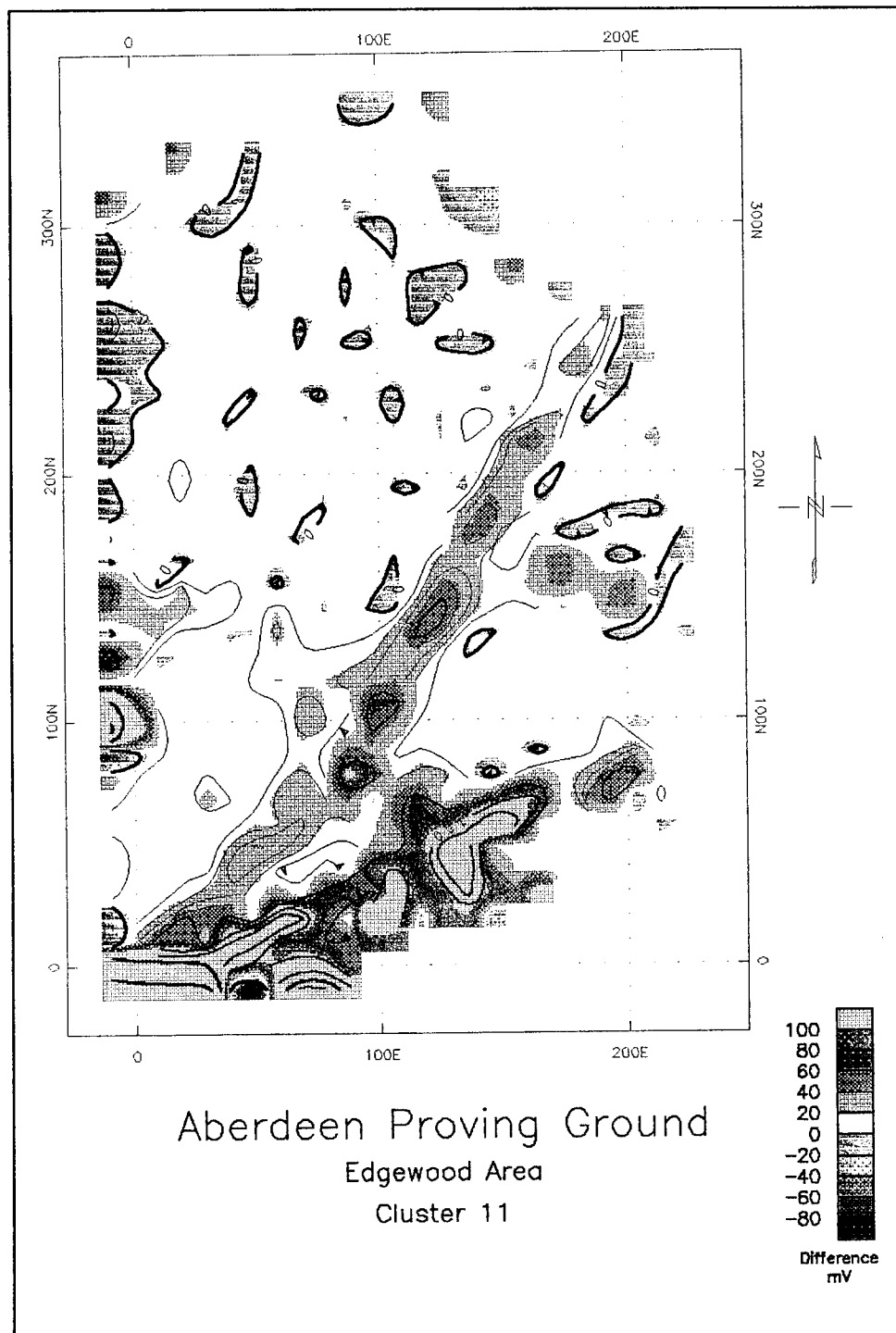


Figure 56. EM-61 difference between top and bottom coils survey for Site 6. Contours are 10 mV, and station intervals are 10 ft (3 m)

Table 5
Anomalies Detected at Site 6

Anomaly	Location	Type	Cause
1	10E,330N	conductive, magnetic	fence
2	140E,300N	conductive, magnetic	fence
3	0E,0N-200E,280N	conductive, magnetic	unknown
4	190E,160N	conductive, magnetic	culvert
5	0E,0N-160E,60N	conductive, magnetic	building
6	0E,100N	conductive, magnetic	sign
7	0E,200N	conductive, magnetic	unknown
8	0E,250N	conductive, magnetic	unknown
9	200E,190N	conductive, magnetic	sign

The results of the survey for offshore Site 2 are shown in Figures 60 through 62. Figure 60 shows the results of the EM-31 conductivity survey with contours every 5 mS/m. This plot shows two very large conductive anomalies. Both anomalies are trending nearly east-west. The first anomaly appears to be from location 0E,0N to location 200E,200N. The second anomaly from location 100W,900N to location 200E,1100N. This particular anomaly is directly associated with the fill that occurred at Site 2. The results of the inphase survey are shown in Figure 61. The same two linear trends as discussed previously are also apparent in this data. The results of the magnetic total field survey are shown in Figure 62 with contours every 50 gammas. The results show only two anomalous areas, that associated with a pier in the southern portion of the plot and that at location 100W,950N.

Based on the surveys performed at this site the following conclusions can be drawn. The cause of the linear trending anomaly located at offshore Site 1 is unknown. There are no onshore structures adjacent to this area that would account for the anomaly's occurrence (pipes, tracks, trash, etc.). Since there was no response from the magnetometer survey, the anomaly is not produced by ferrous material. The most likely cause of this feature is a channelized drainage system, or a non-ferrous structure. The two anomalies that appear in the offshore Site 2 area are also unknown in origin. The anomalous area near the power plant pier is most likely associated with the pier's construction or activity on and around the pier. The other anomalous area near location 1000N, is directly adjacent to the Site 2 area. This can be clearly seen in Figure 2. This area does not appear anomalous in the magnetometer survey, again implying that there is no ferrous material in this location. Since the land survey at Site 2 indicates the presence of fill like material, it is possible that this material may have entered into the offshore area as well. This area also serves as the recipient of drainage for the area associated with Sites 1, 2, and 3, which contributes to the large conductive anomaly.

Table 6
Anomalies Detected at Offshore Site 1

Anomaly	Location	Type	Cause
1	200E,10N	conductive, magnetic	pier
2	150E,900N	conductive, magnetic	pier
3	100E,660N-300E,800N	conductive, magnetic	unknown
4	280E,560N	conductive magnetic	unknown
5	280E,520N	conductive, magnetic	unknown
6	160E,340N	conductive, magnetic	unknown
7	120E,150N	magnetic	unknown
8	60E,100N	magnetic	unknown
9	0E,150N	conductive, magnetic	unknown
10	20E,250N	conductive, magnetic	unknown

Table 7
Anomalies Detected at Offshore Site 2

Anomaly	Location	Type	Cause
1	0E,0N-200E,200N	conductive, magnetic	pier
2	100W,950N	conductive, magnetic	fence
3	100W,900N-200E,1100N	conductive, magnetic	unknown

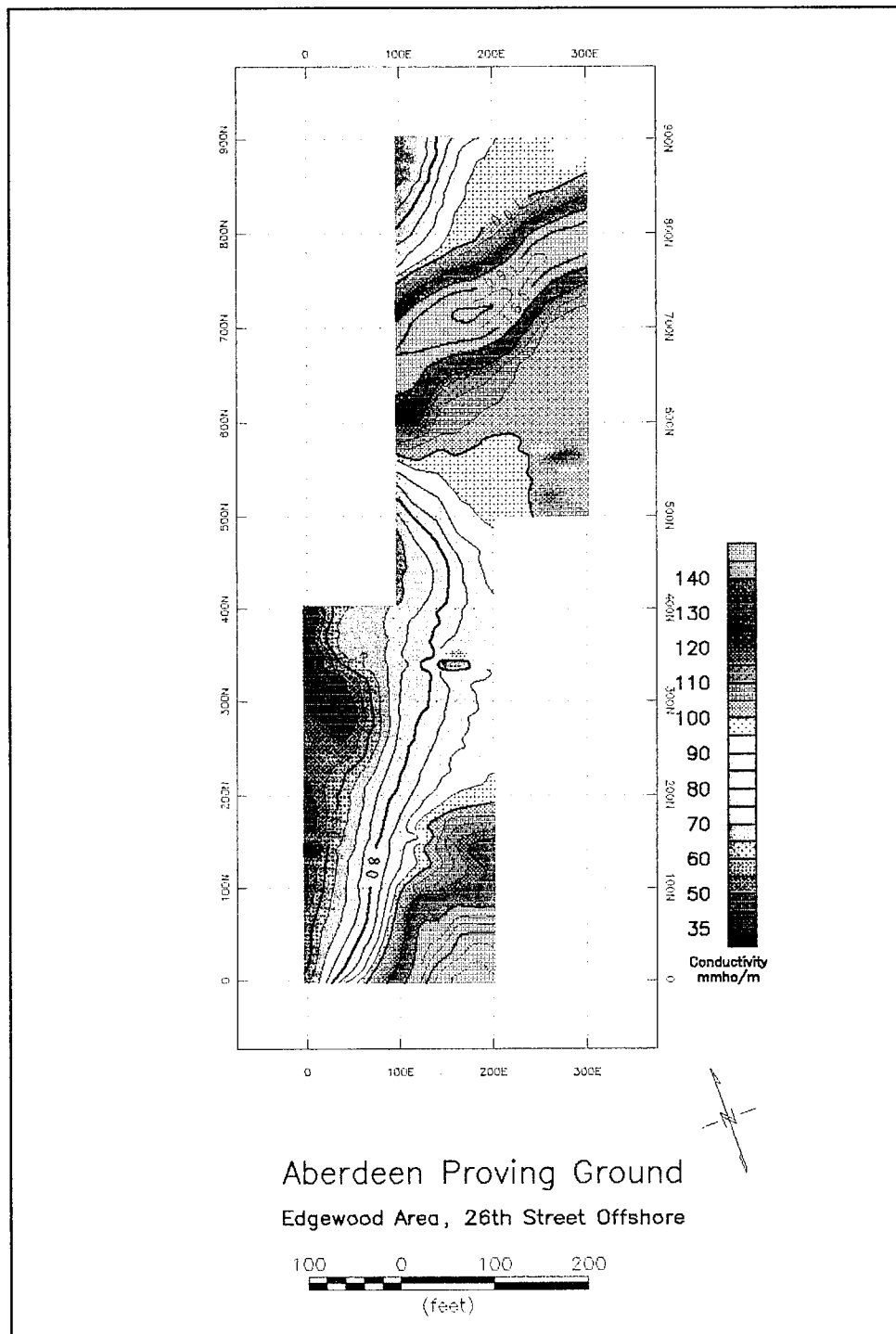


Figure 57. EM-31 conductivity survey for Offshore Site 1. Contours are 5 mS/m, and station intervals are 10 ft (3 m)

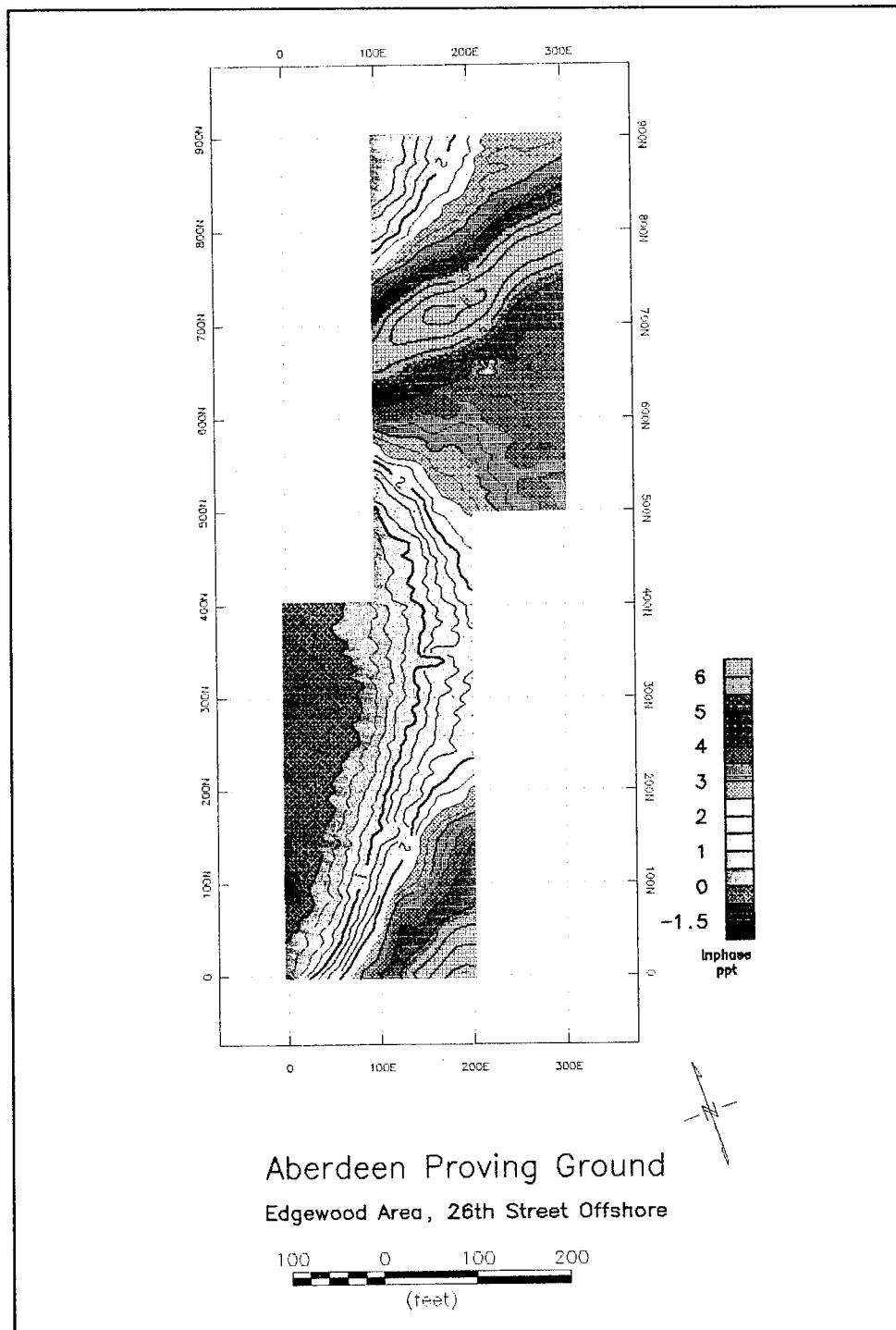


Figure 58. EM-31 inphase survey for Offshore Site 1. Contours are 0.5 ppt, and station intervals are 10 ft (3 m)

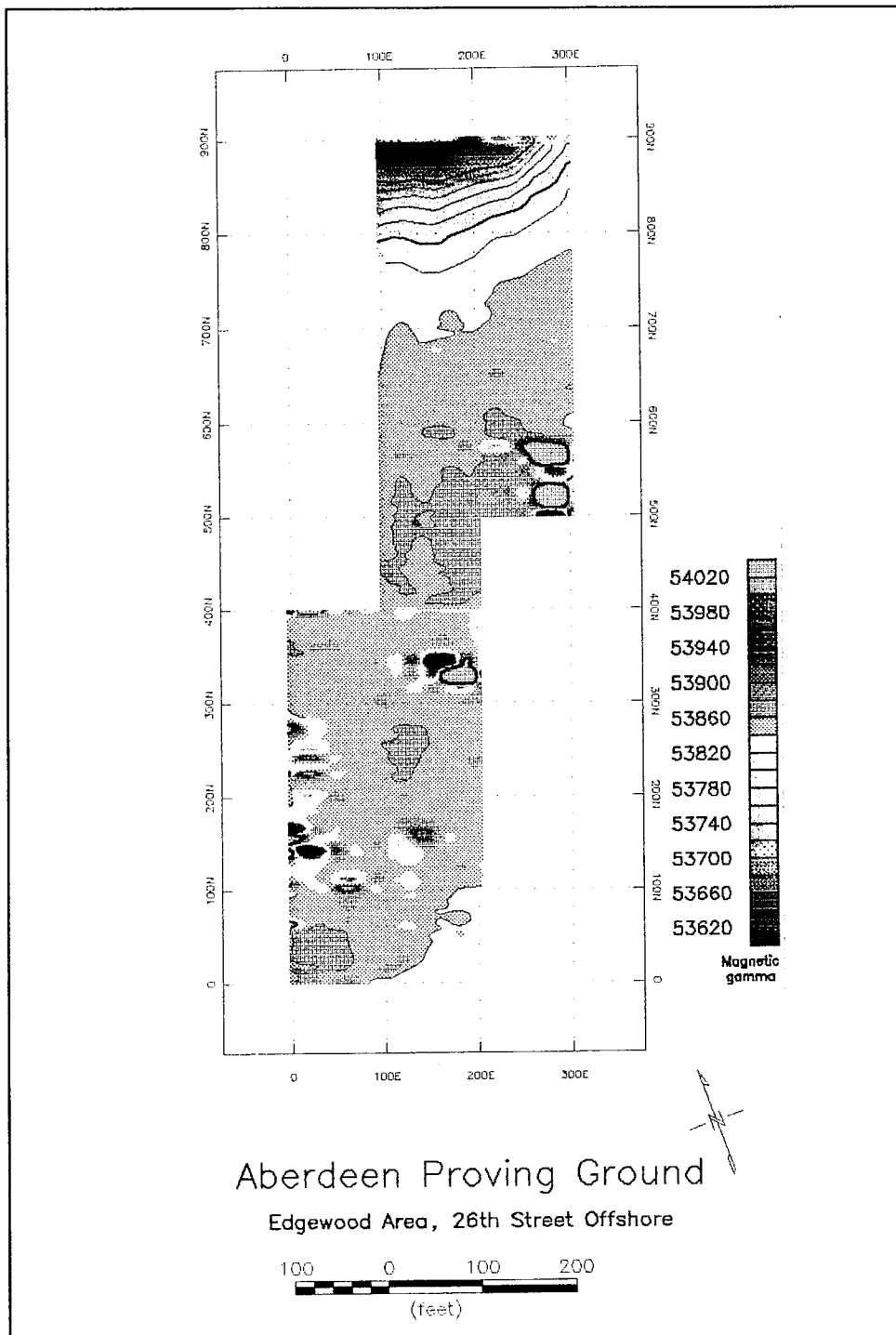


Figure 59. Magnetic total field survey for Offshore Site 1. Contours are 20 gammas, and station intervals are 10 ft (3 m)

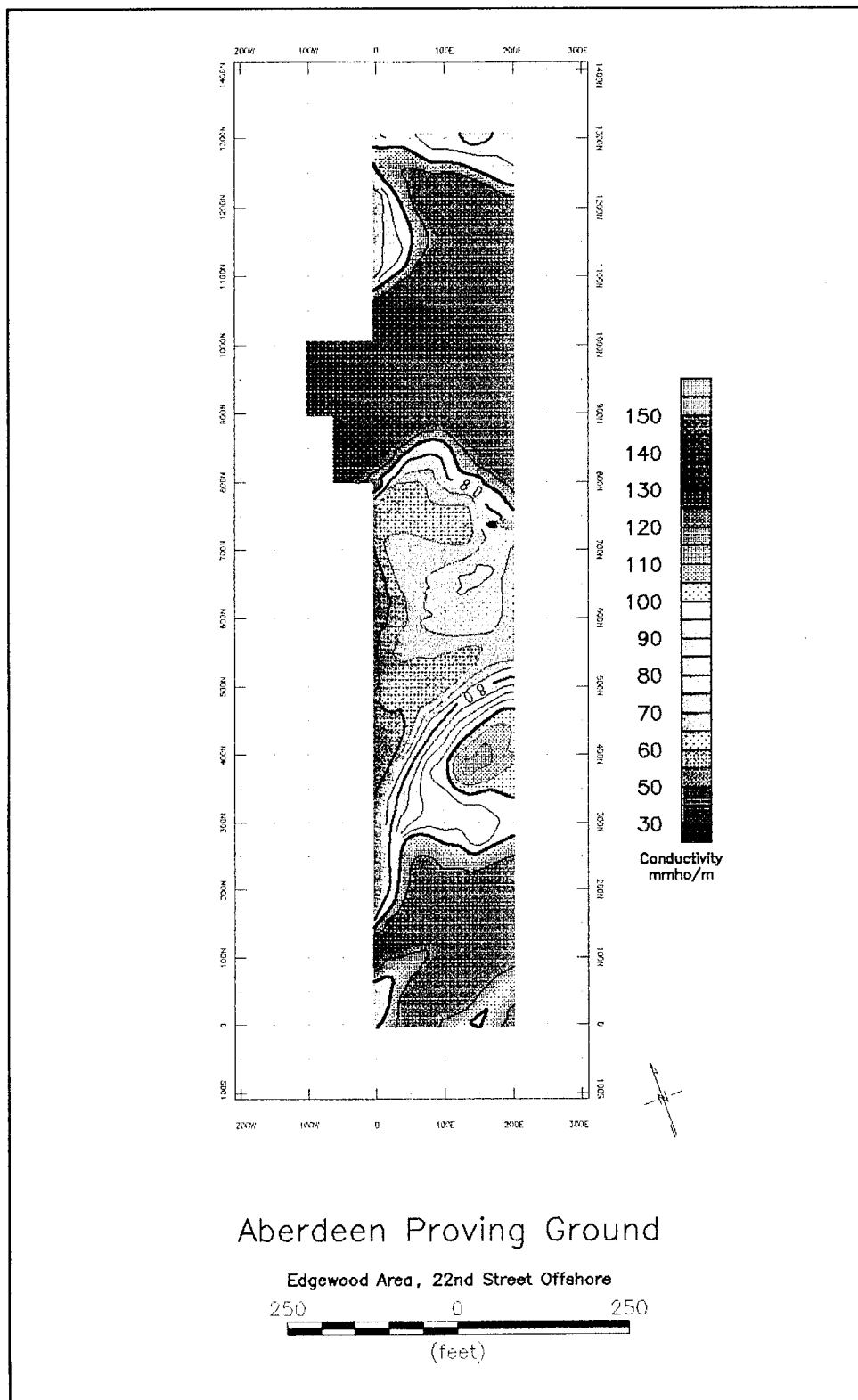


Figure 60. EM-31 conductivity survey for Offshore Site 2. Contours are 5 mS/m, and station intervals are 10 ft (3 m)

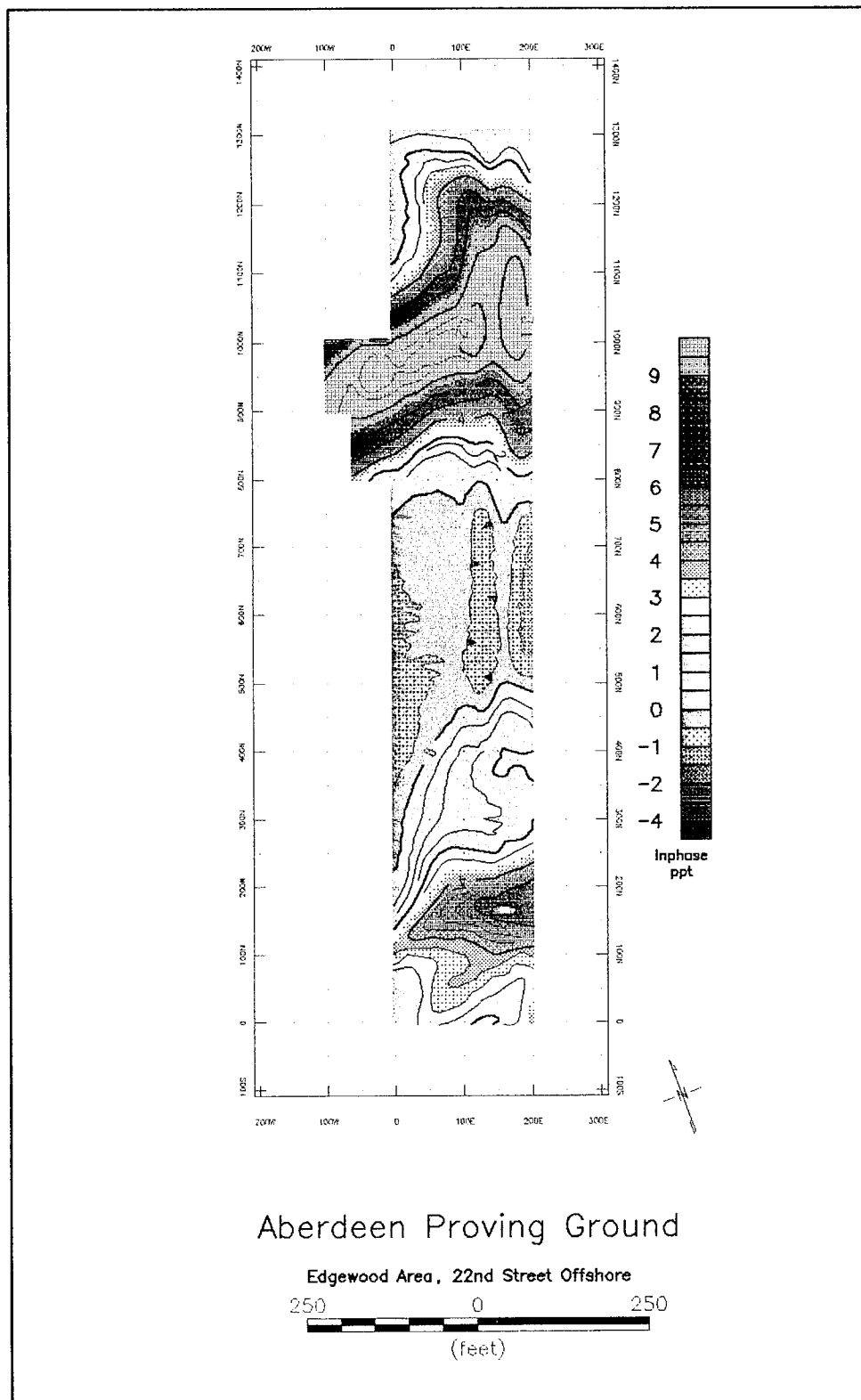


Figure 61. EM-31 inphase survey for Offshore Site 2. Contours are 0.5 ppt, and station intervals are 10 ft (3 m)

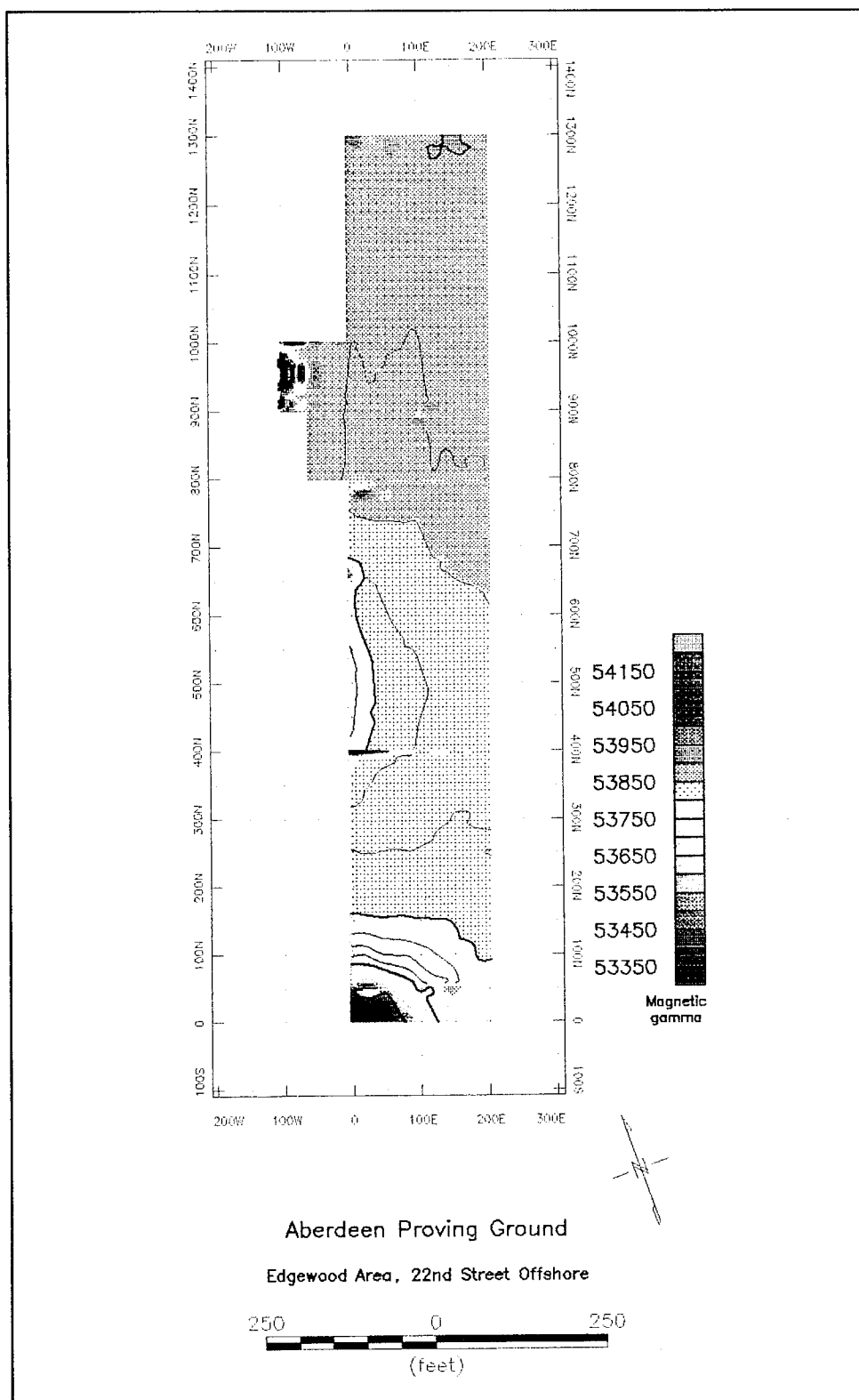


Figure 62. Magnetic total field survey for Offshore Site 2. Contours are 50 gammas, and station intervals are 10 ft (3 m)

5 Summary

A geophysical investigation was conducted on a portion of the Bush River Study Area at APG/EA, designated as Cluster 11. This area consists of four solid waste management units (SWMU) termed 22nd street landfill, ton container steamout site, adamsite storage pit and radioactive material disposal facility. These SWMU's were identified in the RCRA Facility Assessment Report for the EA, APG, by Nemeth 1989. A geophysical investigation was conducted at the Cluster 11 site by WES personnel during August 1994. The objective of the investigation was to delineate anomalies indicative of a landfill or other burial activities (such as tanks, barrels, etc.) and to collect information to aid in the geological site characterization. Five geophysical methods were used in this investigation: electric, magnetic, EM, GPR and surface seismic surveys.

The area to be investigated was initially established and subdivided into smaller areas based upon physical constraints. The Cluster 11 area was divided into six sites, shown in Figure 2. Site 1 was the wooded area just west of the 22nd street landfill and north of Building E2314. Site 2 was the large open area where the major portion of landfilling activity supposedly occurred. Site 3 is located west of the rad yard in a large open area. This site may have also been part of the landfilling activity associated with 22nd street. Site 4 consist of the area associated with the radioactive material disposal facility. Site 5 is located east of Site 4 and is also surrounded by a chain link fence. Site 6 is located just north of the old power plant building that is now abandoned. The area along the shoreline from the old WWII pier north to Eagle point was also surveyed. The grid for this area is shown in Figure 2. The area was divided into two grids based on the orientation of the shoreline. The first grid extended from the WWII pier north to the pier associated with the old power plant building. The second grid extended from the old power plant building pier north to just south of Eagle point.

Onshore Sites 1-6

At Site 1, the Building (E2314) clearly affected each survey and in effect masks any other results that might have been obtained in the area near the building. The area at Station 50W, 50N only appeared in the conductivity survey, which indicates that there is no metallic object associated with this

area. This spot is most certainly a low area where water is collecting and therefore increasing the conductivity values. The remaining anomalous areas at the site can all be attributed to surface features.

At Site 2, the conductivity values are not typical of values expected for material natural to this area. This is an indication that the material is most likely fill material. The presence of a large number of magnetic anomalies, indicated from the other surveys, serve to enhance the interpretation that the area is indeed indicative of a fill. The linear trending feature, most apparent in the conductivity survey, could either be associated with an old drainage path, or possibly a trench.

At Site 3, the northwest corner of the grid is clearly more conductive than the rest of the site and contains many metallic anomalies. There was some amount of surface trash observed in this area which is contributing to the observed readings. This area also slopes in the direction of a nearby creek draining the area, which is contributing to the high conductivity values. However there is clearly a large amount of metallic material in this area that must be located beneath the surface. There is also a very strong possibility that this area might be a continuation of the linear trend observed at Site 2. The other significant anomalous area is that at location 130W, 60N. This area appeared in every test and is not explained by surface features.

At Site 4, although the buildings are hindering anomaly detections, there does appear to be a pipelike feature located beside one of the buildings at location 240E from 20N to 100N. The only other anomalies unaccounted for by surface features occur at locations 140E, 40S and 125E, 225N. The causes of these anomalies are unknown.

At Site 5, several anomalies were detected. These cause - unknown anomalies are most likely due to surface features.

At Site 6, the only anomaly that is not associated with a known surface feature is the large northeast-southwest trending anomaly. This anomaly is both a conductive and magnetic (based on the EM-31) anomaly. However, the results from the magnetometer survey did not indicate a very strong anomaly which would be indicative of ferrous material. The EM-61 did show a very large response to the anomaly since it responds well to metallic and non-metallic material. The possibilities for the cause of the anomaly would be a trench or drainage system containing slightly metallic rocks, or possibly a non-ferrous structure.

Offshore Sites 1 and 2

Several conclusions may be drawn regarding the offshore sites. The cause of the linear trending anomaly located at offshore Site 1 is unknown. There are no onshore structures adjacent to this area that would account for the anomaly's occurrence (pipes, tracks, trash, etc.). Since there was no response

from the magnetometer survey, the anomaly is not produced by ferrous material. The most likely cause of this feature is a channelized drainage system, or a non-ferrous structure. The two anomalies that appear at offshore Site 2 are also unknown in origin. The anomalous area near the power plant pier is most likely associated with the pier's construction or activity on and around the pier. The other anomalous area near location 1000N, is directly adjacent to the onshore Site 2 area. This area does not appear anomalous in the magnetometer survey, again implying that there is no ferrous material in this location. Since the land survey at Site 2 does indeed indicate the presence of fill like material, it is possible that this material may have entered into the offshore material as well. This area also clearly serves as the recipient of drainage for the area associated with Sites 1, 2, and 3. This drainage pattern likely contributes to the very large conductive anomaly.

Geological

Primary geologic interpretation is based on geologic logs. Geophysical applications (such as the GPR, seismic and EM data presented here) complement interpretations of the subsurface geologic framework. The GPR profiles emphasize the lateral inhomogeneity and rapid facies transition typical of riverine or estuarine depositional environments. The reflectors visible in the radar profiles likely represent a depositional contact between a predominantly clay unit and a sandy unit. A possible channel near well WBR-35 extending to the east was indicated on a GPR profile, and its location is supported by monitoring well cross sectional data. The axial minima of this channel is near WBR-35 and WBR-43. Based on borehole and geophysical constraints, the channel may trend to the northwest/southeast.

The seismic profiles provide detail on the lithotypes at depth. The seismic depth sections show stacked reflectors typical of sedimentary depositional sequences. Both lines illustrate the generally southeastward dip of strata which is consistent with the cross section shown in Figure 4 and the work of (Owens 1969; Southwick et al. 1969; Coleman et al. 1990) that is typical of deposition and loading of the Salisbury Embayment. Interpretation of line 200 yields notable features such as the structural dip discussed above, pinch and swell of layers, possible channel features and thinning and truncation of layers.

The following correlations between reflectors and known geology have been drawn. Reflectors at approximately 137-152 m in depth are interpreted to represent Precambrian metamorphic basement. This depth is consistent with other estimates for APG by Owens, 1969; Otton and Mandle, 1984; and McGinnis et al. 1994. A number of unknown and undifferentiated units are seen at depths of 91, 82 and 76 m. At a depth of 64 m there is a strong reflector which likely corresponds to the lower confining unit of the Lower Confined Aquifer seen in Figure 4. At 48 m there is another strong reflector which has been correlated with the top of the Lower Confined Aquifer of Figure 4. At a depth of 39 m there is another strong reflector of variable

coherency that is correlated with the base of the Canal Creek Aquifer. The Canal Creek Aquifer in this portion of the Bush River peninsula appears to be only around 9 m in thickness. A strong and coherent reflector is seen at a depth of 30 m which is likely the top of the Canal Creek Aquifer. Line 200 (Figure 36) shows the Canal Creek Aquifer thinning from a thickness of 15 m near the south end to an estimated 5-6 m near the middle of the line and an apparent thickening again of the aquifer further north. Within the 15 to 23 m interval between Stations 170 to 120 there is a group of intermittent reflectors that dip to the north and south converging around Station 140. This has been tentatively interpreted as a channel feature, but without borehole information the interpretation can not be adequately assessed.

References

Annan, A. P. (1982). "Ground penetrating radar workshop notes," Sensors and Software, Inc., Mississauga, Ontario, Canada.

Bailey, M. (1995). "Hydrology of Cluster 11," COE-BDE, Interim Document.

Barrows, L. and Rocchio, J. E. (1990). "Magnetic surveying for buried metallic objects," *Ground Water Monitoring Review* 10(3), 204-211.

Bevan, B. W. (1983). "Electromagnetics for mapping buried earth features," *Journal of Field Archaeology* 10.

Breiner, S. (1973). "Applications manual for portable magnetometers," Geometrics, Sunnyvale, CA.

Butler, D. K. (1986). "Military Hydrology; Report 10: Assessment and field examples of continuous wave electromagnetic surveying for ground water," Miscellaneous Paper EL-79-6, U.S. Army Engineer Waterways Experiment Station, Vicksburg, MS.

Butler, D. K. and Llopis, J. L. (1990). "Assessment of Anomalous Seepage Conditions." *Geotechnical and Environmental Geophysics, Volume II: Environmental and Groundwater*. Society Explor. Geoph., Tulsa, OK.

Coleman, S. M., Halka, J. P., Hobbs III, C. H., Mixon, R. B. and Foster, D. S. (1990). "Ancient channels of the Susquehanna River beneath Chesapeake Bay and the Delmarva Peninsula," *Geological Society of America Bulletin*, 102, 1268-1279.

Geonics Limited. (1984). "Operating manual for EM31-D non-contacting terrain conductivity meter," Mississauga, Ontario, Canada.

McGinnis, L. D., Daudt, C. R., Thompson, M. D., Miller, S. F., Mandell, W. A and Wrobel, J. (1994). "Environmental Geophysics at Beach Point, Aberdeen Proving Ground". Technical Report Argonne National Laboratory, 118 p.

Minard, J. P., May, F. E. and Christopher, R. A. (1980). "Geology of the Round Bay quadrangle, Anne Arundel County, Maryland." *U.S. Geological Survey Professional Paper 1109*, 30 p.

McNeil, J. D. (1980). "Electromagnetic terrain conductivity measurements at low induction numbers," Technical Note TN-6, Geonics Limited, Mississauga, Ontario, Canada.

Nabighian, M. N. (1988). *Electromagnetic methods in applied geophysics*, Vol. 1, Society Explor. Geoph., Tulsa, OK.

Nemeth, Gary. (1989). "RCRA Facility Assessment Report, Edgewood Area, Aberdeen Proving Ground, Maryland." Vol. 2, pp. 776, Figure 184.

Olhoeft, G. R. (1984). "Applications and limitations of ground penetrating radar," 54th Annual Internat. Mortgage Expanded Abstracts, Society Explor. Geoph., Tulsa, OK, 147-148.

Otton, E. G. and Mandle, R. J. (1984). "Hydrogeology of the upper Chesapeake Bay area, Maryland, with emphasis on aquifers in the Patomac Group." *Maryland Geological Survey Report of Investigations*, No. 39, 62 p.

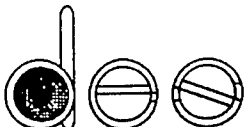
Owens, J. P. (1969). "Coastal Plain rocks of Harford County, Maryland". *Maryland Geological Survey*, p 77-103.

Southwick, D. L., Owens, J. P. and Edwards J. Jr. (1969). "The geology of Harford County, Maryland." *Maryland Geological Survey*.

Telford, W. M., Geldhart, L. P., Sheriff, R. E., and Keys, D. A. (1973). *Applied Geophysics*, Cambridge University Press, NY.

Thurmond, V. (1993). "North-South stratigraphic cross section of the Bush River area." Corps of Engineers, Baltimore District, Internal Document.

Appendix A



dobekci earth sciences, inc.

*geophysics for engineering
and the environment*

September 26, 1994

Mr. Mike Sharp
US Army Engineer
Waterways Experiment Station
P.O. Box 631
Vicksburg, MS 39108

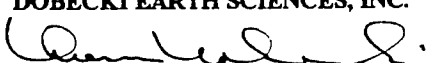
**FINAL REPORT
SEISMIC REFLECTION SURVEY
CLUSTER 11 AREA
PURCHASE ORDER NO. DACA39-94-M-5618**

Dear Mr. Sharp:

This final report represents the results of our seismic reflection project at the Aberdeen Proving Grounds, Edgewood Area, Cluster 11. We have completed all phases (preliminary testing, production data acquisition, seismic data processing, and data interpretation) of the project in accordance with the Statement of Work given in your original request for proposal and as modified in the field during the initial testing phase. This final report incorporates our initial, Interim Report on the Testing Phase (submitted August 22, 1994) and discusses the remaining phases in detail.

Dobekci Earth Sciences, Inc. (DES) appreciates the opportunity to have participated on this WES project. Please let us know if we may clarify any points made in the following report.

Respectfully Submitted,
DOBECKI EARTH SCIENCES, INC.


Thomas L. Dobekci, Principal Geophysicist

11111 Katy Freeway
Telephone: 713-467-0373

Suite 610

Houston, Texas 77079
Facsimile: 713-465-0919

TABLE OF CONTENTS

	Page
1.0 INTRODUCTORY COMMENTS	3
2.0 PHASE I (Testing Program).....	4
2.1 Testing Procedure.....	4
2.2 Initial Testing of P-wave sources.....	4
2.3 Initial Testing of S-wave sources.....	5
2.4 Results of Testing Phase.....	6
3.0 PRODUCTION SEISMIC REFLECTION SURVEY.....	7
3.1 Line Descriptions.....	7
3.2 Estimated Shear Velocities.....	8
3.3 Data Processing.....	10
3.4 Results - Seismic Line 200.....	11
3.5 Results - Seismic Line 100.....	14
4.0 LIMITATIONS.....	15

FINAL REPORT
SEISMIC REFLECTION SURVEY
CLUSTER 11 AREA
PURCHASE ORDER NO. DACA39-94-M-5618

1.0 INTRODUCTORY COMMENTS

The US Army Corps of Engineers, Waterways Experiment Station ("WES") has issued a purchase order (DACA39-94-M-5618) to Dobecki Earth Sciences, Inc. ("DES") to conduct a seismic reflection survey program at the Cluster 11 Area of Aberdeen Proving Grounds, Edgewood, Maryland. WES has been conducting a series of geophysical survey programs, both on and offshore, to characterize the environmental nature and hydrogeologic character of the Cluster 11 area - a site of previous landfilling activities. While some drilling has been performed to evaluate the hydrogeology, most of the work done on land to date has been shallow surveys to define metals accumulations or other hazards. The objective of the subject, seismic reflection survey, then was to supplement any existing borehole information and to determine stratigraphic information (depth, thickness, and continuity) regarding certain hydrogeologic units (aquifers and confining layers) within the upper 250 ft of the subsurface in an area surrounding a former refuse disposal area. The original scope of work called for an initial testing phase to evaluate compressional ("P") and shear ("S") wave techniques at this site and to follow up the testing (if shown to be effective) with a production survey of approximately 1500 line feet of seismic reflection along lines defined by WES personnel. This final report presents the results of the Testing Phase as well as the Production Survey Phase.

2.0 PHASE I (Testing Program) - August 16, 1994

2.1 Testing Procedure

In general terms, DES tested a variety of compressional (P) wave and shear (S) wave sources, both vertical (P) and horizontal (S) geophones, a variety of source to geophone offsets, and two different geophone spacings to determine the proper design and geometries for the production survey.

The tests were acquired in the area immediately west of the road crossing the old refuse area, just west of the fenced off portion of the old refuse area. Surface conditions were grassy and relatively flat. Upon digging shallow pits for the S-wave source and shallow borings for the Buffalo Gun source, we found that the very near surface (to two feet depth, at least) consists of mixed trash including plastics, newsprint, and numerous pieces of brick, ceramic tiles, and some concrete. The area does show refuse disposal which would suggest, depending on thickness of refuse, that seismic data in this area may be poor due to poor transmission characteristics normally found through refuse materials. The ground was dry, but we did encounter water in the shallow (2 ft) borings we augered for the Buffalo Gun tests.

2.2 Initial Testing of P-wave sources

Five source combinations for P-wave energy were tested. The spread of geophones consisted of 24, 40 Hz, vertical geophones spaced at two-foot intervals along the ground. The five sources included:

- An eight-pound sledgehammer striking a steel plate (vertical blow)
- An eight-pound sledgehammer striking a hard plastic cylinder (vertical)
- A small, hand-sledgehammer striking a steel plate (vertical)
- A small, hand-sledgehammer striking a hard plastic cylinder (vertical)
- A Buffalo Gun firing a 12 gauge shell into a 2 ft, vertical bored hole

Each P-wave source was recorded at two positions: 1) 10 ft from the first (end) geophone and 2) 58 ft from the first (end) geophone. These two locations constitute a walk-away noise test which reviews seismic data over a total offset range of from 10 - 102 ft. All sources provided similar results (see Figure 1 as an example) in that the data contained little in the frequency band above 100 Hz (probably due to surficial refuse). The Buffalo Gun had difficulty because of the difficulty in augering holes in this area (lots of brick debris). More significant than the frequency content is that we only observed two, identifiable P-wave reflections, and these occur at times consistent with the deepest of the interfaces seen in the general geologic cross section of the site. This means that almost all of the shallower interfaces of interest could not be mapped using even a two-foot geophone spacing. A final observation is that, even with a maximum offset of 102 ft, we did not observe any clear or even hints of first break arrivals at water table velocity (5,000 ft/sec - see Figure 2). With a suspected depth to water of 15 ft, we would have expected to see such first breaks at an estimated offset distance of 40-50 ft. In summary, we do not feel P-waves, in this area of the site anyway, would have satisfied the survey objectives.

2.3 Initial Testing of S-wave sources

For the shear wave testing, we set out a spread of twenty-four SH-type geophones also at a two-foot spacing (in fact, right next to the P-wave geophones). The same two source positions (at 10 ft and 58 ft offset from the first geophone) were employed but using the shear wave source tested. The sensitivity axis of the geophones was oriented perpendicular to the spread direction. The sources consisted of the same eight-pound sledgehammer and the hand sledge but striking the steel plate lying against the side of a shallow hole as shown on attached Figure 3. Striking the plate in one direction sends a horizontal polarized shear (SH) wave into the ground. Placing the plate against the other side of the hole and striking in the opposite direction sends a SH wave of reversed polarity into the ground. In practice, we strike in one direction and then subtract the strike in the

opposite direction; this enhances the SH wave and reduces any P-wave energy. In this fashion we can produce records which are rich in shear waves.

The two sources were merely a change in hammer weight using the same setup as shown. The resulting raw shear wave shot results (attached figure 4 is an example) showed several strong reflections from as shallow as 0.125 seconds (approximately 45 ft depth) to as deep as 0.850 sec (over 300 ft depth, estimated). The data also show that the reflections are not flat (e.g. several show a dip downwards near geophone position 5 on figure 4). This could either mean that the reflectors themselves have structural ups and downs over short distances or that the near surface fill area is very variable in terms of thickness and velocity causing so-called 'static' shifts.

We also repeated the SH wave testing using a 4 ft geophone spacing. The results were less consistent than using the two foot spacing but were considered acceptable. We did not feel going to a greater spacing was warranted.

2.4 Results of Testing Phase

Based upon our source testing, we suggested that P-waves were inadequate to produce results as required in the Scope of Work. We did feel that using SH waves with no greater than a four-foot geophone spacing, the minimum cited in the original Scope of Work, was appropriate. Our final shooting geometry was decided as:

- Source, SH hammer (8 lb) against sides of shallow holes
- Geophone (SH) spacing of four feet
- Source (off-end) offset of eight feet from near geophone
- Shotpoint interval of four feet to yield the required 12 fold data

3.0 PRODUCTION SEISMIC REFLECTION SURVEY - August 17-19, 1994

3.1 Line Descriptions

After completion of the Testing Phase and determination of production data acquisition parameters, DES acquired shear wave reflection seismic data along two seismic lines (Line 100 and Line 200) in the Cluster 11 Area at APG. The general locations of these two lines are shown on Figure 5.

Line 100 is in the same general area as the site of the testing phase - the open field area suspected of being an old fill area just to the west of the fenced-in landfill area. Total line length was 588 feet (total length available in field area) in a, basically, East-West direction. In the digging of the shallow holes for emplacement of the shear wave steel plate, we noted a great deal of artificial (non-soil) materials including concrete pieces, brick pieces, and some minor amounts of plastic in the upper 6 inches, particularly towards the western half of the seismic line.. This not only caused some difficulty in the preparation of shotpoint, but it also indicated that this may have been a fill area. The implications of a fill area on seismic data quality is that, usually, fill areas are notorious for being poor data areas because of inhomogeneity and high porosity of fill materials causing extensive scattering and dissipation of seismic waves.

Line 200 is a 676 ft long seismic line, basically oriented NS and located in the area to the south of Line 100. It crossed rather flat field extending from near the creek just south of Line 100, across open field, between the old building/berm area and the fenced-off canister storage facility. Two drainage ditches were crossed by the seismic line in the general location just to the east of the canister storage area; the impact of these was to introduce static (time shift) errors into the data set which were later removed during processing.

3.2 Estimated Shear Velocities

In order to convert reflection times to reflector depths, it is important to acquire an estimate of the shear wave velocities of the subsurface materials. The curvature ("Normal Moveout") of the reflections, themselves, offer a measurement estimate for the deeper materials. For the shallower (upper 50 ft or so) materials, we provided a direct measurement of the shear wave velocities by performing a short, reversed refraction profile during our initial testing phase. The test consisted of a forward and reversed refraction spread using a geophone spacing of four feet and two S-source shotpoint situated 8 ft before the first geophone and 8 ft past the 24th geophone. The resulting refraction data were analyzed using two analysis programs (SIPT from Rimrock Geophysics and SeisRefa by Oyo Geospace). Both programs show consistent results of a) an upper, loose soil horizon of less than 3 ft thickness and having an average shear wave velocity value of 250 ft/sec underlain by b) a more compacted (undisturbed), thick (we did not see its base using the given spread geometry) soil layer having average shear wave velocity of 600 ft/sec. As the shear velocity does not increase at the water table, we would not expect any dramatic increases in shear velocity versus depth until we reach the depth of the Pleistocene-Cretaceous contact (roughly, 25 ft taken from the stratigraphic cross section supplied to DES by WES). We would expect an increase in velocity in Cretaceous materials because of their increased age and tendency for increased compaction and partial cementation. Without borehole measurements, we cannot accurately define the velocity versus depth gradient which means we cannot absolutely tie specific reflections to specific reflecting horizons (geology), but using the reflection curvature and the results of the refraction survey, we can define such a velocity versus depth distribution which is likely *close* to the true distribution. Using refraction (upper ten feet velocities) and reflection curvature (RMS stacking velocities converted to average velocities to given reflection times), we have the following time-depth conversions:

<u>Reflection Time (sec)</u>	<u>Equivalent Estimated Depth (ft)</u>
0.000	0
0.100	25
0.200	75
0.300	130
0.400	195
0.500	270 (?)
0.600	370 (?)

The questionable values for the deeper reflection times is due to uncertainty about stacking velocities at these times (reflections are almost flat, so almost any stacking velocity will work). This depth range, however, is beyond the depth of interest (250 ft) for this particular survey. Equivalently, we may produce a time to specific depth distribution (also non-linear) as follows:

<u>Depth (ft)</u>	<u>Equivalent Estimated Reflection Time (sec)</u>
0	0.000
25	0.100
50	0.150
75	0.200
100	0.230
150	0.330
200	0.410
250	0.475

We note that the time to depth relationship is not linear; that is, if reflection time is presented as a linear scale, then depth would not be linear on the same plot. Alternatively, if depth were presented as a vertical, linear scale, then time would be non-linear. To accommodate this, we present both reflection time sections and separate linear vertical depth sections for each line in the following discussions..

We do note that, during the Production Data acquisition phase, we did notice the coming and going of harder layers of limited width wherein shallow shear velocities approached 1000 ft/sec. These, we feel, are probably either small channel-shaped layers

which have only limited continuity and consisted of denser, more compacted materials or areas where the harder Cretaceous layers are closer to the ground surface.. While these may cause local changes in the velocity/depth relationship, we do not feel they change the relationship to such a degree that we need to treat these short intervals separately.

3.3 Data Processing

The resultant seismic reflection data were submitted to Sterling Seismic Services (Denver) for processing. The general stream of data processing on their Advance ProMax processing system is as follows:

- Read seismic data from floppy disks and reformat into Advance internal format.
- Apply predictive deconvolution to seismic traces to reduce the very prevalent reverberation seen on each line and to sharpen the seismic pulse.
- Enter seismic shotpoint and geophone geometries and elevations
- Sort the seismic data from shot files (gathers) into common midpoint (CMP) gathers
- Adjust the seismic trace times for elevation differences (statics)
- Apply additional statics due to variation in the nature of the near surface low velocity layer (refraction statics)
- Compute stacking velocities and adjust for normal moveout (NMO).
- Stack NMO adjusted CMP gathers for 12 fold (max).
- Apply post-stack filtering and coherency enhancement
- Print time section
- Perform time-to-depth conversion
- Print depth section

3.4 Results - Seismic Line 200

Figure 6a is the seismic reflection time section and Figure 6b is the depth-converted, seismic reflection record section for Seismic Line 200. We have chosen to discuss the data from Line 200 first because its data quality is superior to Line 100. Further, our colored interpretations are performed only on the depth sections (e.g. Figure 6b). On the figures, the main vertical scale is in two-way reflection time (seconds) on Figure 6a; the horizontal scale is 1" = 40 ft (the separation between each individual seismic trace is two feet, or one-half of the surface geophone spacing). The reflections are observed as dark band showing coherency (continuity) across the section. On Figure 6b, the depth scale is as shown in feet depth. Again, without borehole data right on the line (actual measured transit times to specific layers), we cannot absolutely correlate a given reflection (e.g. the strong reflection at approximately 0.200 sec/75 ft) with a given geologic horizon (e.g. the Top of the Canal Creek Aquifer), but, using the minimal cross sectional data available and the time-to-depth conversion scheme described, we can state which reflections are most likely which geologic units. For example, the 0.200 sec/75 ft reflection probably *does* represent the Top of the Canal Creek because it is a fairly strong event, which we would expect, and occurs close in time/depth to where we would expect the Canal Creek based upon an approximate 80 ft depth seen in Borings BR-4 and BR-5.

What we note on the section is that there are quite a few reflections ranging in time from 0.050 sec (15 ft depth, approximately) to over 0.600 sec (over 370 ft). Because we estimate a 250 ft depth to occur at a reflection time of 0.475 sec, the deeper reflections represent layers beyond our current depth of interest and for which we have no borehole control. We will, then, try to make correlations of reflections within the upper 0.475 sec with known geologic units and to use both these and the deeper horizons to make overall interpretations of the local geologic structure along this line.

We also note that data quality in the northern end of Line 200 (Stations 100 through 140, roughly the first 160 ft) is rather poor, especially in the upper section (above

0.300 sec). We cannot account for this loss in quality other to say that this end of the line is also in closest proximity to the Line 100 area which is also a poor data quality area.

Specific to Line 200, we have tried to make the following correlations between reflections (cited depths are typical across the section) and major geologic interfaces. Using the published cross section through the borings on site, we try to link a given reflection with a given unit. To this end, we have color-coded dominant reflections as being either a "blue" reflection, representing the top of a dominantly clay unit or "yellow" for the top of a dominantly sand unit. We have colored the deeper reflectors "orange" as we have no information as to their potential stratigraphy.

<u>Depth (ft)</u>	<u>Geologic Interface</u>	<u>Comments</u>
25	Top Cretaceous/Upper Confining Unit	Weak and poor coherency; colored "blue" on Figure 6b
100	Top Canal Creek Aquifer	Strong and coherent colored "yellow"
130	Base Canal Creek/Top Confining Unit	Strong with variable coherency; "blue"
160	Top Lower Confined Aquifer	Strong with variable coherency; "yellow"
190	Bed within Lower Confined Aquifer	Weak with variable coherency; not colored
210	Top Lowest Confining Unit	Strong and coherent colored "blue"
250	Unknown Unit	Very strong and coherent
270	Unknown Unit	
300	Unknown Unit	colored "orange"

From a cross-sectional, structural sense, we do not see any evidence of faulting on this section (Line 200). However, we do see several other features which are notable. These include structural dip on the layers, pinching-out of others, and the interpretation of a channel-like feature.

The structural dip is not uniform. For the central portion of Line 200, the layer interfaces are, generally, flat. We do see a general increase in dip down towards the South beginning at, approximately, Station 230 (130 stations or 520 ft from the northern end of the line = Station 100). However, we also see an increase in dip down to the North (left) going to the north of Station 180. The dip to the South is more apparent on the deeper (>150 ft) interfaces than on the shallower interfaces. This southern dip is in general agreement with the gross cross-sectional picture given by drilling results (Borings BR-1 through BR-5 with Boring BR-4 being the closest to Line 200).

Aside from general dip of the layers, we also see thinning of certain layers and an apparent formation of a channel-like feature. For example, there seems to be a pinching out of a thin bed within the Cretaceous and above the interpreted Canal Creek aquifer at a depth of 50 ft near Station 230; such a possible sand lens is also noted on the stratigraphic cross-section. Also, the (interpreted) Canal Creek aquifer itself shows apparent thinning from a typical 50 ft thickness on the south end of the line down to a minimum thickness (estimated) of 15-20 ft near Station 210. Just north of this area of thinning, we see a downwarping and apparent thickening of the (interpreted) Canal Creek reflection. The overlying reflections continue across without significant downwarping, so this is not a general "statics" problem. This has the appearance of a channel; however, the fill material is unknown other than we feel it is of lower velocity than the 'normal' Canal Creek as we also see a slight downwarping of deeper reflections directly beneath this feature which may also be contributing to the observation of dip to the North cited above. We do not feel that the deeper beds are truly downwarped but, rather, the reflections from these are apparently delayed because of going through an additional thickness of lower velocity

material. Whatever the actual feature may be, it is really the only significant stratigraphic/structural feature seen on Line 200. It is important, however, to note that, in general, as we trend towards the North, several of the beds (e.g. interpreted Canal Creek) appear to be thinner than at the southern end of the line which also agrees with trends shown on the stratigraphic cross-section. This northern end of the line is the point of closest approach to Line 100, so we would hopefully be able to tie the reflections at the northern end of Line 200 (of admittedly poorer quality) to those seen on Line 100 whose description follows.

3.5 Results - Seismic Line 100

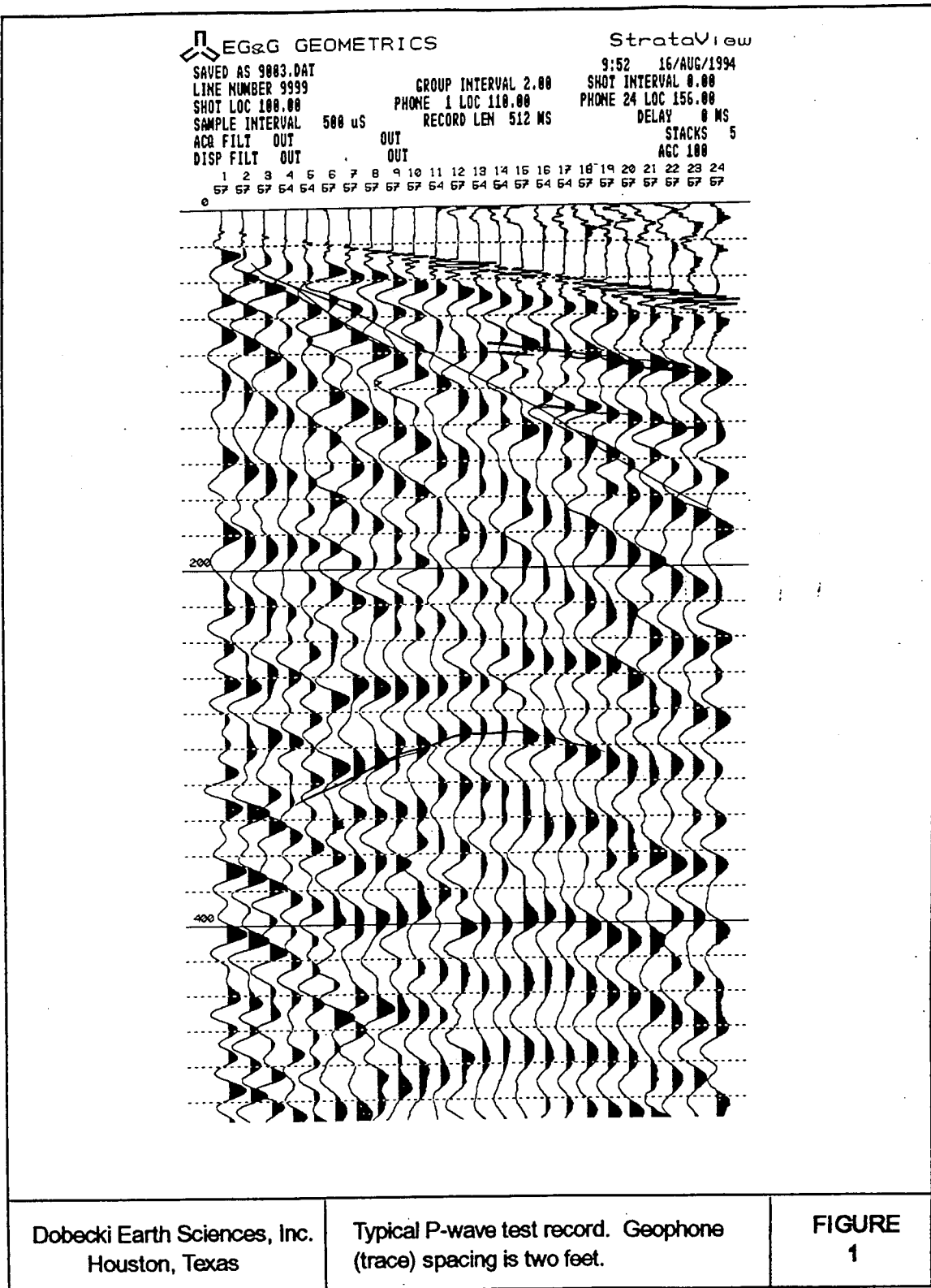
Figure 7a is the time-record section and Figure 7b is the converted depth reflection section for seismic Line 100. In general, the very shallow section (<100 ft depth) on Line 100 shows better quality than Line 200, but, overall, the data quality is poorer as reflections are quite a bit weaker and less coherent. We can, however, overlay the reflection section from the northern end of Line 200 on the Line 100 data and correlate most of the same reflection events at nearly the same times/depths. The most obvious feature lacking from the Line 100 data are the strong, very deep (orange) reflections. While we are able to see these in segments, they are not as strong or coherent as on Line 200. This may be, in part, because of the fill materials seen at the surface all along Line 100 while we only saw such materials in the northern end of Line 200. Introduction of looser fill materials has an overall tendency to reduce the strength of observed reflections because of scattering and high attenuation of seismic energy going through such materials. The fact that both Lines 100 and 200 were acquired using identical seismic sources and acquisition parameters and yet yield quite different quality data attests to the difference in near surface conditions (filled versus non-filled) between the two areas which are less than one-half mile apart. In spite of weak reflections, we have been able to correlate events with Line 200, and we make, therefore, the same correlations and coloring scheme of

reflections to interpreted geologic interfaces as we did with Line 200. Given this, we make the following comments about observations along Line 100.

The interfaces above 150 ft all exhibit slight dip from left to right (West to East), while the deeper interfaces show a possible reversal of dip at the western end (Station 230-190). This appears to result in a thickening again of the interpreted Canal Creek aquifer from only 20 ft or so at the eastern end to about 50 ft at the western end of Line 100. We do not, however, see any indications of faulting or major pinching out (discontinuity) of any of the key horizons.

4.0 LIMITATIONS

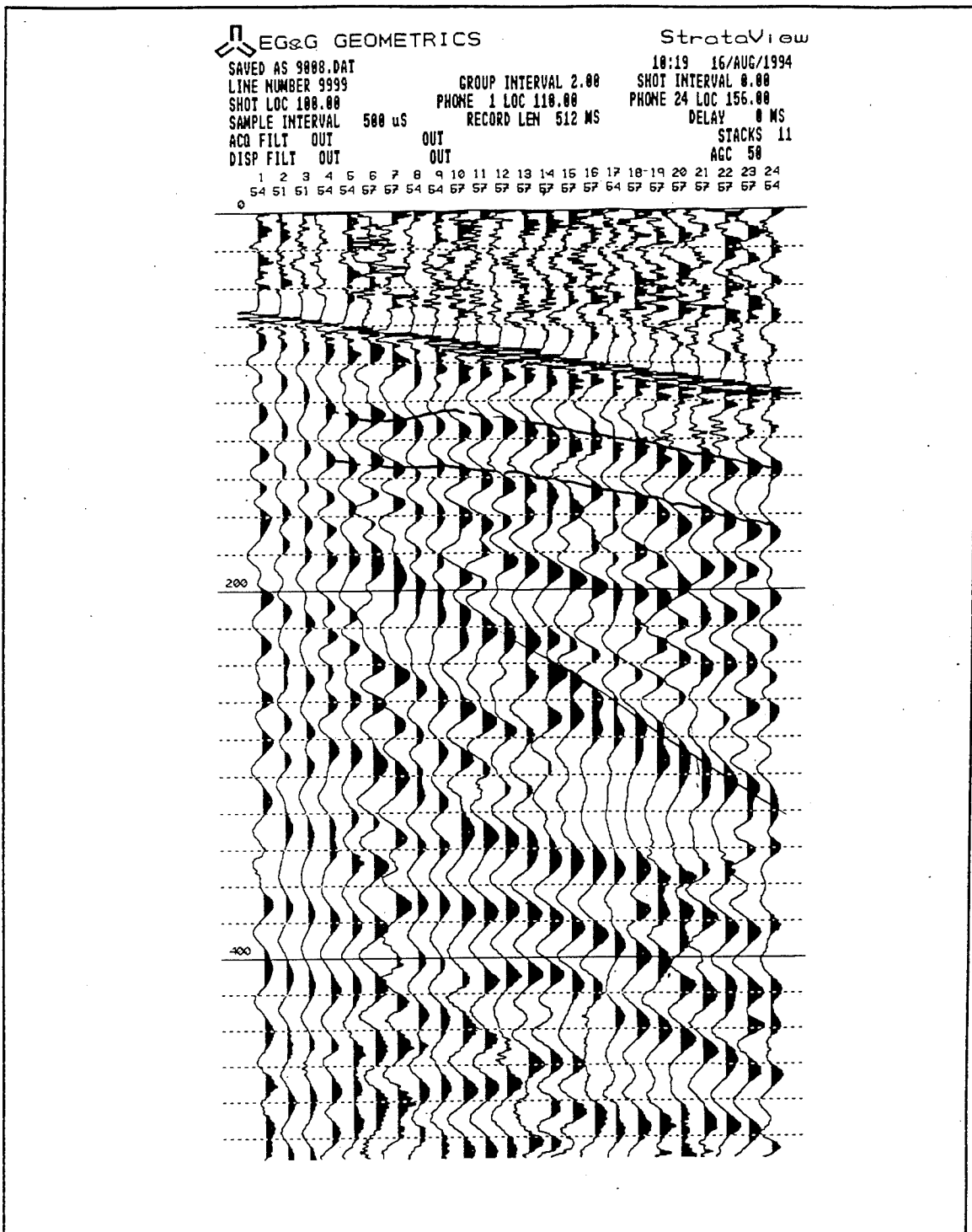
The field data acquisition and data processing methods employed in this seismic reflection survey meet the standards of care and practice of our profession. The interpretation of said reflection data in terms of linking observed reflections with suspected hydrogeologic units (aquifers and aquitards) is based only upon our estimated velocity distribution and resulting depth conversion but without any borehole information for absolute correlation aside from the stratigraphic cross-section provided by WES. Therefore, while the tying of specific reflections to specific geologic units remains speculative and highly dependent upon that stratigraphic section, comments made regarding continuity and thickness variation and structural behavior on those layers (whatever they actually may be) are a more valid part of our interpretation.



Dobecki Earth Sciences, Inc.
 Houston, Texas

Typical P-wave test record. Geophone
 (trace) spacing is two feet.

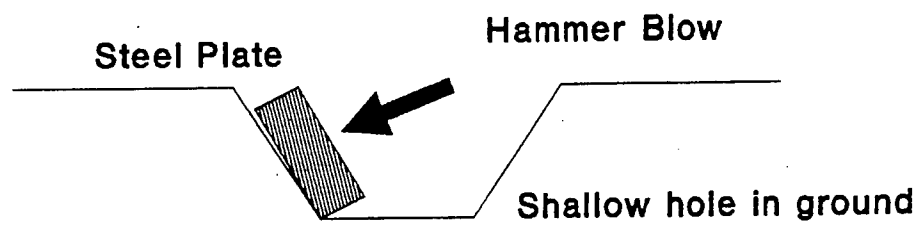
FIGURE
1



Dobecki Earth Sciences, Inc.
Houston, Texas

Long offset P-wave test record.
Note: no water table first breaks.

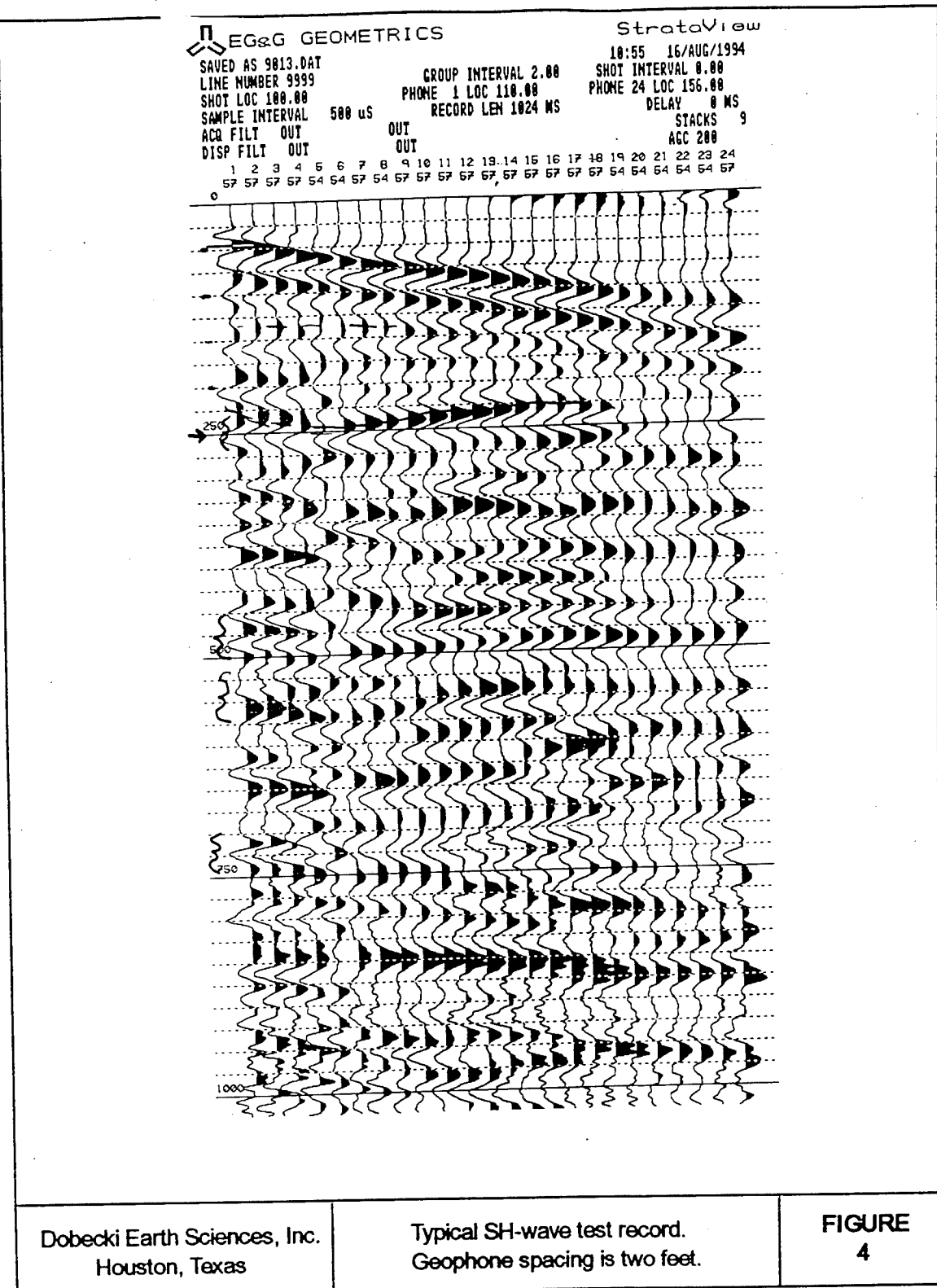
FIGURE
2



Dobecki Earth Sciences, Inc.
Houston, Texas

Diagram of the SH wave source.
View is looking along the line.

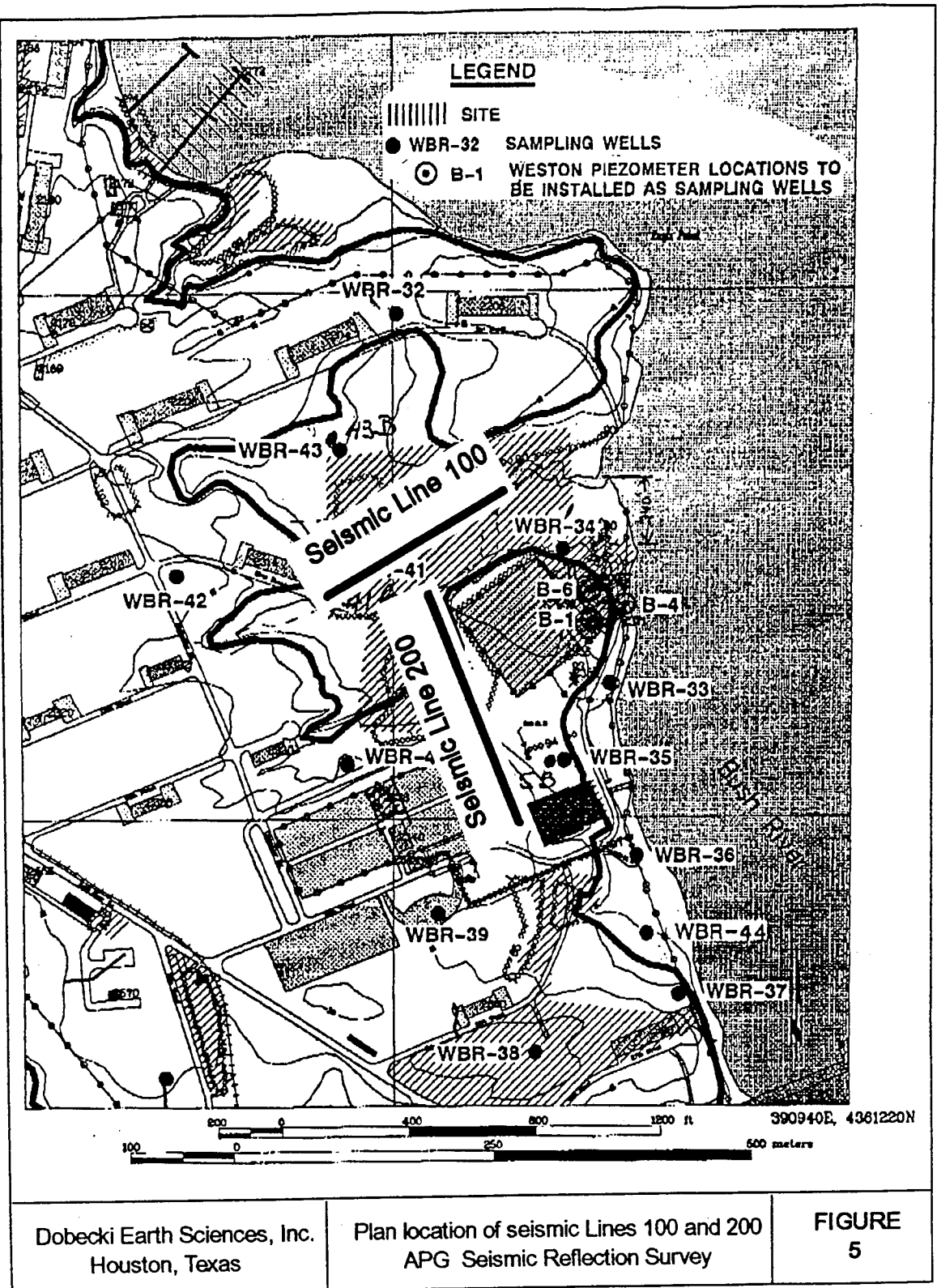
**FIGURE
3**



Dobecki Earth Sciences, Inc.
Houston, Texas

Typical SH-wave test record.
Geophone spacing is two feet.

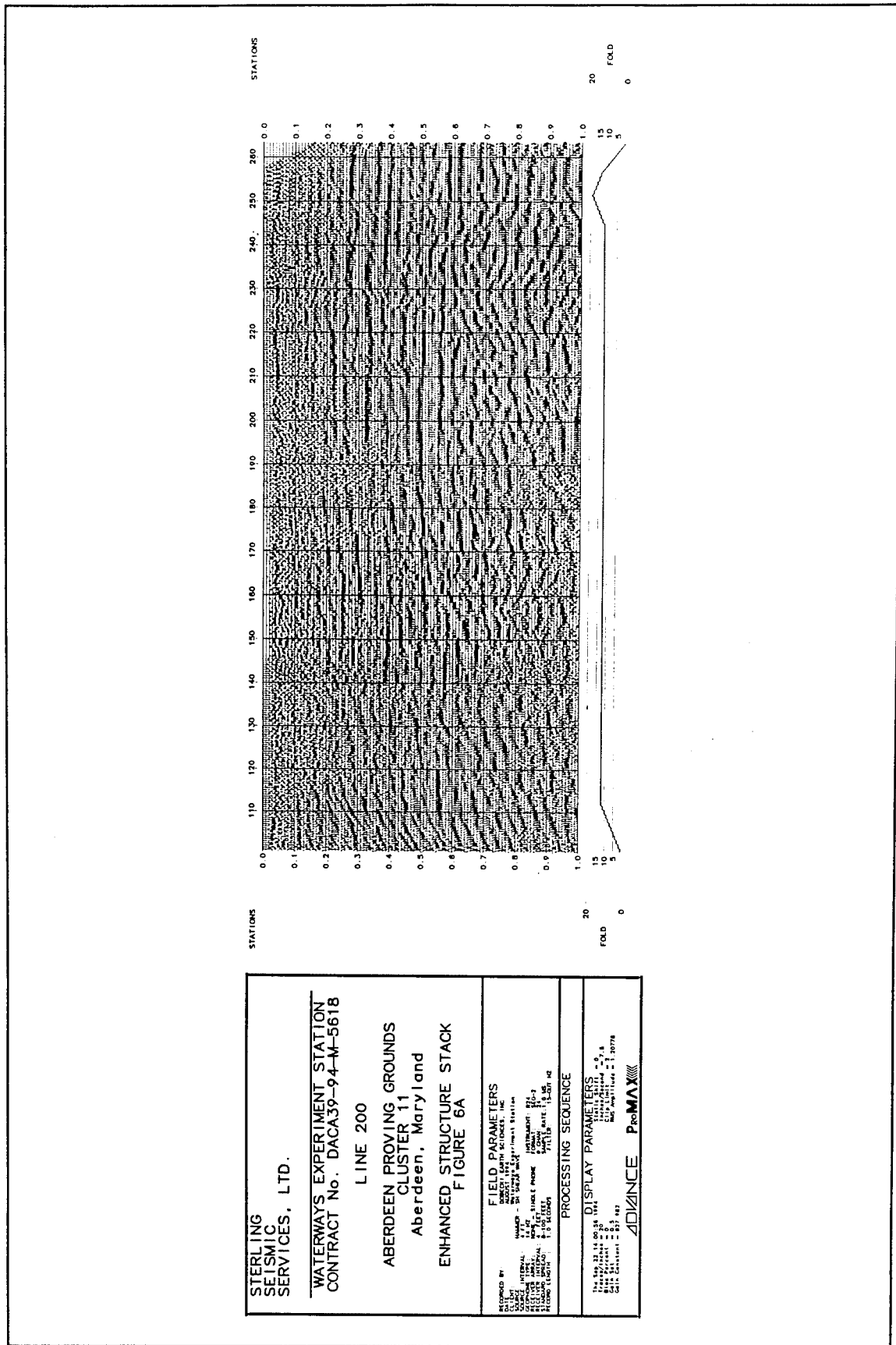
FIGURE
4

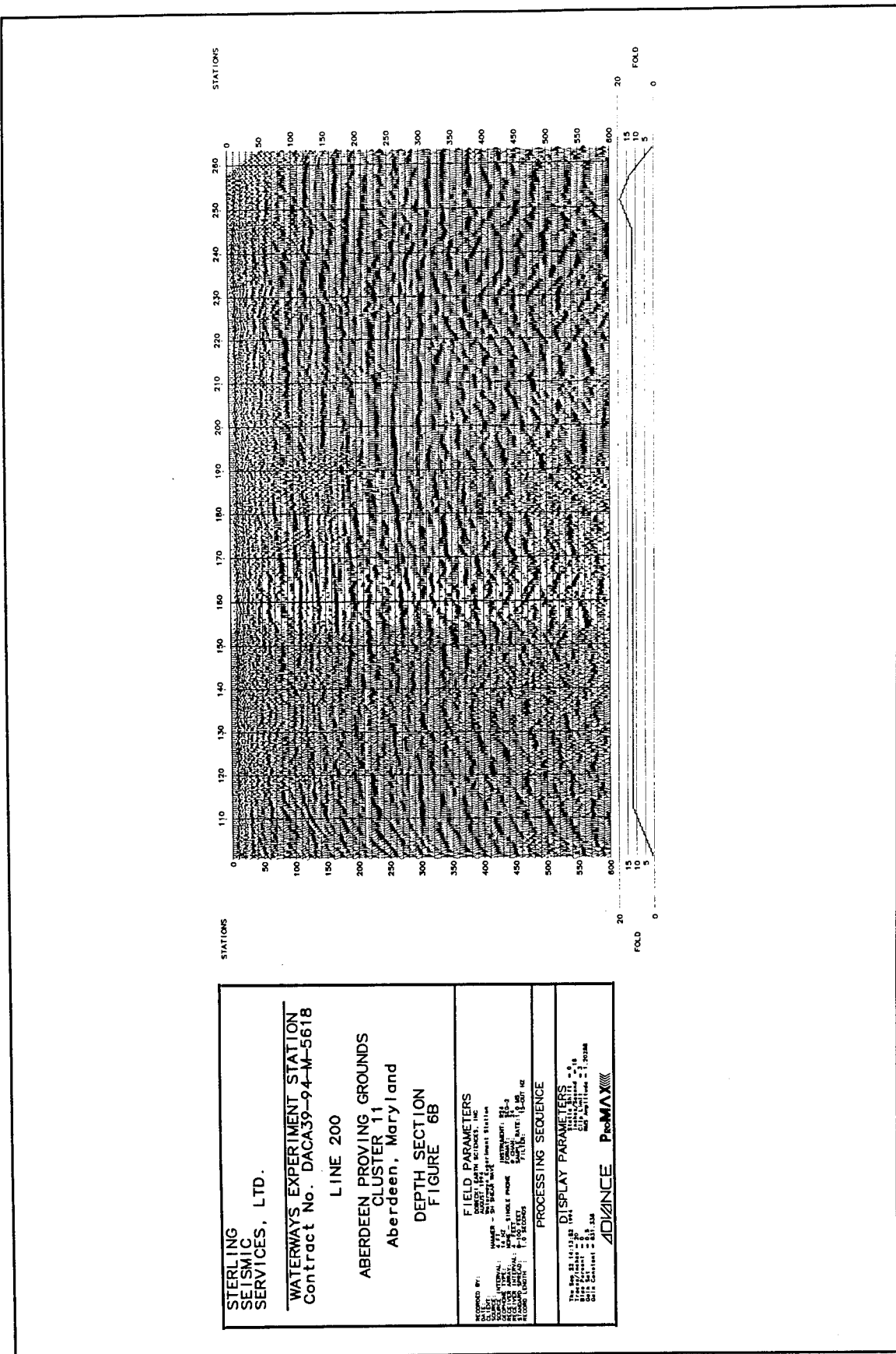


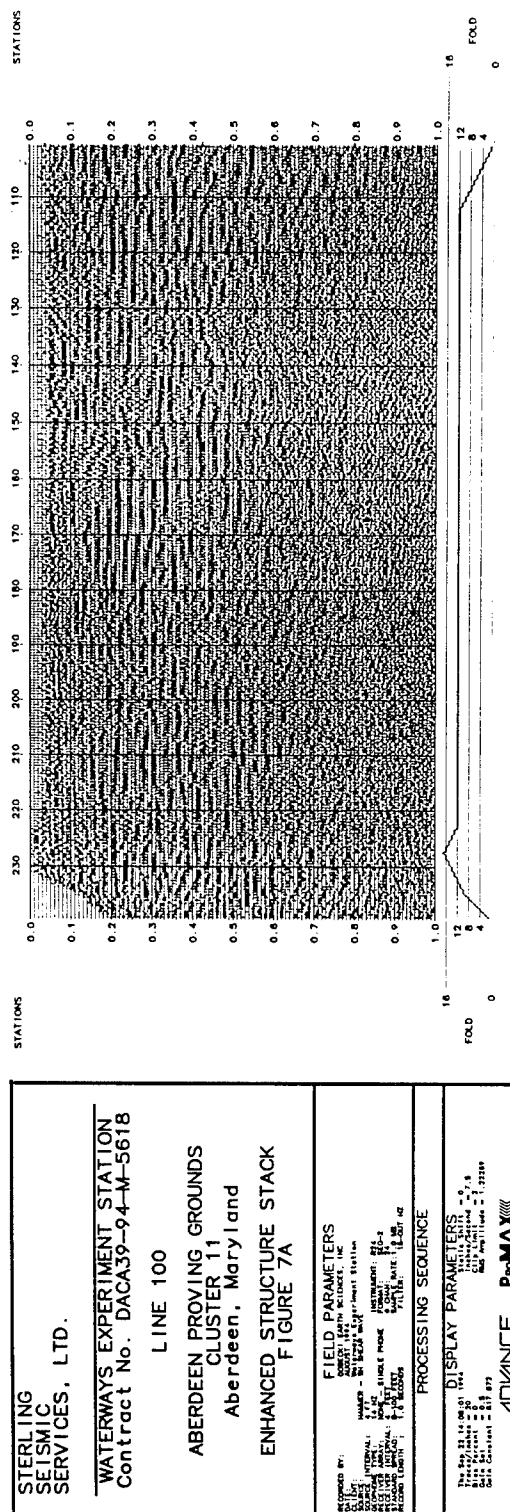
Dobecki Earth Sciences, Inc.
Houston, Texas

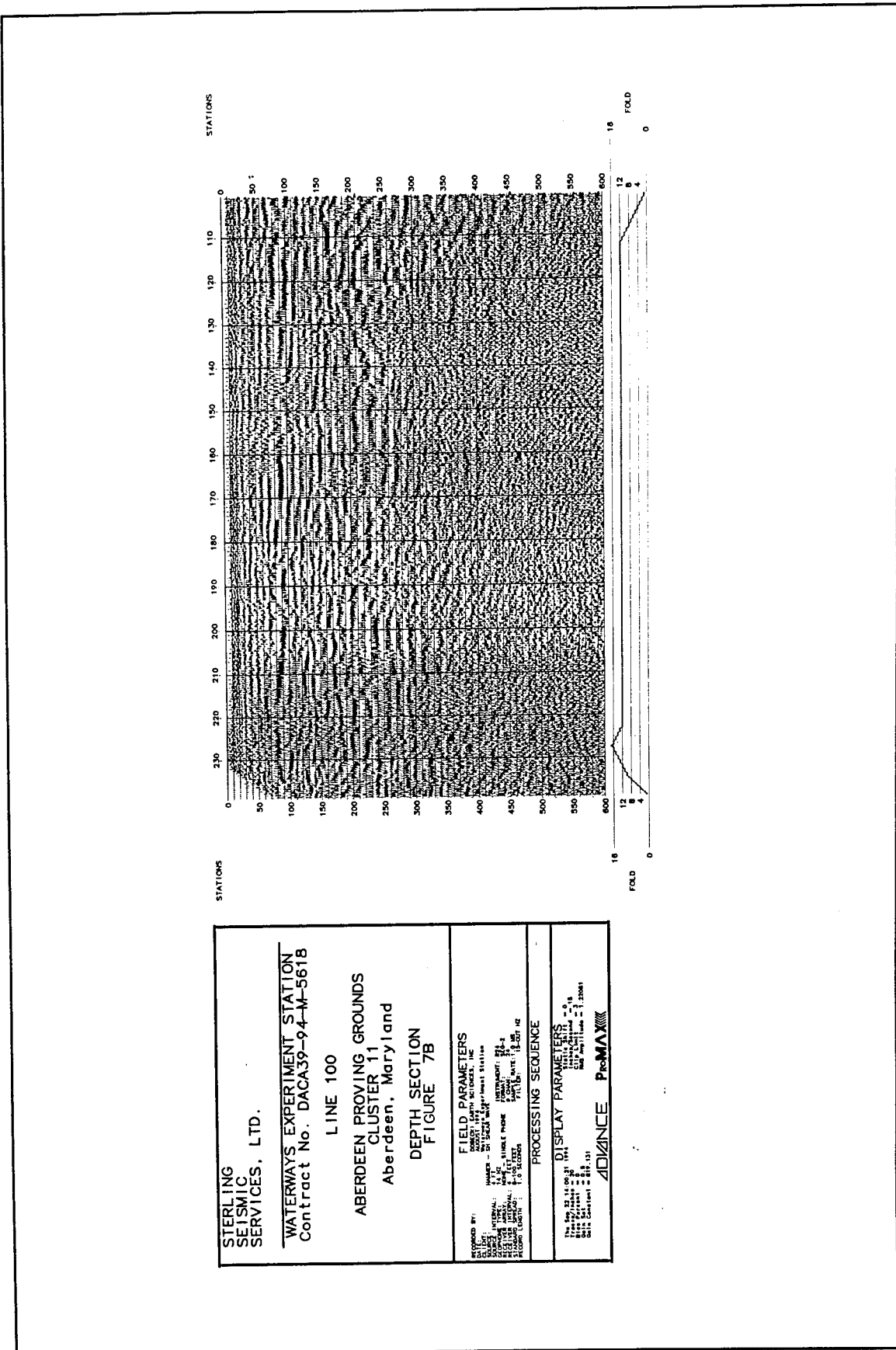
Plan location of seismic Lines 100 and 200 APG Seismic Reflection Survey

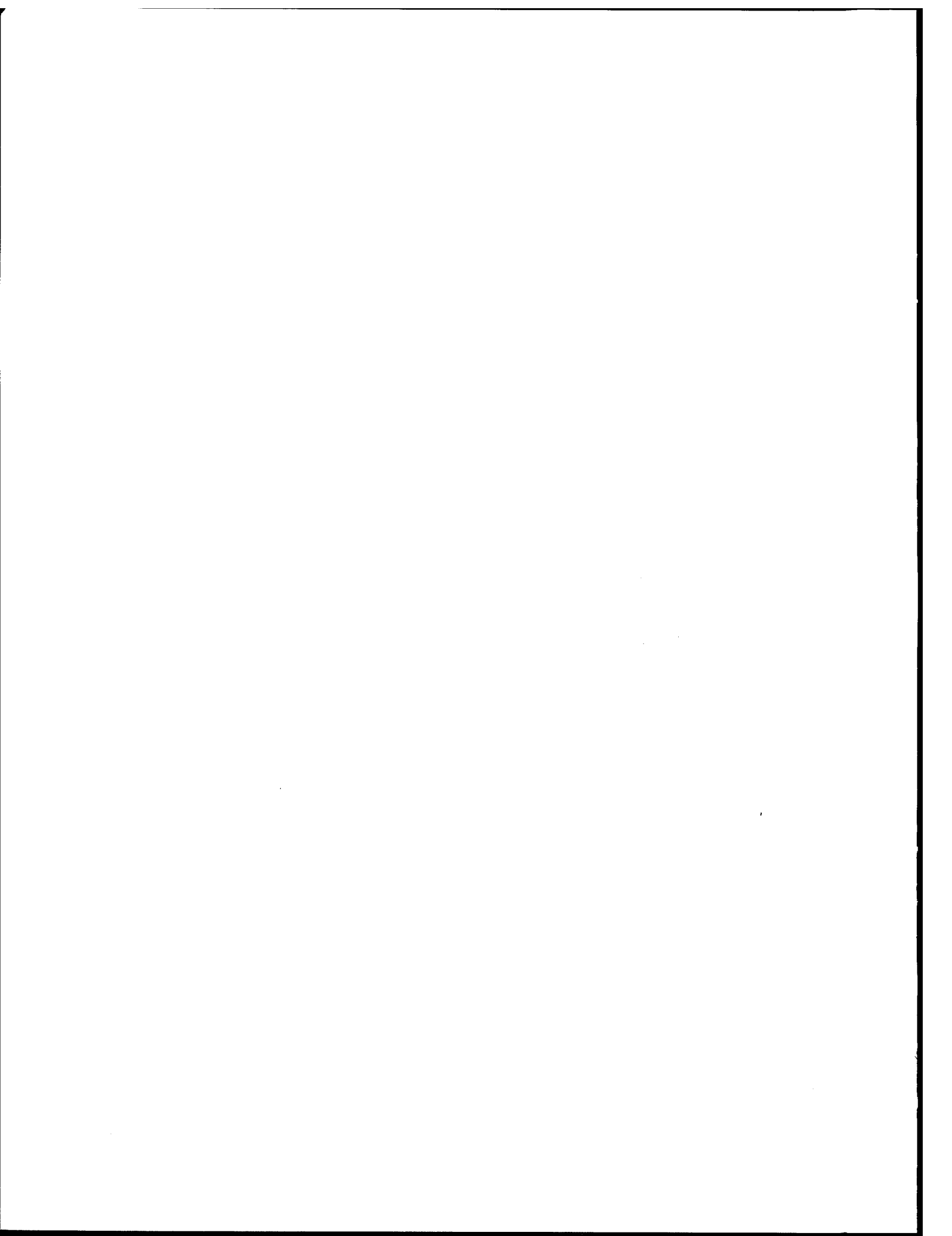
FIGURE 5











REPORT DOCUMENTATION PAGE

Form Approved
OMB No. 0704-0188

Public reporting burden for this collection of information is estimated to average 1 hour per response, including the time for reviewing instructions, searching existing data sources, gathering and maintaining the data needed, and completing and reviewing the collection of information. Send comments regarding this burden estimate or any other aspect of this collection of information, including suggestions for reducing this burden, to Washington Headquarters Services, Directorate for Information Operations and Reports, 1215 Jefferson Davis Highway, Suite 1204, Arlington, VA 22202-4302, and to the Office of Management and Budget, Paperwork Reduction Project (0704-0188), Washington, DC 20503.

1. AGENCY USE ONLY (Leave blank)	2. REPORT DATE March 1996	3. REPORT TYPE AND DATES COVERED Final report	
4. TITLE AND SUBTITLE Geophysical Investigation of Cluster 11, Edgewood Area, Aberdeen Proving Ground, Maryland			5. FUNDING NUMBERS
6. AUTHOR(S) Michael K. Sharp, Janet E. Simms, Landris T. Lee, Jr., Jerry L. Burgess			
7. PERFORMING ORGANIZATION NAME(S) AND ADDRESS(ES) U.S. Army Engineer Waterways Experiment Station 3909 Halls Ferry Road, Vicksburg, MS 39180-6199; Aberdeen Proving Ground, MD 21005			8. PERFORMING ORGANIZATION REPORT NUMBER Miscellaneous Paper GL-96-4
9. SPONSORING/MONITORING AGENCY NAME(S) AND ADDRESS(ES) U.S. Army Aberdeen Proving Ground, Installation Restoration Program, Directorate of Safety, Health, and Environment, Aberdeen Proving Ground, MD 21005			10. SPONSORING/MONITORING AGENCY REPORT NUMBER
11. SUPPLEMENTARY NOTES Available from National Technical Information Service, 5285 Port Royal Road, Springfield, VA 22161.			
12a. DISTRIBUTION/AVAILABILITY STATEMENT Approved for public release; distribution is unlimited.		12b. DISTRIBUTION CODE	
13. ABSTRACT (Maximum 200 words) A geophysical investigation consisting of surface seismic, electric, electromagnetic, magnetic, and ground penetrating radar methods was conducted at the Cluster 11 site located in the Edgewood Area of the Aberdeen Proving Ground, Maryland. The purpose of the investigation was to locate underground structures such as barrels and tanks. The results indicated the presence of unknown underground anomalies at each site, and their locations were mapped.			
14. SUBJECT TERMS Aberdeen Proving Ground Electromagnetic Geophysics Ground penetrating radar			15. NUMBER OF PAGES 183
			16. PRICE CODE
17. SECURITY CLASSIFICATION OF REPORT UNCLASSIFIED	18. SECURITY CLASSIFICATION OF THIS PAGE UNCLASSIFIED	19. SECURITY CLASSIFICATION OF ABSTRACT	20. LIMITATION OF ABSTRACT